Universidad de Concepción
Dirección de Postgrado
Facultad de Ciencias Naturales y Oceanográficas
Programa de Doctorado en Oceanografía

Mortalidad y degradación bacteriana de copépodos pelágicos asociadas a las Zonas de Mínimo de Oxígeno (ZMOs)

Tesis para optar al grado de Doctor en Oceanografía

SONIA ELIZABETH YAÑEZ
TENORIO
CONCEPCIÓN-CHILE
2018

Profesor Guía: Dra. Pamela Hidalgo Díaz
Dpto. de Oceanografía, Facultad de Ciencias Naturales y Oceanográficas
Universidad de Concepción

Universidad de Concepción
Dirección de Postgrado

La Tesis de Doctorado en Oceanografía titulada "MORTALIDAD Y DEGRADACIÓN BACTERIANA DE COPÉPODOS PELÁGICOS ASOCIADAS A LAS ZONAS DE MÍNIMO DE OXÍGENO (ZMOS)", de la Sra. SONIA ELIZABETH YÁÑEZ TENORIO" y realizada bajo la Facultad de Ciencias Naturales y Oceanográficas, Universidad de Concepción, ha sido aprobada por la siguiente Comisión de Evaluación:

Dra. Pamela Hidalgo Díaz
Profesora Guía
Universidad de Concepción _____

Dr. Rodrigo De la Iglesia
Miembro de la Comisión Evaluadora
Pontificia Universidad Católica _____

Dr. Osvaldo Ulloa
Miembro de la Comisión Evaluadora
Universidad de Concepción _____

Dra. Nicole Trefault
Directora
Miembro de la Comisión Evaluadora
Universidad Mayor _____

Dra. Lidia Yebra
Evaluador Externo
Instituto Español de Oceanografía _____

Dr. Rubén Escribano
Director
Programa de Doctorado en Oceanografía
Universidad de Concepción _____

A mis padres, mis abuelas y mi marido.

AGRADECIMIENTOS

Deseo agradecer profundamente a todos quienes con su colaboración y apoyo hicieron posible el desarrollo y término de esta tesis.

En primer lugar, agradezco a los miembros de mi comisión de tesis. A mi profesora guía, Dra. Pamela Hidalgo, por apoyarme tanto académica como emocionalmente en estos más de 10 años de formación desde el pregrado hasta hoy, por confiar en mí y nunca ponerle límites a mi creatividad, por dejarme partir y esperarme en cada viaje, por ser mi referente. Al Dr. Rodrigo De la Iglesia, por permitirme desarrollar esta idea y abrirme las puertas de su laboratorio, por enseñarme, orientarme y avanzar conmigo todo el camino que significó esta tesis, con sus altos y bajos, sobretodo por su confianza. Al Dr. Osvaldo Ulloa y Dra. Nicole Trefault por su apoyo desde el proyecto de tesis. Al Dr. Rubén Escribano por ser siempre mi mentor.

También quiero agradecer al Dr. Kam Tang, quién a la distancia fue un gran apoyo, muchas gracias por su dedicación y sus muchas horas de reunión en línea durante este tiempo. Al Dr. David Elliott y Dr. Paul Bukabeckas, por recibirme en Richmond, Estados Unidos y enseñarme a modelar datos de mortalidad que por tanto tiempo busqué resolver. Al Dr. Ronnie Glud y Dr. Peter Stief, por recibirme en Odense, Dinamarca, abrir las puertas de su laboratorio, y transmitir, siempre, con una sonrisa la mejor disciplina para desarrollar experimentos que he obtenido hasta ahora.

Con mucho cariño, agradezco a mis compañeros y amigos del Grupo de Estudio en Ecología y Biodiversidad del Plancton, Pamela Fierro, Belén Franco, Guillermo Feliú, Paula Ruz y Richard Cobo. Por su colaboración en distintos aspectos académicos, pero por sobre todo, por su cariño, alegría y por su amistad infinita que persiste aunque ahora estemos esparcidos por el mundo. Agradezco también al grupo de trabajo del Laboratorio de Microbiología Marina de la PUC, especialmente a Benjamín Glasner, Isidora Morel y Leslie Daille por la enseñanza y paciencia en mi aprendizaje de las técnicas de análisis molecular, pero por sobre todo por su cariño y amistad.

También, deseo agradecer al equipo de extensión del Instituto Milenio de Oceanografía, especialmente a Bárbara Léniz por la posibilidad que me entregaron de socializar los conocimientos científicos a la comunidad de la región Metropolitana, donde pude aportar a

la divulgación de las ciencias como parte del rol social de los científicos. A Geraldine e Irlin.

Agradezco a las distintas fuentes de financiamiento que me permitieron estudiar este Doctorado: Beca de Doctorado Nacional CONICYT (CONICYT-PCHA/Doctorado Nacional/2013-21130213), Beca para postgrados del Instituto Milenio de Oceanografía, Proyecto de colaboración internacional CONICYT Chile-USA 2012-0006 de la Dra. Pamela Hidalgo. Agradezco a Red Doctoral en Ciencia, Tecnología y Ambiente, REDOC CTA. por financiar mi estadía en Center for Environmental Studies en Virginia Commonwealth University, Virginia, Estados Unidos.

Finalmente, no me alcanzan las palabras para expresar lo agradecida que estoy de mi familia y amigos. Agradezco profundamente a mi marido, Patricio, por todo su apoyo durante este largo proceso, pero principalmente por su infinito amor cada día, su paciencia y confianza depositada en mi en todo momento, por su impagable sonrisa al comenzar el día. A mi madre, Adriana, a mi padre, René, a mi viejo, Isaías, por ser mi inspiración, a mis hermanos Diego y Fredy, a mis hermanas Ignacia y María de los Ángeles, por su apoyo constante y amor incondicional.

CURRICULUM VITAE

Sonia Elizabeth Yáñez Tenorio
Nacida el 28 de mayo de 1987, en Coyhaique, Chile

2015−2018: Doctor en Oceanografía, Universidad de Concepción, Chile.

2010−2012: Magister en Ecología de Sistemas Acuáticos, Universidad de Antofagasta, Chile.

2005−2009: Biología Marina, Universidad de Concepción, Chile.

2005−2008: Licenciatura en Biología Marina, Universidad de Concepción, Chile.

AREAS DE INVESTIGACIÓN

Principal: Oceanografía Biológica

Secundaria: Ecología pelágica

PUBLICACIONES

Yañez S., Pors R., Hidalgo P., Stief P., and Glud R. (en prep). Degradation of sinking copepods, and to explore their importance for N cycling in oxygen depleted water.

Yañez S., Hidalgo P., Trefault N., Ulloa O & De la Iglesia R. (en prep). Bacterial community and decomposition of copepods carcasses associated to aerobic and anaerobic conditions.

Yañez S., Hidalgo P. & Tang K. (en prep). Mortality in dominant copepod species in the northern Chile (23°S) Humboldt Current Ecosystem.

Yañez S., Hidalgo P., Ruz P. & Escribano R. 2018. Live and dead zooplankton determined by Neutral Red Method in the upwelling zones of the Humboldt Current Ecosystem. Enviado a Marine Biology.

Yañez S., Hidalgo P., Ruz P. & Tang K. 2018. Copepod secondary production in the sea: errors due to uneven molting and growth patterns and incidence of carcasses. Progress in Oceanography. 165, 257-267. https://doi.org/10.1016/j.pocean.2018.06.008

Ruz P., Hidalgo P., Yáñez S., Escribano R. & J. Keister. 2015. Eggs Production and hatching success of *Calanus chilensis* and *Acartia tonsa* in northern Chile upwelling zone (23°S), Humboldt Current System. Journal of Marine System. 148: 200-212.

Yañez S., Hidalgo P. & R. Escribano. 2012. Mortalidad natural de *Paracalanus indicus* (COPEPODA, CALANOIDA) en áreas de surgencia asociada a la zona de mínimo oxígeno en el Sistema de Corrientes de Humboldt: Implicancias en el transporte pasivo del flujo de

carbono. Revista de Biología Marina y Oceanografía 47(2): 295-310.

Hidalgo P., Ferrari F., Pino P., Yañez S. & R. Escribano. 2012. Development of *Rhincalanus nasutus* (Giesbrecht, 1888) (COPEPODA: RHINCALANIDAE) from the Humboldt Currents System. Crustaceana. 85(9): 1025-1053.

EXPERIENCIA DOCENTE

2017– 2018 : Clases particulares de Química, Física y Biología de pre-grado como miembro asociado a Tutores Universidad de Chile

- Miembro del comité de tesis

2014: Srta. Carol González, Biología Marina, Universidad de Concepción. Tutor: Dra. Pamela Hidalgo.

2013: Sr. Danilo Soto, Biología Marina, Universidad de Concepción. Tutor: Dra. Pamela Hidalgo.

- Estudiantes de pregrado

2013: Srta. Marcela Andrea Henríquez Brunet, Biología Marina, Universidad Católica de la Santísima Concepción. Co-guía: Sonia Yañez. Tutor: Dra. Florence Tellier.

- Ayudantías en cursos de pregrado

2015: Curso Microbiología Marina, Pontificia Universidad Católica de Chile, Santiago, Chile.

2008-2009: Ecología de sistemas acuáticos y biodiversidad en sistemas pelágicos. Universidad de Concepción, Chile.

2014-2015: Zoología II y sistemas pelágicos. Universidad de Concepción, Chile.

- Profesor de pregrado

2010: Docente colaborador en la asignatura de Ecología Pelágica para la carrera de Ecología Marina (OC-723). I Semestre. Instituto de Investigaciones Oceanológicas, Universidad de Antofagasta, Chile.

CURSOS

2018. Open ECODIM Simposium. Microbial Symbiosis in the marine environment. Austral Summer Institute XVIII (ASI XVIII). 12 de enero, Universidad de Concepción.

2018. Trabajo y participación en el grupo Milenio-BCN/ATP en 2017.

2017. III Versión encuentro “Jóvenes Consciencia, pensando en Chile desde la Ciencia”. 27,28 y 29 de septiembre de 2017, Mantagua, Concón.

2016. Open ECODIM Symposium. Exploring the deepest and most mysterious Regions of the Ocean. Austral Summer Institute XVII (ASI XVII), 15 de enero, Universidad de Concepción, Chile

2016. IX Curso Internacional “Ecology and Diversity of Marine Microorganisms” (ECODIM), Austral Summer Institute (ASI). Estación de Biología Marina, Universidad de Concepción, Dichato, Chile. 11 al 30 de enero de 2016.

2014. ASI XIV. "Mulltidisciplinary satellite Oceanography : Platforms, data an applications". Professor Dr. Andrew Thomas, School of Marine Sciences at the University of Maine, USA. 6–10 Enero, 2014.

2012. ASI XII. "Coastal Upwelling Time Series in the Humboldt Current System (CUTS-HCS)". 9 – 13 Enero, 2012.

EXTENSIÓN Y DIVULGACIÓN CIENTÍFICA

2017 – 2018. Monitora en talleres del Océano, Explora Sur- Oriente y Poniente, Santiago de Chile. Instituto Milenio de Oceanografía.

2015: Monitora científica en Proyecto de Proyección al Medio Externo "Muestra Audiovisual Científica Itinerante (MACI)". IMO y PAR Explora Biobío.

2015: ¿Cómo afectará el cambio climático a la distribución de los copépodos? Colegio Salesiano, Concepción. Primer lugar categoría experimental, Feria Antártica Escolar. 5—8 de noviembre de 2015. Punta Arenas, Chile.

2015: Zoofertilizante: potenciador marino en la agricultura. Colegio Salesiano, Concepción. Tercer lugar categoría Enseñanza Media. XVIII Feria Nacional de la Ciencia y la Tecnología, Universidad del Bio-Bio, Concepción Chile.

CRUCEROS OCEANOGRÁFICOS

2018: Monitoreo estacional de zooplancton y variables oceanográficas en Valparaíso. Proyecto STOV. Escuela de Ciencias del Mar, Pontificia Universidad Católica de Valparaíso.

2013 – 2015: Monitoreo estacional de zooplancton y variables bio-oceanográficas en Bahía de Mejillones. Proyecto USA 2012 – 0006.

2010 – 2012: Muestreos mensuales de zooplancton y obtención de variables bio-oceanográficas en Bahía Mejillones. Proyecto FONDECYT 11090146**.**

ESTADÍAS DE INVESTIGACIÓN O ENTRENAMIENTO

2014 – 2018: Análisis biología molecular: extracción DNA, PCR y enzimas de restricción. Análisis de datos de secuenciación con software bioinformáticos. Laboratorio de microbiología marina. Pontificia Universidad Católica de Chile. Profesor tutor: Dr. Rodrigo De la Iglesia

2016 – 2017. The degradation of sinking copepods, and to explore their importance for N and C cycling in O_2 depleted waters: insight in biogeochemistry with particular focus on O_2 dynamics, CO_2 production rates, and DOC release rates within and from copepod carcasses. Profesor tutor: Dr. Peter Stief y Dr. Ronnie Glud. del Nordic Center for Earth Evolution (NordCEE) de University of Southern Denmark, Odense, Dinamarca. Diciembre 2016 – Marzo 2017.

2015. Zooplankton ecology with the goal of using population dynamics modelling to develop estimates of non-predatory mortality from data on abundances and live-dead composition of copepods from Mejillones (23°S), Northern Chile. Profesor tutor: Dr. David Elliott y Dr. Paul A. Bukaveckas del Center of environmental Studies en Virginia Commonwealth University, Richmond, Virgina, Estados Unidos. Enero – Marzo 2015.

Tabla de Contenidos

Índice de Figuras

Índice de Tablas

Resumen

Mortalidad y degradación bacteriana de copépodos pelágicos asociadas a las Zonas de Mínimo de Oxígeno (ZMOs)

Sonia Elizabeth Yáñez Tenorio
Doctorado en Oceanografía
Universidad de Concepción, 2018
Dra. Pamela Hidalgo D., Profesor Guía

La mortalidad es tal vez el parámetro menos conocido en la dinámica poblacional de copépodos. Las investigaciones tradicionales por mucho tiempo han asumido que la mortalidad es causada por la depredación, que regula los cambios en la abundancia de sus poblaciones. Las consecuencias de estas prácticas es que simplemente se ignore el estado vital de los animales *in situ*. Pero es simplemente ilógico creer que todos los copépodos *in situ* están vivos. Los copépodos y otros miembros del zooplancton están sometidos a mortalidad no-depredatoria, observada como la presencia de carcasas en el ambiente. Un meta-análisis realizado en base a datos de literatura indica que al menos un tercio de la mortalidad de copépodos *in situ* no puede de ninguna manera ser explicada por depredación. Por lo tanto, ignorar la presencia de estas carcasas también podría provocar errores en otros parámetros poblacionales porque los copépodos muertos obviamente no mudan, crecen o se reproducen. Tanto así, que un modelo de estudio demostró que ignorar, aunque sea en pequeñas magnitudes las abundancias de las carcasas y la mortalidad no-depredatoria podría llevar a proyecciones poco realistas del crecimiento poblacional. Recientes avances en métodos de tinción para distinguir entre individuos vivos y muertos en muestras de campo, junto los ajustes realizados para condiciones locales realizados en este estudio han abierto la oportunidad de realizar una cuantificación detallada de la abundancia de carcasas de copépodos en Sistema de Corrientes de Humboldt (SCH). Así, un alto porcentaje de mortalidad de copépodos asociados a las Zonas de Mínimo de Oxígeno (ZMOs) presentes en el SCH, aumenta la abundancia de carcasas de copépodos, que representan un substrato concentrado de materia orgánica (MO) para *hotspots* bacterianos. La descomposición por bacterias de la MO en las carcasas de copépodos marinos podría sustentar

una alta producción bacteriana a partir de procesos anaeróbicos en la ZMO, que no ocurren en la capa superficial oxigenada de la columna de agua. Esto, puede darnos indicios de una vía alternativa del flujo de MO y energía en la cadena trófica clásica en la ZMO, mostrando una relación directa entre copépodos y bacterias considerados hasta ahora como independientes. El presente estudio abordó desde la perspectiva experimental, la problemática asociada a las estimaciones de degradación y comunidad bacteriana de carcasas del copépodo *Acartia tonsa* y desde la perspectiva *in situ*, los potenciales efectos de las bajas concentraciones de oxígeno en la ZMO sobre las tasas de mortalidad de copépodos pelágicos dominantes en el SCH. Los resultados observados son 1) Usando datos de abundancia de copepoditos vivos y muertos, junto con la duración de estadíos y las tasas de muda, obtuvimos tasas de mortalidad depredatoria y no-depredatoria de las tres especies principales de copépodos marinos dentro del Sistema de Corriente de Humboldt (HCS) de Chile: *Paracalanus* cf. *indicus*, *Acartia tonsa*, y *Calanus chilensis*, y examinamos por primera vez su relación con factores ambientales. Las tasas de mortalidad total aumentaron con los estadíos de desarrollo en las tres especies. Las tasas de mortalidad total de C5 fueron 3-4 veces más altas que las de C1. En promedio, la depredación representó 53,7 de la mortalidad total en *P.* cf. *indicus*, 56,4% en *A. tonsa* y hasta un 65,2% en *C. chilensis*. Mientras tanto, la mortalidad no depredadora representa entre 34.8 al 46.3% de la mortalidad total, y esto refleja la importancia del estrés ambiental sobre el control de la dinámica poblacional de copépodos en el HCS; 2) Mediante el uso de experimentos de laboratorio, nosotros seguimos el curso de la degradación de carcasas del copépodo marino *A. tonsa*. Ambos tratamientos presentaron curvas de degradación diferentes, pero alcanzando máximos similares a las 36 hrs de incubación. Distintas comunidades bacterianas fueron observadas entre los diferentes tratamientos de los experimentos de degradación. Mediante el uso la secuenciación masiva del gen 16S se logró una identificación detallada de los miembros de la comunidad bacteriana asociada a la degradación de carcasas del copépodo marino *A.tonsa*. Los análisis filogenéticos permiten concluir que las carcasas de *A.tonsa* están asociados con tres phyla mayoritarios: Proteobacteria, Bacteroidetes y Verrucomicrobia. Vibrionaceae, Pseudoalteromonadaceae, Rhodobacteraceae, Flavobacteriaceae and Verrucomicrobiaceae fueron las familias de bacterias más abundantes. La presencia de los genes *nirK* y *nosZ*, marcadores de desnitrificación (producción N_2 y N_2O, respectivamente) fueron encontrados bajo condiciones anóxicas, principalmente asociados con el estadio final de degradación de las

carcasas de *A.tonsa*. Entonces, la investigación de bacterias asociadas a carcasas de copépodos es necesaria para entender la funcionalidad de estas carcasas y su degradación bacteriana como *hotspots* pelágicos que tienen implicancias biogeoquímicas en el ciclo del nitrógeno, a través de la desnitrificación; y 3) En otros estudios de laboratorio se evidenció que, la producción de amonio (NH_4^+) a partir de la degradación bacteriana de carcasas de *A. tonsa* fue observada en todos los tratamientos en donde el oxígeno estaba muy bajo y estaría siendo provocada por la mineralización del nitrógeno orgánico; la cual, podría potencialmente contribuir a la reducción disimilatoria del nitrato al amonio (DNRA, del ingles Dissimilatory nitrate reduction to ammonium). Además, aquellas carcasas de copépodos que sedimentan podrían pasivamente transportar nitrógeno orgánico hacia aguas profundas, donde al ser degradadas, este se podría liberar parcialmente como NH_4^+ y allí las bacterias de vida libre podrían utilizar ese NH_4^+ y oxidarlo a N_2. Por lo tanto, estas carcasas estarían contribuyendo, indirectamente, a procesos de pérdida de N, a través de la oxidación anaeróbica del amonio (anammox, del inglés ANaerobic AMMonium OXidation).

Así, la pérdida de N en el pélagos se ve potencialmente incrementada por las carcasas de copépodos tanto directamente a través de la producción de N_2 y N_2O, como indirectamente a través de la producción de NH_4^+ que podría contribuir a anammox. Entonces, dado que los copépodos son algunos de los organismos del mesozooplancton más abundantes en el océano, por lo que el ciclo anaeróbico del nitrógeno asociado con estos individuos podría tener grandes implicancias sobre los ciclos biogeoquímicos del océano, y la pérdida de nitrógeno orgánico desde los ecosistemas pelágicos.

Palabras claves: Mortalidad no-depredatoria, carcasas de copépodos, degradación de carcasas, comunidad bacteriana, remineralización, ciclos biogeoquímicos.

Abstract

Mortality and bacterial decomposition of pelagic copepods associated to Oxygen Minimum Zone (OMZs)

Sonia Yañez Tenorio

Ph. D in Oceanography

University of Concepción, 2018

Dra. Pamela Hidalgo D., Advisor

Mortality is perhaps at least constrained in copepod population dynamics. Traditional research for convenience assumes that mortality is driven solely by predation and therefore can be derived from changes in population abundances. A corollary to this practice is that field sampling simply ignores the live/dead status of the animals. It is, however, illogical to believe all copepods *in situ* are alive. Copepods and other zooplankton can suffer non-predation mortality that leaves behind carcasses. A meta-analysis of literature data suggests that up to one-third of *in situ* copepod mortality cannot be explained by predation. Ignorance of carcasses occurrence also causes errors to other population parameters because dead copepods obviously do not molt, grow or reproduce. A modelling study showed that ignoring even a small magnitude of carcasses abundance and non-predation mortality could lead to unrealistic projection of population growth. Recent advances in staining methods for distinguishing between live and dead individuals in field samples opened the opportunities to make detailed quantification of copepod carcasses in the Humbolt Current System (HCS). A high percentage of zooplankton mortality associated to Oxygen Minimum Zone (OMZ) present in the HCS, could increase the abundance of copepods carcasses, representing a concentrated pool of labile organic substrates for bacterial hotspots. Deceased copepods tend to sink because of higher density than surrounding water, but sinking is modulated by bacterial decomposition. Bacterial decomposition remineralizes carcasses' organic materials and could support high bacterial production from anaerobic processes into the OMZ, which do not occur in the oxygenated water of surface layers. This can serve as a hint for evaluating alternative pathways of material and

energy fluxes in the classic food web into the OMZ, presenting copepods and bacteria as directly connected functional groups. The present research, from an experimental perspective, dealt with copepod and bacterial composition of the calanoid copepod *Acartia tonsa* under oxic and anoxic conditions. From the *in situ* perspective, the non-predatory mortality of dominant pelagic copepods associated with the OMZ were studied in northern Chile within the HCS. The results found were the following: (1) Using detailed data of live/dead compositions, along with stage durations and molting rates, we derived both predatory and non-predatory mortality rates of the three main copepod species, *Paracalanus* cf. *indicus*, *Acartia tonsa* and *Calanus chilensis*, within the Chilean Humboldt Current System (HCS), and examined their relations with the environmental factors for the first time. Total mortality rates, calculated as the sum of average predatory and non-predatory mortality rates over the two annual cycles, increased with developmental stages in all three species. The total mortality rates of C5 were 3-4 times higher than those of C1. On average, predation accounted for 53.7 of the total mortality in P. cf. indicus, 56.4% in A. tonsa, and up to 65.2% in C. chilensis. Meantime, non-predatory mortality accounts for 34.8 to 46.3 % of the total mortality, and this reflects the importance of environmental stresses in controlling the copepod population dynamics within the HCS; (2) From laboratory experiments, we followed the course of decomposition of the carcass of the marine copepod *A. tonsa*. In oxic conditions, decomposition begun rapidly, later it remained relatively stable, and slowly increased towards the last hours of the incubations. In contrast, the decomposition process was much slower in the anoxic conditions, increasing greatly and quickly over the last hours of the incubations. Different bacterial communities among different treatments of decomposition experiments were found, whereas changes and succession were observed throughout both incubations. Using Illumina sequencing of the 16S rRNA gene we identified members of the bacterial community associated with carcass decomposition of *A. tonsa*. From the phylogenetic analysis, it could be concluded that the investigated copepod was associated with bacteria of three phyla: Proteobacteria, Bacteroidetes and Verrucomicrobia. Vibrionaceae, Pseudoalteromonadaceae, Rhodobacteraceae, Flabobacteriaceae and Verrucomicrobiaceae were the most abundant bacterial family. Expression of *nirK* and *nosZ* marker genes for denitrification (N_2 and N_2O production, respectively) were found to occur under anoxic conditions and showed an increase with time, mainly associated with the late stage of decomposition. Then, the investigation of bacteria associated to decomposition of copepod

carcasses is very important, due to the functioning of those carcasses as pelagic hotspots for bacterial decomposition may have implications in nitrogen cycling via denitrification; and (3) Another laboratory study showed that the production of NH_4^+ from decomposition of carcasses was observed in all treatments under low oxygen saturation levels and came from mineralization processes; thus, DNRA may contribute. Moreover, the production of NH_4^+ further suggests that sinking of copepods' carcasses passively transports bound nitrogen to depths where it could be partially released as ammonium and may fuel free-living anammox bacteria and thus contribute to pelagic N-loss by anammox.

Then, pelagic N-loss is potentially enhanced by carcasses of chitinous zooplankton directly through N_2 and N_2O production, as well as indirectly through NH_4^+ production that may contribute to anammox. As copepods are some of the most abundant mesozooplankton in the oceans, anaerobic nitrogen cycling associated with these animals may have large implications for biogeochemical cycling in the oceans, and the fixed-nitrogen loss from marine pelagic environments.

Keywords: Non-predatory mortality, copepod carcasses, carcasses decomposition, bacterial community, remineralization, biogeochemical cycles

1. INTRODUCCIÓN

1.1. Sistema de Corrientes de Humboldt y Zonas de Mínimo de Oxígeno

El Sistema de Corriente de Humboldt (SCH) se caracteriza por ser uno de los ecosistemas marinos más productivos del mundo, en donde el estrés inducido por el viento paralelo a la costa y con dirección hacia el Ecuador desplaza las aguas superficiales costa afuera, dando lugar al ascenso de aguas subsuperficiales más frías, ricas en nutrientes y pobres en oxígeno disuelto hacia la zona eufótica, sosteniendo elevados niveles de producción biológica en la capa superficial (Mann & Lazier 1991).

Debido a la surgencia, la alta productividad primaria en aguas superficiales y un alta demanda de oxígeno por la respiración aeróbica microbiana, el SCH presenta una Zona de Mínimo Oxígeno (ZMO) muy extensa y somera (Ulloa et al., 2013), asociada a la masa de Agua Ecuatorial Subsuperficial (AESS) (Escribano & Schneider, 2007). Las concentraciones de oxígeno disuelto observadas son $\leq$ 22 μM (0,5 mL L^{-1}) (Fig. 1.1).

El ambiente reductor de las ZMOs favorece el reciclamiento de nutrientes como fosfatos y silicatos, la biodisponibilidad de metales traza (*e.g.* Fe^{+2}) y la acumulación de carbono inorgánico disuelto (CID >2225 μmol kg^{-1}), constituyendo grandes reservorios de CO_2 (Paulmier et al., 2011). Las ZMOs se encuentran enriquecidas en nitrito (NO_2^-) y empobrecidas en nitrato (NO_3^-), siendo responsables del 50% del déficit relativo de nitrógeno inorgánico, debido a que este elemento es perdido como nitrógeno molecular (N_2) y óxido nitroso (N_2O) a través de procesos como la desnitrificación y la oxidación anaeróbica del amonio (ANAMMOX, del inglés ANaerobic AMMonium OXidation) (Ulloa & Pantoja, 2009; DeVries et al., 2013). De esta forma, las ZMOs cumplen un rol fundamental en los ciclos biogeoquímicos y en el reciclamiento de la materia orgánica (MO) (Paulmier & Ruiz-Pino 2009; Ulloa et al., 2012; Gilly et al., 2013).

La ZMO en el Pacífico Suroriental (PSO) se basa parcialmente de aguas viejas de bajo contenido de oxígeno que provienen de profundidades intermedias del Pacífico, que agotan su oxígeno fuera de las costas de México y Perú, y son advectadas dentro de la región a lo largo de la costa del Pacífico oriental (Schneider et al., 2006).

Las ZMOs además han sido descritas como áreas de baja biodiversidad de macrofauna

e inhóspitas para la mayoría de los recursos marinos comerciales (Ulloa & Pantoja, 2009). Contrario a esto, se observa que una alta diversidad de comunidades microbianas está asociada positivamente con ZMOs en la columna de agua (Stevens & Ulloa, 2008). Por lo que, las ZMOs tienen un papel clave en la estructuración de las comunidades marinas (Stewart et al., 2012), tales como, las zooplanctónicas y bacterianas del sistema pelágico.

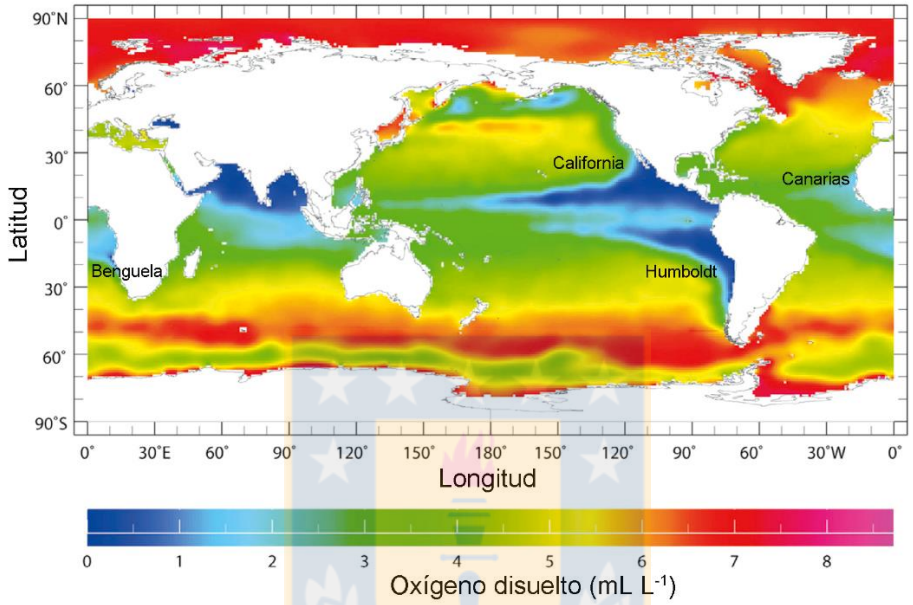

Figura 1.1.- Distribución del oxígeno disuelto (mL L^{-1}) a 200 m de profundidad. zonas de mínimo oxígeno (color azul) asociadas a los sistemas de surgencia de las corrientes de Canarias, Benguela, California y Humboldt. Datos obtenidos en IRI/LDEO Climate Data Library, Columbia University (http://iridl.ldeo.columbia.edu/). Datos originales desde World Ocean Atlas 2005 (Garcia et al. 2006), figura modificada desde Riemann et al 2010.

Las ZMOs constituyen verdaderos laboratorios naturales para el estudio de las variaciones del ecosistema pelágico ante problemáticas ambientales asociadas al cambio climático global, tales como la desoxigenación del océano (Paulmier et al. 2011). La variabilidad del sistema pelágico suele ser estudiada mediante respuestas fisiológicas del plancton, debido a que son considerados buenos bioindicadores de cambios en las condiciones oceanográficas, principalmente debido a sus cortos ciclos de vida y rápidas respuestas a cambios ambientales (Hays et al. 2005).

En la bahía de Mejillones (23°S) en el norte de Chile, el borde superior de la ZMO se ha definido con una concentración de oxígeno disuelto de 1 mL L^{-1}, siendo observado muy

somero en periodos de surgencia activa, inclusive por sobre los 20 m de profundidad (Hidalgo et al., 2005b). Particularmente, esta bahía, pertenece al sistema de surgencia de Punta Angamos, descrito como el centro de surgencia más productivo de la zona norte de Chile (Escribano, 1998; Escribano & Hidalgo, 2000; Sobarzo & Figueroa, 2001), con valores de productividad primaria que alcanzan los 1,070 g C m^{-2} $año^{-1}$ (Marín et al., 2003), albergando a su vez una alta abundancia y diversidad zooplanctónica (Escribano & Hidalgo, 2000; Hidalgo & Escribano, 2001).

1.2. Ecología del zooplancton en el SCH

Los copépodos son organismos de la subclase Copepoda y son, típicamente, uno de los componentes zooplanctónicos más abundantes en los océanos del mundo (Omori & Ikeda, 1984). Constituyen el taxón más importante entre los metazoos pelágicos marinos (Böttger-Schnack, 1995) siendo aproximadamente el 80% de la composición y abundancia del SCH (Escribano & Hidalgo 2000; Hidalgo & Escribano 2001; Escribano et al., 2007; Hidalgo et al., 2010), por lo que han sido ampliamente utilizados como grupo modelo para el estudio de estimaciones de producción zooplanctónica, principalmente a través de tasas vitales (*e.g.* tasas de crecimiento), para una mejor comprensión de la ecología de poblaciones y los factores que controlan la producción secundaria en el océano (Huntley & López, 1992; Hirst & Lampitt, 1998; Runge & Roff, 2000). Los copépodos utilizados en este estudio son las especies: *Acartia tonsa*, *Paracalanus* cf. *indicus y Calanus chilensis* (ver Fig. 1.2).

Figura 1.2: Fotografías de copépodos utilizados en este estudio. A) *Acartia tonsa. Créditos para Minh Vu desde http://www.impaq.ruc.dk/Pictures/. Acceso 26.04.2018.* B) *Paracalanus* cf. *indicus. Créditos para Moira Galbraith desde* http://www.marinespecies.org/photogallery. y C) *Calanus chilensis. Créditos para Paula Ruz.*

A.tonsa y *P*. cf. *indicus* son copépodos calanoideos de pequeño tamaño, su prosoma mide < 1.2 mm, y poseen distribución cosmopolita (Hidalgo & Escribano, 2001; Escribano *et al*., 2007, 2014), mientras que *C.chilensis* es de mayor tamaño, > 2 mm (Escribano et al., 2016) y corresponde a una especie endemica del norte de Chile (Escribano & Rodriguez, 1994, 1995; Escribano, 1998). Estas especies tienen un complejo ciclo de vida, con 13 estadios de desarrollo (Fig. 1.3). El primero es el huevo (estadio embrionario), que eclosiona en seis estadios naupliares (N1 – N6) y se desarrollan en seis estadios copepoditos (CI – CVI). El estadío final de copepodito (CVI), corresponde al estado adulto con dimorfismo sexual (separado entre machos y hembras) (Trujillo-Ortiz, 1986; Peterson, 1998; Hidalgo et al., 2012). El proceso de desarrollo de un estadío al subsiguiente es llamado "muda" y ocurre en todos los estadios de desarrollo, excepto en el final, el adulto.

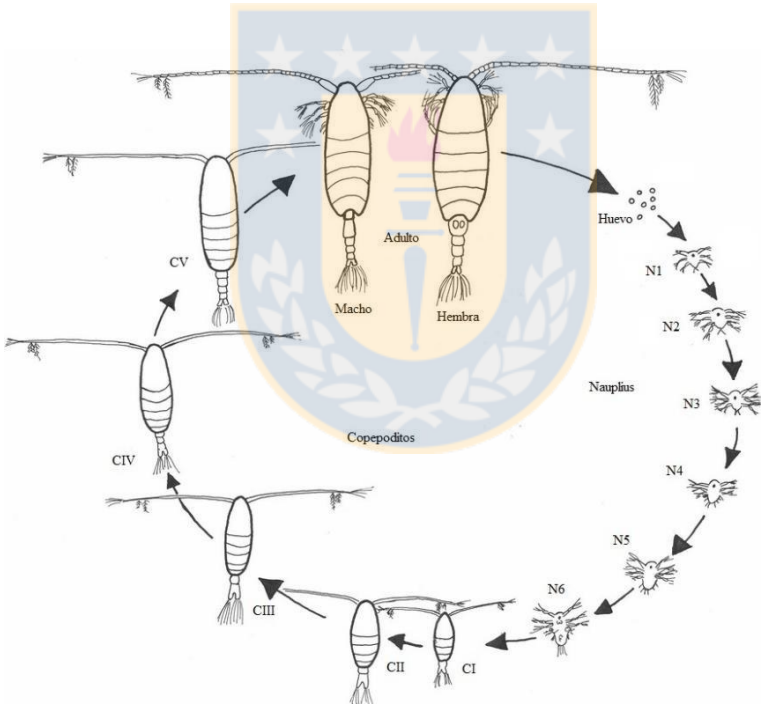

Figura 1.3. Ciclo de vida de un copépodo *(Fuente: http://www.st.nmfs.noaa.gov/copepod, último acceso 25 de abril de 2018).*

La alta variabilidad espacio − temporal del ambiente pelágico regula los patrones de distribución y las tasas de producción de estas especies de copépodos en el SCH. Las estimaciones de producción secundaria en la Bahía de Mejillones muestran un complejo ciclo de vida y diferenciado para cada especie.

El crecimiento de estos organismos ha sido descrito como dependiente tanto de la temperatura (Bèlehràdek, 1957; Fernández-Álamo & Färber-Lorda, 2006), como de la calidad y cantidad de alimento disponible (Hirst & Lampitt, 1998). Se ha demostrado que floraciones algales con baja calidad nutritiva u organismos tóxicos son capaces de reducir el crecimiento y la fecundidad en copépodos (Turner & Tester, 1997; Ianora et al., 1999; Poulet et al., 2007). Asimismo, procesos advectivos (Escribano, 1998), la intensidad de la surgencia (Escribano et al., 2012) y bajas concentraciones de oxígeno disuelto en la columna de agua pueden actuar como reguladores de la distribución, abundancia, producción (Roman et al., 1993; Stalder & Marcus, 1997; Manríquez et al., 2009; Hidalgo et al., 2010) y mortalidad zooplanctónica (Yañez et al., 2012; e.g. revisar capitulo siguiente).

1.3. Tasas de mortalidad no-depredatoria en copépodos planctónicos

La mortalidad sigue siendo el parámetro menos conocido y pobremente cuantificado de la dinámica poblacional del zooplancton (Ohman & Wood, 1995), dado que existe una incertidumbre en las estimaciones de las tasas de mortalidad debido a las inherentes dificultades para estimarlas *in situ*, tales como la distinción entre organismos vivos y muertos. Las investigaciones tradicionales por mucho tiempo han asumido que la mortalidad es causada por la depredación (Genin et al. 1995), y que es esta quién regula los cambios en la abundancia de sus poblaciones. Las consecuencias de estas prácticas es que simplemente se ignore el estado vital de las animales *in situ*. Pero es simplemente ilógico creer que todos los copépodos *in situ* están vivos. Los copépodos y otros miembros del zooplancton están sometidos a mortalidad no-depredatoria, observada como la presencia de carcasas en el ambiente (Tang et al., 2014).

Hoy en día, las carcasas, que son los copépodos muertos en la columna de agua, han sido observadas alrededor del mundo (Tang et al., 2009; Yañez et al., 2012, 2018; Martínez et al., 2014) debido al desarrollo de un método de tinción que está ahora disponible para distinguir entre organismos vivos y muertos en sistemas de aguas dulces, estuarios (Elliott & Tang, 2009; Tang et al., 2009; Martínez et al., 2014) y marinos (Elliott et al., 2013; Yañez et al., 2012, 2018; Martínez et al., 2014). Usando este método, se ha observado que en promedio el porcentaje de copépodos muertos puede llegar a ser superior al 50% del total de la

abundancia (Elliott & Tang, 2009; Tang et al., 2009; Yañez et al., 2012, 2018; Tang et al., 2014; Martínez et al., 2014).

La cuantificación de la abundancia de estas carcasas intactas, son estimaciones potencialmente utilizables para evaluar *in situ* la mortalidad no-depredatoria en el ambiente pelágico (Elliott & Tang, 2011). Las causas comunes de la mortalidad no-depredatoria de copépodos incluyen senescencia (Ceballos and Kiørboe 2011; Saiz et al., 2015), estrés físico y químico (Carpenter et al. 1974; Roman et al., 1993; Bickel et al., 2011), parasitismo (Kimmerer and McKinnon 1990; Burns 1985; Ohtsuka et al., 2004; Duffy et al., 2005) y/o factores relacionados con el alimento (Tsuda 1994; Tang et al., 2014).

Un meta-análisis realizado en base a datos de literatura indica que al menos un tercio de la mortalidad de copépodos *in situ* no puede de ninguna manera ser explicada por depredación (Hirst and Kiørboe 2002). Por lo tanto, ignorar la presencia de estas carcasas también podría provocar errores en otros parámetros poblacionales porque los copépodos muertos obviamente no mudan, crecen o se reproducen. Tanto así, que un modelo de estudio demostró que ignorar, aunque sea en pequeñas magnitudes las abundancias de las carcasas y la mortalidad no-depredatoria podría llevar a proyecciones poco realistas del crecimiento poblacional (Elliott and Tang, 2011). Así, las variaciones en las tasas de mortalidad del zooplancton pueden afectar drásticamente los resultados de los modelos de dinámica poblacional y de nutrientes-fitoplancton-zooplancton (Steele & Henderson, 1992; Proude et al., 2009a; Elliott & Tang, 2011), por lo que es, a menudo, necesario un ajuste *a posteriori* de las tasas de mortalidad junto a modelos predictores observacionales (Runge et al., 2004).

La formulación de este parámetro de mortalidad *in situ* en modelos poblacionales e individuales permite predecir las respuestas de la población ante los cambios ambientales (Ohman, 2012; Martínez et al., 2014). Es por ello por lo que, es un gran desafío para los ecólogos planctónicos estimar las tasas de mortalidad estadío-específico y sus causas para comprender la dinámica poblacional de copépodos (Tang et al., 2014) y su rol en el ecosistema del SCH (Yáñez et al., 2012).

1.4. Bacterias asociadas a las carcasas de copépodos

Las bacterias y los copépodos coexisten en el sistema pelágico, sin embargo, las investigaciones de ecología convencional los ven como dos grupos funcionales, leve e indirectamente relacionados (e.j Azam & Malfatti, 2007). Sin embargo, estudios recientes han

mostrado que su ocurrencia y función ecológica puede estar estrechamente relacionada (ej. Møller et al., 2007; Tang et al., 2009). Esta relación se observa en una fracción no menor de copépodos (11,6 – 59,8 %) que maduran fisiológicamente, envejecen, completan su ciclo de vida y finalmente mueren (esto es, mortalidad no-depredatoria). Estos organismos muertos, corresponden a las carcasas que se mezclan con el pool del detrito orgánico y particulado, quedando disponibles (como substratos orgánicos lábiles) para la utilización heterotrófica bacteriana en el ambiente pelágico (Tang et al., 2006; Bickel & Tang, 2010; Tang et al., 2014) (Fig. 4).

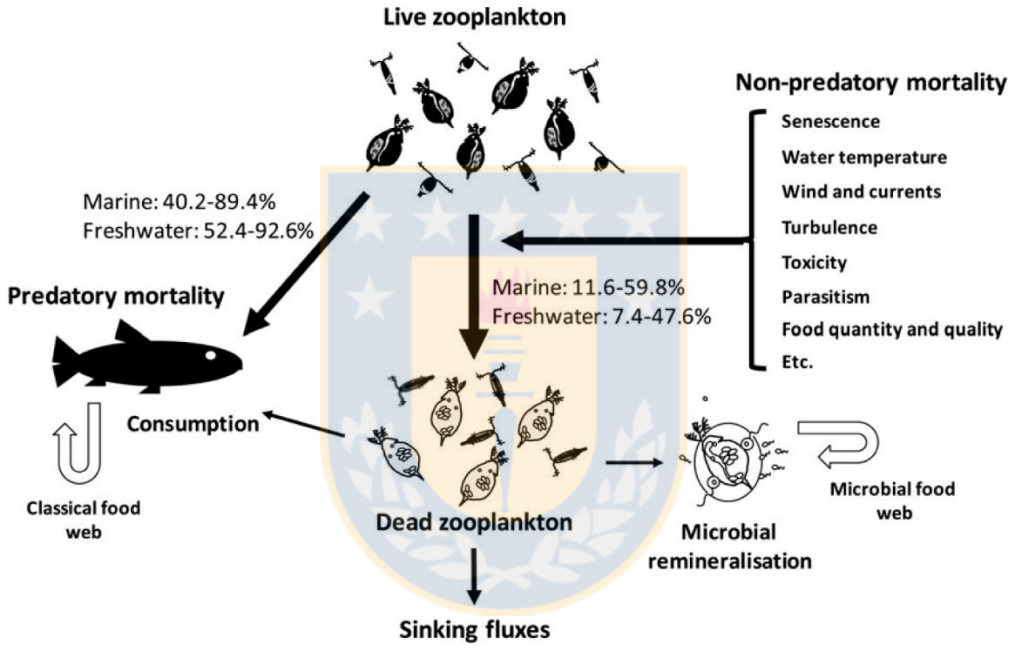

Figura 1.4. Relación entre las carcasas de copépodos y las bacterias en el ecosistema pelágico (Modificado desde Tang et al., 2014).

La abundancia bacteriana asociada con estas carcasas de copépodos puede ser incluso órdenes de magnitud mayores que en el ambiente acuático, indicando una colonización bacteriana activa en ellas, siendo las carcasas verdaderos microambientes para su desarrollo (Tang, 2005; Tang et al.,2014).

En el pélagos, las bajas concentraciones de oxígeno en las ZMOs han sido señaladas como el factor responsable del incremento de carcasas de copépodos en esta capa, principalmente en aquellas especies que no posean adaptaciones fisiológicas para habitar en

ella (Yañez et al., 2012). Este incremento puede ser un importante substrato orgánico lábil para comunidades bacterianas, formando puntos de alta biodiversidad (*hotspot*) microbiana en el océano (Tang et al., 2010), ya que naturalmente contienen bacterias, particularmente sobre la superficie de su cuerpo y dentro de sus intestinos (Nagasawa & Nemoto, 1988; Carman & Dobbs, 1997; Tang, 2005).

En relación con los cambios que pueda experimentar la comunidad bacteriana durante el tiempo de degradación, se ha observado que la comunidad de bacterias de las carcasas degradadas es muy diferente a la comunidad del agua del ambiente, indicando un cambio en la comunidad bacteriana con el inicio de la descomposición (Tang et al., 2006 a, b) (Fig. 5). Durante la descomposición, los cambios que pueda sufrir la comunidad bacteriana, tanto dentro como fuera de la carcasa, sugieren que pueden existir bacterias más eficientes que otras al degradar y explotar la MO de las carcasas, llevando a cambios importantes en la composición de la comunidad bacteriana (Tang & Elliott, 2014). Al final de la descomposición, mucho del tejido de las carcasas y las bacterias pueden desaparecer, quedando el exoesqueleto quitinoso y porciones traza de tejidos internos. Aunque las bacterias quitinolíticas existen o están presentes en lagos, sistemas estuarinos y marinos, la degradación de quitina por bacterias en la naturaleza tiende a ser muy baja. Por ejemplo, incubaciones *in situ* de purificación de partículas muestran una "tasa de pérdida" < 1% por día (Kirchner, 1995; Kirchman &White, 1999; Tang & Elliott, 2014).

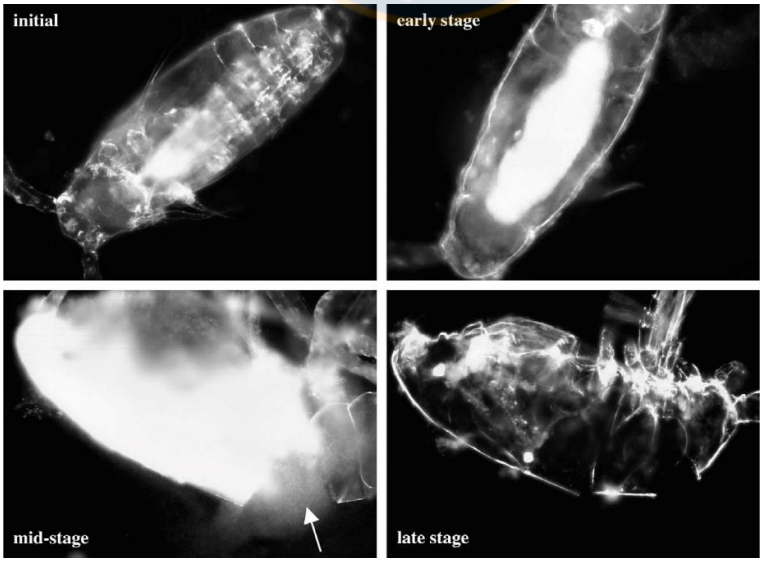

Figura 1.5. Degradación microbiana de carcasas de copépodos (Tang et al., 2006 b).

La degradación microbiana hidroliza y remineraliza el material orgánico de las carcasas en altas tasas, en este proceso, además, se reduce la densidad de las carcasas y cabe la posibilidad de que estas carcasas por boyantés neutra, permanezcan en la columna de agua (Tang & Elliott, 2014). En contraste, una rápida sedimentación ha sido reportada para *Acartia tonsa* de 60 m/día (Elliott et al., 2010) y para *Paracalanus* cf. *indicus* de 40 m/día (Yáñez et al., 2012) en el transporte pasivo de carbono hacia aguas profundas y el fondo marino (Sampei et al., 2009, Tang et al., 2014).

Así entonces, la descomposición bacteriana de MO desde carcasas de copépodos puede sustentar una alta producción bacteriana en la ZMO. Además, a diferencia de la degradación de los fitoagregados, que raramente es anóxico (Ploug, 2001), su degradación podría albergar procesos bacterianos anaeróbicos que no ocurren en otro lugar de la columna de agua (Bickel & Tang, 2010), por ejemplo, la capa superficial oxigenada. La descomposición y desintegración de las carcasas por bacterias heterótrofas podrían proveer una vía alternativa de regeneración de nutrientes (Harding, 1973; Bickel & Tang, 2010). Esto podría, además, influir en el anillo microbiano, por incorporación de estas carcasas, como Materia Orgánica Particulada (POM, del inglés Particulate Organic Matter) sujeta a la degradación bacteriana para la producción de DOM y permitirnos conocer el potencial desvío y flujo de materia y energía desde su ruta clásica (fitoplancton-zooplancton-peces), lo cual puede tener implicancias al momento de estimar producción secundaria en copépodos asociados a las ZMOs.

Estudios sobre la ocurrencia y destino de las carcasas de copépodos asociados a las ZMOs podrían, entonces, ser importantes para nuestra comprensión y conocimiento no solo de la mortalidad y dinámica poblacional de copépodos, sino que también conocer la relación que existe entre los copépodos, la cadena trófica microbiana y los flujos biogeoquímicos.

Estos antecedentes, nos permiten afirmar que las ZMOs tienen un rol clave en la estructuración de las comunidades marinas (Stewart et al., 2012), tales como copépodos y bacterias. Por ejemplo, incrementando la mortalidad de aquellos copépodos que no posean adaptaciones fisiológicas para habitar en ella. Siendo entonces, esta mortalidad evidenciada mediante la presencia de carcasas de copépodos, que al permanecer en la columna de agua puedan ser utilizadas como un substrato orgánico y degradadas por aquellas bacterias heterótrofas que habitan en el sistema pelágico y su ZMOs asociada. No obstante, aún existen

preguntas abiertas por responder. Entre ellas, poco se sabe sobre cuáles son las tasas de incorporación de las carcasas de copépodos al ambiente, o acerca de la función e identidad de las comunidades bacterianas asociadas a estas carcasas (Tang et al., 2006 a,b). Además, existe escaso conocimiento acerca de los cambios que pueden existir en la degradación de carcasas a diferentes concentraciones de oxígeno y las implicancias de ésta, tanto para la remineralización de MO y la cadena trófica microbiana como para los flujos de biogeoquímicos.

El presente estudio abordó desde una perspectiva ambiental, la problemática asociada a las estimaciones tasas de mortalidad de copépodos pelágicos y los potenciales efectos de las bajas concentraciones de oxígeno en las ZMOs y desde la perspectiva experimental, las influencias de esta capa sobre la degradación y comunidad bacteriana directamente asociada a carcasas de copépodos en el SCH. Finalmente, como estas perspectivas pueden influir en las estimaciones de producción secundaria de copépodos pelágicos en el Sistema de Corrientes de Humboldt.

2. HIPÓTESIS Y OBJETIVOS

Considerando que la presencia de las carcasas de copépodos está influenciada por las condiciones ambientales a las que estos organismos se ven expuestos; ambientes particulares como la ZMO frente al norte de Chile podrían estar influyendo no solo en las tasas de mortalidad no-depredatoria (incrementado la abundancia de carcasas), sino también en las tasas de degradación y composición de la comunidad bacteriana asociada a estas carcasas. Por esto, las hipótesis a someter a prueba en la presente investigación plantean que:

H1: “La disminución en la concentración de oxígeno en la columna de agua incrementa las tasas de mortalidad no-depredatoria de copépodos pelágicos, produciendo carcasas como material lábil para la degradación bacteriana en la Zona de Mínimo de Oxígeno del Sistema de Corrientes de Humboldt”.

H2: “La disminución en la concentración de oxígeno en la columna de agua incrementa las tasas degradación bacteriana de carcasas de copépodos en la Zona de Mínimo de Oxígeno del Sistema de Corrientes de Humboldt”.

H3: “La disminución en la concentración de oxígeno en la columna de agua modifica la comunidad bacteriana asociada a carcasas de copépodos pelágicos en la Zona de Mínimo de Oxígeno del Sistema de Corrientes de Humboldt”.

2.1. OBJETIVO GENERAL

Comprender el impacto de la disminución de la concentración de oxígeno en la columna de agua sobre la mortalidad de copépodos pelágicos, la degradación de sus carcasas y las comunidades bacterianas asociadas, en la zona de surgencia del norte de Chile en el SCH.

2.2. OBJETIVOS ESPECÍFICOS

1. Estimar las tasas de mortalidad no-depredatoria de copépodos pelágicos asociadas a la concentración de oxígeno en la columna de agua en la zona de surgencia del norte de Chile.
2. Determinar la degradación bacteriana de carcasas de copépodos pelágicos asociadas a la concentración de oxígeno en la columna de agua en la zona de surgencia del norte de Chile.
3. Determinar la composición bacteriana potencialmente responsable de la degradación de carcasas de copépodos pelágicos asociadas a la concentración de oxígeno en la columna de agua en la zona de surgencia del norte de Chile.

3. MATERIALES Y MÉTODOS

3.1. Área de estudio

La presente investigación se desarrolló en la Bahía de Mejillones (23°S) dentro del SCH. Esta región es conocida por su activa e intermitente surgencia costera (Marín et al., 1993) que les confiere a las aguas superficiales, masas de agua ricas en nutrientes, frías y pobres en oxígeno disuelto asociadas a la zona de mínimo de oxígeno (OMZ, del inglés Oxygen Minimum Zone) (Marín and Olivares, 1999), siendo estos eventos de surgencia los responsables de los altos niveles de producción primaria (Daneri et al., 2000) y pesquerías (Alheit & Bernal, 1993; Arcos et al., 2001).

Fueron realizados muestreos mensuales y estacionales durante los años 2010-2015 utilizados para el ajuste del método de rojo neutro. Los muestreos mensuales durante los años 2010 - 2011, fueron utilizados principalmente en las estimaciones de mortalidad de zooplancton. En estos periodos, se obtuvieron muestras ambientales (T, S, DO, Chla; ver sección 3.2) y zooplanctónicas desde 3 estaciones de muestreo, denominadas como St-1 (23º, 04 S – 70º, 25 W; zmáx = 60 m), St-2 (23º, 02 S - 70º 27 W; zmáx = 90m) y St-3 (23º, 03S - 70º 28 W; zmáx = 120m). Estas estaciones se distribuyen costa- océano, siendo la St-1 la estación costera, la St-2 representa la zona de transición, mientras que la St-3 es oceánica (Fig. 3.1). Adicionalmente a este muestreo, se obtuvieron muestras desde las estaciones St-2 y St-3 en una transecta costa-océano, las que fueron utilizadas para los experimentos de tasas de degradación y determinación de la comunidad bacteriana asociada a las carcasas desde el ambiente realizados durante los años 2015-2016.

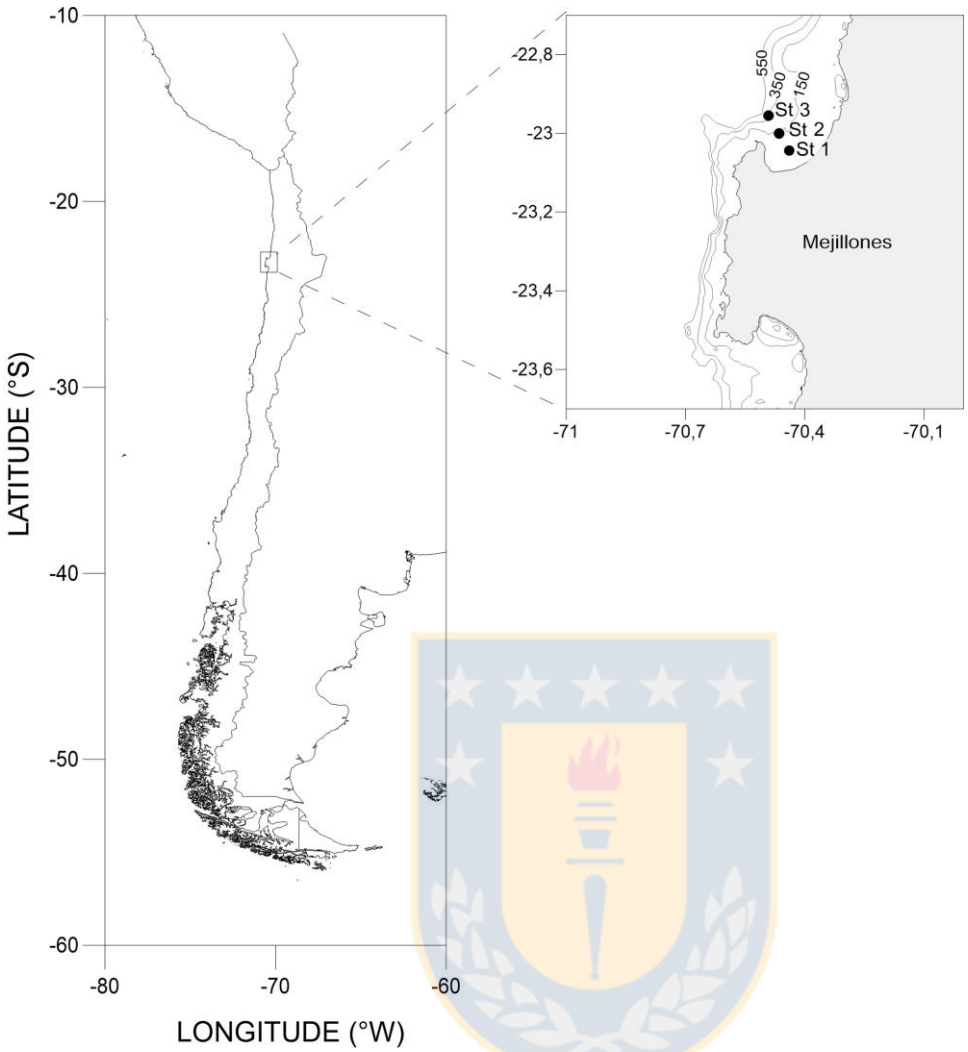

Figura 3.1 Área de estudio en la Bahía de Mejillones en el norte de Chile. Las estaciones de muestreo se encuentran indicadas por un punto negro.

Objetivo 1: Estimar las tasas de mortalidad no-depredatoria de copépodos pelágicos asociadas a la concentración de oxígeno en la columna de agua en la zona de surgencia del norte de Chile.

3.2. Trabajo de campo

La información ambiental fue obtenida mediante perfiladores oceanográficos autónomos tipo CTD (del inglés Conductivity, Temperature, Depth), modelo SeaBird 19, y una Sonda multiparámetro modelo YSI 200 Exo 2, que permitieron obtener información de conductividad, temperatura, profundidad y oxígeno disuelto en la columna de agua. También se colectaron

muestras de agua con una botella Niskin de 10 L, para estimar clorofila a dos profundidades (10, 50 m).

3.2.1. Muestra de zooplancton para estandarizar rojo neutro

La colección de zooplancton fue tomada desde diferentes periodos de tiempo en una ventana de 6 años, entre marzo del 2010 y marzo 2015, con un total de 141 muestras analizadas. En los muestreos, fueron utilizadas diferentes redes de zooplancton de 200 y 100 µm dependiendo de la plataforma y área de estudio, tales como Multinet, WP-2 y Tucker trawl, todas equipadas con fluorómetro.

Con la finalidad de ajustar el método de rojo neutro a las condiciones locales, además de examinar las muestras obtenidas de diferentes redes, también las muestras fueron incubadas en las siguientes condiciones: diferentes concentraciones de solución de rojo neutro (2, 4 y 6 mL). Diferentes tiempos de incubación (10 y 20 minutos). Las muestras obtenidas fueron transferidas a frascos etiquetados de 500 mL, e inmediatamente fueron tratadas con el método de rojo neutro (Elliott & Tang, 2009; modificado por Yañez, 2009 y de Yañez et al., 2012, 2018 para condiciones locales). Brevemente, cada muestra fue incubada con 2-4 mL de una solución de rojo neutro (0,5 % p/v) por 10-20 minutos. Posteriormente, las muestras teñidas fueron concentradas y enjuagadas con agua de mar filtradas para remover el exceso de tinción, inmediatamente fueron preservadas con formalina neutralizada con acetato de sodio al 4%. En el laboratorio fueron almacenadas en condiciones de oscuridad para posteriormente ser analizadas. En el laboratorio, las muestras fueron enjuagadas para quitar el exceso de formalina, y luego fueron analizadas agregando aprox. 0,3 mL de ácido acético ($C_2H_4O_2$) 1M para activar el color de la tinción. Primero, testeamos el efecto de la preservación y almacenamiento sobre la tinción de la muestra, tomando 10 mL de submuestra desde un frasco aleatorio por un periodo de 3 a 6 meses. Bajo un estereoscópico óptico (20x y 40x), se identificaron y cuantificaron organismos de algunos grupos de zooplancton: huevos, nauplios, copepoditos y adultos de especies dominantes de copépodos (< 4 mm), hidromedusas, cladóceros, ostrácodos, apendicularias, larvas de peces y quetognatos. Los organismos vivos fueron reconocidos de color rojo y aquellos no teñidos o incoloros como organismos muertos.

3.2.2. Muestras de zooplancton para estimaciones de mortalidad

Los copépodos fueron recolectados con arrastre vertical desde la capa superficial oxigenada (0–30 m de profundidad) usando una red tipo WP-2 (con copo no filtrante) de 200 micras de apertura de malla (50–cm de apertura de boca), equipada con un fluorómetro.

Las muestras obtenidas fueron transferidas a frascos etiquetados de 500 mL, y fueron tratadas con el método de rojo neutro siguiendo el protocolo ajustado a las condiciones locales (descrito en la sección 3.2.1). En el laboratorio, y bajo un estereoscópico óptico (20x y 40x), se identificaron y cuantificaron los estadios de copepoditos y adultos de las especies de copépodos dominantes: *Acartia tonsa*, *Paracalanus* cf. *indicus* y *Calanus chilensis*. Los organismos vivos /muertos fueron identificados y cuantificados y estandarizados a ind. m^{-3}, esto con el fin de poder estimar las tasas de mortalidad no-depredatoria de copépodos en la zona de estudio (ver sección 3.4).

3.2.3. Muestra de copépodos para experimentos de tasas de desarrollo

Los copépodos fueron recolectados mediante arrastre oblicuo con una red WP-2 sobre los 50 m de profundidad desde las St-3 a St-3. Las muestras fueron diluidas en agua de mar y transportadas al laboratorio dentro de 2 horas. Adicionalmente, una muestra de agua de mar fue recolectada con una botella Niskin a 10 m para la incubación.

3.3. Trabajo en laboratorio

3.3.1. Estimación del tiempo de Duración de Estadios.

En las especies de copépodos en estudio *P.* cf. *indicus, A. tonsa y C. chilensis*, la duración de estadios ha sido estudiada en laboratorios y se ha encontrado que varía por estadío, y que podría depender de la temperatura y la disponibilidad y calidad del alimento (Kimmerer and McKinnon, 1989; Peterson 2001; Giraldo et al., 2002; Escribano 1998; Vargas et al., 2010).

En este estudio se estimó la duración de estadios temperatura-dependiente usando la equación de Bèlehràdek (1935):

$$Di = a_i (T - \alpha)^b \qquad (1)$$

Donde T es la temperatura in C°, a_i es el tiempo de desarrollo (días, se determinó desde experimentos de tasas de desarrollo, ver sección 2.3.2), y los parámetros α y b fueron estimados mediante una regresión no lineal de mínimos cuadrados (función *nls* en el programa R).

3.3.2. Experimentos de tasas de desarrollo

Los experimentos de tasas de desarrollo en copépodos están basados principalmente en la presunción que los individuos recién capturados y mantenidos en incubaciones cortas (horas) manifiestan tasas de desarrollo y crecimiento similares a aquellas *in situ* donde han sido capturado (Harris, 2000). Básicamente, la ocurrencia de mudas y la duración de los estadios se determinan a partir de los cambios observados en la frecuencia de aparición de estadios consecutivos en el transcurso del desarrollo hasta el estadio adulto. El tiempo de desarrollo hasta un determinado estadio se define como el intervalo entre el inicio del experimento y el momento cuando el 50% de la cohorte ha mudado al estadio, mientras que la duración queda determinada por el intervalo entre el tiempo de desarrollo hasta el estadio y el correspondiente al estadio subsiguiente.

Desde los muestreos de zooplancton vivo, los organismos fueron identificados y separados por estadios para las actividades experimentales. Se realizaron incubaciones de 30 individuos por cada estadío en agua de mar filtrada a temperatura controlada de 15°C. Los organismos que se incubaron fueron seleccionados de acuerdo su estado de condición en cuanto a su capacidad natatoria, pigmentación, cuerpos y antenas completas. Luego, cada 24 h, los estadios iniciales, subsecuentes, mudas y muertos fueron cuantificados. En total, fueron realizados 29 experimentos con *P*. cf. *indicus*, 42 experimentos con *A. tonsa* y 31 experimentos *con C.chilensis*.

Las estimaciones de cambios en la frecuencia de estadios durante las actividades experimentales, permitieron componer la función que describe la tasa de muda (*MR*):

$$MR = ((N_i - N_{i+1})/(t/24) \quad (2)$$

donde *MR* es la tasa de muda (1/d) , *t* es el tiempo (*d*), *i* y *i+1* son los estadios iniciales y subsecuentes, descontados los organismos muertos.

La tasa de desarrollo corresponde entonces, a la tasa de individuos (obtenida desde *MR*) que van ingresando en cada estadio de la población durante la escala diaria. Esto es, el número de individuos reclutados a la población durante el período de muestreo.

Por lo tanto, el tiempo de desarrollo (α, d) se estima con la siguiente ecuación,

$$ai = 1/MR \quad (3)$$

3.4. Estimaciones de tasas de mortalidad no-depredatoria de copépodos

Las estimaciones de tasas de mortalidad no-depredatoria (m, d^{-1}) de estadios de copepoditos en este estudio se calcularon desde el método aproximaciones de tablas de vida vertical (VLT, del inglés Vertical Life Tables), modificado desde Aksnes et al., (1997) por Elliott and Tang, (2011). En este método, ambos, copépodos vivos y carcasas intactas son tratados como sobrevivientes de la mortalidad depredatoria. La tasa de mortalidad depredatoria es estimada utilizando ecuaciones de VLT modificadas. La tasa de mortalidad no−depredatoria, entonces, es calculada como la diferencia entre el total y las tasas de mortalidad depredatoria, ambos derivados desde cálculos de VLT.

Los parámetros principales son: i) proporción de abundancia ($ind.m^{-3}$ organismos vivos y muertos por el total (π); ii) duración de estadios (D_i, desde la ecuación de Belehràdek) y iii) tiempo de residencia de las carcasas en el agua (τ, en inglés carcasses turnover time) (Elliott and Tang., 2011); y iv) tasas de mortalidad depredatoria (δ, d^{-1}):

i) Proporción de organismos vivos y muertos (π): Este parámetro fue estimado desde la identificación y cuantificación de los estadios de copepoditos (C1−C5) y adultos vivos y muertos (carcasas). La identificación de organismos vivos y carcasas se realiza gracias a la aplicación del método de rojo neutro (ver sección 3.2.1). Los datos fueron estandarizados a $ind.m^{-3}$ y luego calculadas sus proporciones para organismos vivos vs total y organismos muertos vs total. Utilizadas luego en la ecuación (5) y (6).

ii) Tiempo de duración de estadios (D_i, días): Estimaciones del tiempo de duración de estadios (D_i, para el estadío i, d) son requeridos en el modelo como *"inputs"* para el método de estimaciones de tasas de mortalidad no-depredatoria y fueron calculadas usando la ecuación (1) (ver sección 3.3.1) desde experimentos de laboratorio (sección 2.3.2) para las tres especies de estudio.

iii) Tiempo de residencia de las carcasas en el agua (τ): Este parámetro fue estimada de acuerdo con Elliott et al., (2010), quién encontró que la turbulencia *in situ* en la bahía de Virginia podría retener carcasas en la columna de agua por un tiempo determinado. Sin embargo, la sedimentación de estas carcasas puede tardar debido a que la degradación

microbiana reduce las carcasas de copépodos a una fina capa de quitina (8,35 % del peso seco inicial; Cauchie et al., 1997), y fue calculado como la siguiente ecuación:

$$\tau = e^{\left(\frac{3,83}{4,166\left(1-e^{-0,008T}\right)+0,046DO}-1,39\right)} \quad (4)$$

Donde la tasa de residencia o turnover time (horas desde la muerte hasta capa de quitina mencionada anteriormente). T es la temperatura y DO es el oxígeno disuelto del agua. Entonces la ecuación (4) predice el tiempo de residencia de una carcasa de copépodo (días, meses, años), a T y DO ambiental.

iv) Tasas de mortalidad depredatoria (δ, d^{-1}): La fórmula utilizada para estimar este parámetro relaciona la información entre estadios sucesivos (*i* and *i*+1) a través de la ecuación de la razóo entre sus abundancias (A_i y A_{i+1}) observados en el mismo tiempo y locación, la razón de reclutamiento desde sus respectivos tiempos de duración de estadíos (D_i y D_{i+1}), asumiendo una tasa de mortalidad constante dentro de los dos estadios.

$$\frac{Ai}{Ai+1} = \frac{1-\pi_1 e^{(-\delta i Di)}-\pi_2 e^{(-\delta i \tau)}}{\pi_1 e^{(-\delta i Di)}\left[1-\pi_3 e^{(-\delta i Di+1)}-\pi_4 e^{(-\delta i \tau)}\right]} \quad (5)$$

$$\frac{Ai}{Aq} = \frac{1-\pi_1 e^{(-\delta i Di)}-\pi_2 e^{(-\delta i \tau)}}{\pi_1 e^{(-\delta i Di)}\left[1-\pi_4 e^{(-\delta i \tau)}\right]} \quad (6)$$

Donde π_1 y π_2 son la proporción de individuos vivos y muertos, respectivamente, en el estadío *i*; π_3 y π_4 son la proporción de individuos vivos y muertos, respectivamente, en el estadío *i+1*; τ es la duración de carcasas de copépodos en la columna de agua (τ) y δ es la tasa de mortalidad depredatoria.

Para esta tesis, la ecuación (5) fue utilizada para estimar la tasa mortalidad depredatoria (δ, d^{-1}) de los estadios C1-C4. En el caso de que el estadío sucesivo es un adulto (A_q, el estadío adulto, no muda) la ecuación utilizada fue la (6).

Las tasas de mortalidad no pueden ser calculadas directamente usando las ecuaciones (5) y (6), por lo que son necesarios métodos numéricos para resolverlos. El software R posee una rutina para encontrar el algoritmo necesario, las funciones en *fzero* fueron entonces utilizadas para resolver las ecuaciones de tasas de mortalidad iterativamente, δ, en las ecuaciones (5) y (6).

v) Mortalidad total (*mt*, d^{-1}): Este parámetro fue estimado una vez estimadas las razones de

las abundancias (A_i y A_{i+1}), duración de estadios (D_i y D_{i+1}) y mortalidad depredatoria (δ, d^{-1}) aplicados a la siguiente ecuación:

$$Mortalidad\ total\ (mt, d^{-1}) = \mathrm{Ai} + 1\ (\frac{e^{(\delta iDi)} - 1}{1 - e^{(\delta iDi+1)}}) \quad (7)$$

Una vez calculadas las tasas de mortalidad total y depredatoria, las tasas de mortalidad no-depredatoria fueron estimadas como la diferencia entre las tasas mortalidad total y la depredatoria. Esta aproximación de tasa de mortalidad no-depredatoria solo fue aplicada para aquellas muestras donde los valores de mortalidad depredatoria fueron positivos.

Objetivo Específico 2: Determinar la degradación bacteriana de carcasas de copépodos pelágicos asociadas a la concentración de oxígeno en la columna de agua en la zona de surgencia del norte de Chile.

3.5. Trabajo de campo

3.5.1. Muestra de zooplancton para experimentos

Para las actividades experimentales, se obtuvieron 3 muestras de zooplancton vivo entre las estaciones St-2 y St-3 (Fig.2), aproximadamente a 7-8 millas náuticas desde la costa. Se realizaron arrastres oblicuos sobre los 30 metros de profundidad con una red WP-2 (200 micras), sin copo filtrante, por un tiempo aproximado de 15 minutos de manera de obtener una muestra concentrada. Las muestras fueron cuidadosamente transportadas en neveras con ice pack para mantener la temperatura del medio, se obtubo agua de mar con una botella oceanográfica antes mencionada. Adicionalmente, se realizó un lance de CTDO hasta los 90 metros para obtener los gradientes de temperatura, salinidad y oxígeno disuelto. Las muestras fueron almacenadas en una nevera y transportadas al laboratorio en un tiempo de 1 hora.

3.6. Trabajo en laboratorio

3.6.1. Experimentos degradación de carcasas

En el laboratorio, las muestras de zooplancton fueron mantenidas en la nevera, y se esperó un tiempo de manera que el zooplancton muerto decante al fondo del recipiente y el vivo se mantenga en superficie nadando. El zooplancton vivo fue cuidadosamente removido con una pequeña malla. Luego, el agua de la nevera fue filtrada por un tamiz de 200 µm. Entonces, y con

el fin de obtener carcasas frescas, el zooplancton vivo fue expuesto brevemente (10 seg aproximadamente) a una solución de ácido acético al 10%, posteriormente el exceso de ácido acético fue removido, enjuagando las carcasas varias veces con agua de mar filtrada 0,2 micras.

Los experimentos de degradación bacteriana fueron realizados bajo condiciones de laboratorio con temperatura y oxígeno disuelto controlado. Las incubaciones fueron realizadas en agua de mar filtrada a 0,2 micras en botellas Duran Shot de 250 mL previamente cebadas con ácido clorhidico (HCL) al 1%. El oxígeno disuelto en el agua fue medido con un sensor óptico OXY - 4 Optode PreSens (nivel de detección 0,1 μLL^{-1}) y controlado mediante la inyección de nitrógeno gaseoso (N_2). El sensor de oxígeno fue previamente calibrado usando dos puntos de calibración, 100% y 0% de saturación, siguiendo las instrucciones del fabricante. Se obtuvieron mediciones de OD al inicio y al final de las incubaciones. La temperatura fue controlada con un termostato y un baño termorregulado a 15ºC. Esta temperatura seleccionada corresponde a la temperatura *in situ* promedio de la columna de agua durante el periodo de estudio. Se realizaron 2 niveles de concentración de oxígeno disuelto, en condiciones anóxicas (0 µM o 0 mL L^{-1}) y normóxicas (378−45 µM o 8−1 mL L^{-1}).

Los individuos de la especie *A. tonsa* fueron separados bajo lupa estereoscópica SMZ 1000 zoom stereomicroscope (Nikon) y se formaron grupos de 35 individuos por botella de incubación en triplicado, para ambas condiciones de concentración de oxígeno disuelto. Posteriormente las botellas fueron rebalsadas con agua desoxigenada/saturada en oxígeno y tapadas (sin dejar burbujas) para realizar la incubación y obtener la tasa de degradación cada 6 horas por 36 horas. Pasadas 6, 12,18,24,39 y 36 horas, el contenido de la botella fue filtrado con un tamiz de 23 micras. 25 individuos fueron separados y congelados en nitrógeno líquido (-195,8ºC) y luego almacenados a -20°C. Los 10 restantes fueron separados para análisis de microscopía (ver sección 2.5.5).

3.6.2. Microscopía

Desde los experimentos de tasas degradación 10 individuos fueron analizados y fotografiados bajo lupa estereoscópica modelo CH2 marca Olympus para estimaciones de tiempo de degradación.

3.7. Estimación de degradación

Las tasas de degradación fueron estimadas de acuerdo con el tiempo de incubación de cada botella y el estado de degradación de las carcasas. El estado de degradación se estimó utilizando un software para edición de imágenes, que permite obtener una imagen con contraste. Esta imagen editada, es marcada asimilando una esfera, de manera de estimar el área de esta esfera degradada en el tiempo (Fig. 3.2).

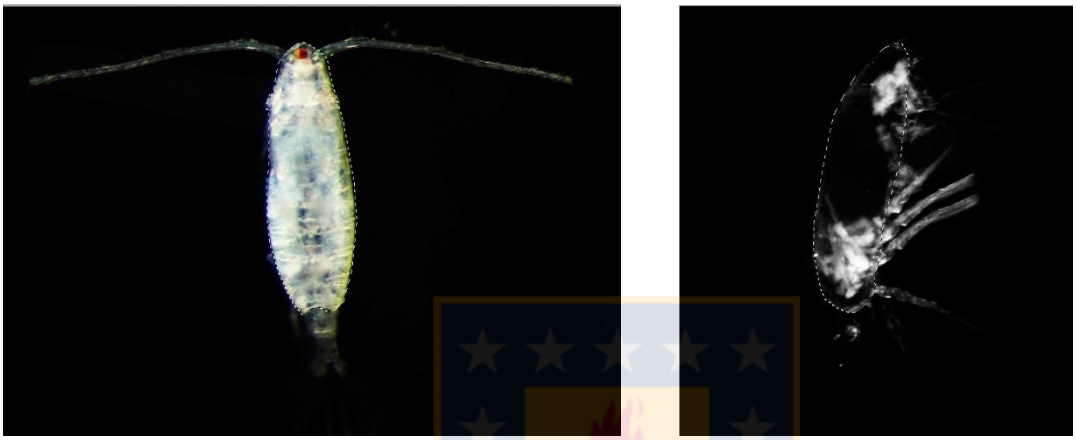

Figura 3.2: Análisis de imágenes para obtener aproximaciones de tasas de degradación de carcasas de copépodos, la línea discontinua representa el total de área seleccionada. A) Carcasa con 0 -30% del prosoma degradado; B) carcasa con 30-70% del prosoma degradado.

Objetivo 3: Determinar la composición bacteriana potencialmente responsable de la degradación de carcasas de copépodos pelágicos asociadas a la concentración de oxígeno en la columna de agua en la zona de surgencia del norte de Chile.

3.8. Trabajo de campo

3.8.1. Muestra de zooplancton para análisis moleculares

Para el análisis de la composición bacteriana inicial asociada a carcasas de copépodos. 25 carcasas fueron separadas desde la muestra de zooplancton tomada en terreno (ver sección 3.5.1), transferidas a un tubo eppendorf estéril de 2mL, preservadas en nitrógeno líquido (-198°C), para posteriormente ser almacenadas a -20ºC.

Adicionalmente, para el análisis de la composición bacteriana asociada a la degradación de las carcasas de copépodos, fueron también tomadas 25 carcasas de copépodos desde los experimentos de tasas de degradación (ver sección 3.5.4), transferidas a un tubo eppendorf estéril de 2 mL, preservadas en nitrógeno líquido (-198°C), para posteriormente ser

almacenadas a -20ºC.

3.9. Trabajo en laboratorio

3.9.1. Análisis de extracción de ADN

Las extracciones de ADN total de las bacterias asociadas a carcasas de copépodos provenientes del experimento de degradación fueron extraídas siguiendo el protocolo del Kit de extracción NucleoSpin Tissue XS (Macheley-Nagel). Para verificar la integridad del ADN extraído, las muestras fueron observadas en un gel de agarosa al 1%, teñido con bromuro de etidio y visualizado en un transiluminador de luz ultravioleta. El ADN fue concentrado utilizando SpeedVac. Finalmente, la calidad y cantidad de ADN fue chequeado en un espectofotómetro Nanodrop ND-1000 y en un fluorómetro V 1.27 (Invitrogen).

3.9.2. Comunidad bacteriana asociada a carcasas de copépodos

Para evaluar la composición de las comunidades bacterianas asociadas a carcasas de copépodos, las muestras obtenidas en la sección 3.7.2 fueron enviadas para ser analizadas vía secuenciación masiva dirigida (Illumina taq-sequencing) en la plataforma Fluidigm (https://www.fluidigm.com) en Functional Genomics Laboratory de University of Illinois. Allí se amplificó la región V4 del gen 16S rRNA utilizando los partidores 349F-806R. Los amplicones fueron secuenciados utilizando Illumina MiSeq.

3.9.3. Genes funcionales

Para estudiar la presencia de genes funcionales, se obtuvieron amplicones desde el mismo ADN templado utilizado para el gen 16S. Los partidores utilizados para cada gen fueron los siguientes: *nosZ*, 1F-1R, *nirK*, 876F-1040R; *amoA*: 1F-2R; petbf-petbr; RbIIf-RbIIr. Los genes elegidos fueron óxido nitroso y nitrito de reductasa (*nosZ* y *nirK*, respectivamente); transferencia de electrones en metanógenos, citocromo b6 (*petB*); nitrificación, amonio-monooxidasa (*amoA*); y fijación de CO_2, Ribulosa-bifostato (*rbcS*).

3.10. Análisis de datos

Las secuencias obtenidas desde el análisis de secuenciación masiva, fueron analizadas con el Software MOTHUR (http://www.mothur.org/wiki/MainPage), el cual permite detectar, reducir y eliminar los errores asociados a la secuenciación, las secuencias de baja calidad y las quimeras. Luego, las muestras fueron clasificadas taxonómicamente comparando la data obtenida con la base de datos SILVA132. Finalmente, las secuencias que no pueden ser

clasificadas fueron eliminadas; con las secuencias restantes se armaron las OTUs (del inglés, Operational Taxonomic Unit).

Debido a la gran cantidad de datos obtenidos desde la secuenciación masiva dirigida (Taq-seq), fue necesario analizarlos con el uso de herramientas estadísticas multivariadas. Para el análisis exploratorio y visualización de las muestras se utilizó un análisis de cluster y el escalamiento multidimensional no paramétrico (nMDS). El análisis de cluster agrupó las muestras en categorías, basado en las abundancias de OTUs dentro de la muestra de tiempo de degradación.

El Análisis de Similitud (ANOSIM) fue utilizado para probar estadísticamente si existen diferencias entre los grupos visualizados en el análisis nMDS. El análisis de Porcentaje de Similitud (SIMPER) fue utilizado para evaluar que taxones fueron los mayormente importantes y responsables de las diferencias observadas entre los grupos de muestras. Para el análisis de todas estas variantes se utilizó el software PRIMER 6 (Primer-E, Plymouth, UK).

4. RESULTADOS

4.1. CAPÍTULO 1: Copépodos pelágicos en el Sistema de Corrientes de Humboldt: aproximaciones de tasas de mortalidad

4.1.1. Live and dead zooplankton determined by the Neutral Red Method

Artículo enviado: Marine Biology (MABI-D-18-00372)

Sonia Yañez

Doctorado en Oceanografía

Universidad de Concepción

Resumen

Se describe un protocolo estandarizado para recolectar, teñir y analizar zooplancton marino desde muestras obtenidas en terreno, con el fin de determinar *in situ* los organismos vivos y muertos. El protocolo fue testeado utilizando tres redes de zooplancton diferentes en dos sitios de surgencia en el Sistema de Corrientes de Humboldt frente a Chile. Este protocolo fue aplicado a un grupo de zooplancton tales como huevos, estadios naupliares y copepoditos de copépodos más en detalle. Nosotros recomendamos el uso de este simple protocolo *in situ* para la determinación del estatus vivo/muerto de grupos comunes de zooplancton en muestras marinas. Este avance en el método de tinción permite a los investigadores acceder a la rápida distinción entre individuos vivos y muertos en terreno, otorgando la oportunidad de obtener en detalle la cuantificación de carcasas de zooplancton. Acceder a esta cuantificación de carcasas en terreno, podría ayudar a los estudios de mortalidad natural de zooplancton asociado a la variabilidad oceanográfica.

Palabras claves: Método de rojo neutro, mortalidad no-depredatoria, zooplancton

Live and dead zooplankton determined by the Neutral Red Method

Sonia Yáñez[1,2], Pamela Hidalgo[2], Paula M. Ruz [3,2], Rubén Escribano[2]

1. Graduate Program in Oceanography, Department of Oceanography, University of Concepción, Chile
2. Department of Oceanography and Millennium Institute of Oceanography, Faculty of Natural Science and Oceanography, University of Concepcion, P.O. Box 160 C, Concepción, Chile.
3. Escuela de Ciencias del Mar, Pontificia Universidad Católica de Valparaíso, Valparaíso, Chile.

Corresponding author: pahidalg@udec.cl

Highlights:

- A simple and reliable protocol for *in situ* determination of the living/dead status of common zooplankton groups in marine field samples.
- This advance in the staining method allows researchers to rapidly distinguishing live and dead individuals in the field, opening the opportunity to obtain detailed quantification of zooplankton carcasses.
- The access to quantify carcasses in field samples will also help the studies on natural mortality of zooplankton associated with oceanographic variability

.

Abstract

Here we describe a standardized protocol for collecting, staining, and analyzing marine zooplankton from field samples for determination of *in situ* live and dead animals. The protocol was tested after using three different sampling nets and from two upwelling sites in the Humboldt Current System off Chile. Its applicability to a range of common marine zooplankton groups was also determined in eggs, naupliar stages, and advanced stages of copepods as addressed in detail. We suggest this is a simple and reliable protocol for *in situ* determination of the living/dead status of common zooplankton groups in marine field samples. This advance in the staining method allows researchers to rapidly distinguishing live and dead individuals in the field, opening the opportunity to obtain detailed quantification of zooplankton carcasses. The access to quantify carcasses in field samples will also help the studies on natural mortality of zooplankton associated with oceanographic variability

Keywords: Neutral red stain method, non-predatory mortality, zooplankton

Introduction

One of the most basic needs in copepod research is having an accurate assessment of population abundance, from which researchers can derive many ecological parameters, such as grazing (feeding) impact, population growth and food availability for higher trophic levels. In a traditional field sampling, copepods are trapped and concentrated by nets into collectors (cod ends), and indiscriminately preserved and enumerated without knowledge of the original live/dead status of the sampled animals. Subsequently, researchers often assume that all copepods counted were originally alive, and that *in situ* mortality is caused solely by predation, which can be deduced from changes in abundance. However, there is no a priori reason to believe that copepods would be exempt from non-predatory mortality, which may leave intact carcasses or dead bodies behind. Without distinguishing between live and dead copepods in field samples, researchers may have overlooked evidence of non-predatory mortality and erred in understanding many potential ecological processes (Tang et al., 2014; Tang and Elliott, 2014).

Copepod carcasses can be distinguished from live copepods before preservation in various ways, such as: i) lack of movement even upon stimulation (probing); ii) lack of heart beats; iii) lack of gut peristaltic movement; iv) signs of decomposition such as development of rigor mortis, missing body tissues, or colonization by microbes. Carcasses are also clearly different from exuviae because carcasses contain traces of tissues even at advanced stage of decomposition (Elliott and Tang 2009). These methods, however, require close and lengthy examination of individual copepods, and are therefore impractical in field surveys. A simple method to quickly and reliably differentiate live and dead zooplankton in preserved field samples is therefore needed. Here we describe such a method using the vital stain neutral red. Dressel et al. (1972) first described the use of neutral red staining to differentiate live and dead marine copepods. The method is promising for determining live/dead status of zooplankton in field samples for a number of reasons. It provides a clear color distinction between live and dead animals, making it less subjective and less time consuming than inspecting for signs of injury or decomposition. It also allows for identification of recently dead individuals that may have no visible signs of decomposition. The method is inexpensive, the stain is nontoxic, and the protocol for staining is simple, making it easy to incorporate into routine field sampling.

This method and has a serie of older studies behind it, such as, Dressel et al. (1972), Crippen and Perrier (1974), Fleming and Coughlan (1978); Carpenter et al. (1974), Hoffmeyer et al. (2005), Vinogradov et al. (1997, 1998) and Tang et al. (2006) and their limitations where

carefully and fully described by Elliott and Tang (2009). Furthermore, Elliott and Tang (2009) described that the limitations associated with neutral red staining of zooplankton field samples can be resolved by testing the accuracy and precision of the results of a single standardized protocol, and with regard to the factors (variable staining pattern/intensity, variable environmental conditions, and artifact mortality). This will ensure the accuracy of *in situ* live and dead composition data obtained by neutral red staining. However, this study has some limitations with the maximum time of the species take up the stain and retain it for an adequate period during preservation and samples analysis. Finally, the protocol proposed by Elliott and Tang, 2009 was modified by Yanez, 2009 and Yanez et al., 2012 for local conditions. Here we describe a standardized protocol for collecting, staining, and analyzing marine zooplankton field samples for *in situ* live and dead determinations of animals. The protocol was tested in two upwelling sites in the Humboldt Current System off Chile, its applicability to a range of common marine zooplankton groups was determined and also in eggs, naupliar stages, and advanced stages of copepods. The outcome is a simple and reliable protocol for *in situ* determining the vital status of common zooplankton groups in marine field samples which can be associated to oceanographic conditions.

Materials and methods

Preparation of neutral red stock solution – The stock solution was prepared diluting 0.5 g neutral red powder (Neutral Red high purity biological stain; Merck) in 1000 mL deionized water. After preparation, the stock solution was stored at dark at room temperature in a sealed amber borosilicate glass vial. This stock solution should be replaced every three months or less, if the storage conditions were not the ideal (e. g., excessive heat or light exposure).

Preparation of buffered formalin stock and activation of neutral red – Formalin stock is buffered (pH > 7) with Sodium Acetate (NaOH), diluting 4.0 g of NaOH in 1000 mL of 40% formalin solution. Samples are acidified to pH< 7 with Acetic Acid ($C_2H_4O_2$) to develop the stain´s color inside the animals.

Collecting zooplankton – The zooplankton collections were carried out in different sampling periods in a 6 years' window, between March of 2009 and 2015, with a total of 141 samples (Table 1). In the sampling we used different plankton nets of 200 and 100 μm mesh size depending of the platform of study and location (Table 1), as Multinet plankton, WP2 and Tucker trawl (Table 1). The neutral red was applied immediately after the collection of the samples on board.

Staining efficiency and sample storage – To test the efficiency of the method, each collected sample was transferred to the staining jar of 500 mL, and neutral red stock solution was incubated with 2 − 4 mL of Neutral Red stock solution (0.5% w/v) (Table 2). For samples with an exceptionally high number of animals, and samples with high concentrations of phytoplankton or detritus, additional neutral red stock may be added to increase stain uptake without damaging the animals. As a rough guideline, the water should appear bright red and not pink (scarce stain) or dark red (excess of stain). After stain addition, samples were incubated for 10 − 20 min. Afterward, samples were concentrated onto fine nylon mesh disks and rinsed briefly with filtered *in situ* sea water to remove excess of stain. In the laboratory samples should be stored at dark until their analysis.

Right before starting sample analysis under the stereo-microscope (20 – 40 X), we washed with water to remove excess of formalin solution and, then we should add 0.3 mL or less of Acetic Acid ($C_2H_4O_2$) to the sample to activate the stain.

Results

First, we tested the effect of preservation and storage on staining results, taking 10 mL subsamples from a single zooplankton sample for variable periods of time between 3 to 6 months. There was significant effect of preservation method on the staining results (Table 3).

Incubation time– For incubating times, we observed that samples stained during 10 min and preserved resulted in lower and more variable percentages of stained organisms compared with samples incubated during 20 min. We also observed that a significant effect of preservation method of the staining results associated with different volumes of neutral red stock solutions (Table 3). The preservation with volume of 2 mL of neutral red resulted in lower and more variable percentages of stained specimens, compared with samples stained with 4 mL (Table 3). Finally, we observed that samples retained the stain for 115 days (more than 3 months); after 4 months, sorting dead and live organisms was difficult for zooplankton samples from Coliumo bay. Meantime, for those zooplankton samples taken in Mejillones bay (where the temperature from the upper 50 m is in average 15°C), we observed that this time was longer than that of Coliumo. The latter samples were further processed in the laboratory within 6 months. Regarding these results, we recommend that samples should be stained by adding 4 mL of neutral red stock solution in 200 mL of sample, incubated for 10 min, preserved in 4% buffered formalin solution, stored in the dark, and processed within 3 months after collection in those areas where the

temperature is lower than 8°C.

Microscopic analyses of stained samples – Preserved samples were acidified to pH < 7 to develop the red stain's color inside the animals. Acidification could be done using any acidic solution (Dressel et al.,1972) and the addition of 0.3 mL of 1 M Acetic Acid ($C_2H_4O_2$) per 15 mL sample works well from our experience. Samples are then observed with a stereo-microscope (20 – 40 X). Microscopy lighting is an important factor, and excessive lighting may cause stained animals to appear pale and unstained animals to appear pink. For copepodid and adult copepods a dark field lighting should be used.

Live animals at the time of sampling stained bright red in part or all of their tissues (mainly prosome tissue); animals dead before the staining will appear unstained, cloudy-white, or light pink. Color will begin to fade in 2 hours after re-suspension and acidification. Adding 0.3 - 0.5 mL additional acetic acid reduces this problem.

Assessment

Considering that this protocol for neutral red staining of zooplankton was described early by Dressel et al. (1972), and most recently by Elliott and Tang (2009), some questions still remain about the potential limitations of the method associated with specific environmental conditions (e.g. in the coastal upwelling zone). Our goal was to describe and test a standardized protocol for staining and live/dead sorting which can be applied easily to field samples. For the method to be incorporated as a regular part of the field sampling, it is important to assess the accuracy and precision of staining results when applied to different zooplankton groups. We observed that neutral red worked well for small zooplankton samples (e. g., small copepods (< 4 mm), medusae, cladocerans and ostracods), but it did not work well with large-sized zooplankton samples (e. g. fish larvae and chaetognatha). For these cases, we therefore recommend that staining be done with > 4 mL of neutral red stock solution.

General methodology – A series of laboratory tests was done with mixtures of known numbers of live and dead zooplankton. In all of them, a large number of live and active animals were collected from a single station in Coliumo Bay off Concepcion (36ºS; 73ºW) and Mejillones Bay (23ºS; 70ºW).

Validation and Application of Neutral red method – For all the tests described in this study, samples were stained, preserved, and analyzed according to the protocol described in "Materials and procedures". To date, neutral red has been applied mainly to calanoid copepods (Dressel et al. 1972, Tang et al. 2006) and to several common marine zooplankton groups (Elliott and Tang

2009). As part of the method development, we assessed the applicability of our protocol to several common marine zooplankton groups: the dominant copepod species; eggs and nauplii, copepodites of *Paracalanus* cf. *indicus*, *Acartia tonsa*, *Calanus chilensis* and *Calanoide patagoniensis*; hydromedusae, cladocerans, appendicularian, siphonophora, ctenophores, ostracods, chaetognatha, fish and crab larvae.

The eggs were stained by adding 0.1 mL of Neutral Red solution [0.5% p/v, 1:1000] in 2 mL of seawater (Ruz et al., 2018). After 10 minutes the samples were preserved in 4% formalin solution buffered with sodium acetate for later analysis. Within two months after the experiments, the samples were analyzed to avoid the degradation of the stain. In the laboratory we sieved (200 µm) and rinsed the formalin solution from the samples prior to place them in counting chambers. Then the samples were acidified to pH < 7 by the addition of five drops (~ 0.5 mL) of acetic acid ($C_2H_4O_2$), to obtain the red stain's color in the organisms that were alive at the end of the experiments.

The results showed that the neutral red method applied for all tested groups were highly effective by Staining Efficiency Test > 99.2%, an exception were fish and crab larvae, which were not stained (Table 4). However, the usefulness of the method depends not only on the initial staining efficiency, but also on the ease of visibility of absorbed stain and retention of stain after uptake. Live fish larvae took up the stain, but the staining was confined to weak pink coloration at body surface. Live crab larvae also took up the stain, but the stained was confined to weak pink and white coloration at joins. Copepod eggs and nauplii and small copepodid, hydromedusae, cladocerans, appendicularia, siphonophora, ctenophores, ostracods, chaetognatha, all stained efficiently. In conclusion, the use of neutral red staining for some zooplankton groups requires special attention. Samples of fish and crab larvae need to be analyzed quickly after thawing and need to be inspected closely for stain uptake. Other groups, such as copepod eggs, nauplii and copepodid, can be confidently determined as live or dead with relative ease.

Discussion

The neutral red method provides a relatively simple way to quantify carcasses (Elliott and Tang, 2009). Two coastal upwelling zones of Humboldt Current Ecosystem were studied where the copepod carcasses were a persistent feature in plankton samples from 2009-2015.

Neutral Red staining was found to be a robust method, broadly applicable to many taxa, and performed well on the tested copepods. Live copepods that have taken up Neutral Red stain

appeared bright red under the microscope, whereas dead copepods are only slightly stained or unstained (see Fig. 1 for photos). The clear color contrast makes counting live and dead copepods in field samples rapid and easy.

In this paper we described an improved a protocol for neutral red staining of marine zooplankton in field samples and provided detailed guidelines for visual examination of staining results. We verified that the method was reliable for determining live/dead zooplankton compositions across a range of environmental conditions and for different zooplankton groups. This advance in the staining method allows researchers to rapidly distinguishing live and dead individuals in the field, opening the opportunity to obtain detailed quantification of copepod carcasses. The access to quantify carcasses in field samples will also help the studies on natural mortality of zooplankton associated with oceanographic variability. Equally important is the observation of future studies, insights into recurring patterns of carcass abundance and distribution within an upwelling system will allow for re-examination of past studies of the same system where live/dead zooplankton composition was not considered. Nevertheless, a dead copepod obviously "behaves" very differently than a live one, and understanding the fate of the carcasses will improve our knowledge of how they can influence the ecosystem.

In this study, the neutral red method was evaluated under high productivity coastal upwelling zones for most abundant marine zooplankton groups. The methods are mostly well suited for copepods, the most abundant zooplankton in the coastal upwelling zone.
Here, was observed that stain uptake varies with different taxa coincidently with Omori and Ikeda (1984) and Elliott and Tang (2009). The use of the method in environments with high concentration of phytoplankton and zooplankton requires additional considerations. For example, if there is a need to carefully evaluate the addition of extra 2 mL of neutral red.

Acknowledgements

The authors thank Dr. David Elliott for helping with data analysis, Captain Juan Menares and the crew of R/V Menachos for assistance in the field. This work is a contribution to the CONICYT-FONDECYT Postdoctoral Project 3180177 (P. M. Ruz) and the Millennium Institute of Oceanography ICM 120019.

Compliance with ethical standards

Funding This study was funded by by the CONICYT- FONDECYT 1080037 (R. Escribano), CONICYT-FONDECYT 11090146 (P. Hidalgo) and CONICYT Collaborative Project CHILE–

USA No. USA2012–0006 (P. Hidalgo). Yañez was supported by the Scholarship of CONICYT-PCHA/Doctorado Nacional/2013-21130213.

Conflict of interest S. Yáñez declares that he has no confict of interest. P. Hidalgo declares that she has no confict of interest. P. Ruz declares that he has no confict of interest. R. Escribano declares that he has no confict of interest.

Ethical approval All applicable international, national, and/or institutional guidelines for the care and use of animals were followed.

References

Carpenter, E. J., Peck B. B., Anderson, S. J. 1974. Survival of copepods passing through a nuclear power station on northeastern Long Island Sound, USA. Mar. Biol. 24:49-55

Crippen, R. W., Perrier J. L., 1974. The use of neutral red and Evans blue for live-dead determinations of marine plankton (with comments on the use of rotenone for inhibition of grazing). Stain Technol. 49:97-104

Dressel, D. M., Heinle D. R., Grote M. C., 1972. Vital staining to sort dead and live copepods. Chesapeake Sci. 13:156-159

Elliott, D.T., Tang, K.W., 2009. Simple staining method for differentiating live and dead marine zooplankton in field samples. Limnol. Oceanogr. Methods 7, 585–594.

Fleming, J. M., Coughlan J., 1978. Preservation of vitally stained zooplankton for live/dead sorting. Estuaries 1:135-137.

Hoffmeyer, M., Biancalana S. F., Berasategui A., 2005. Impact of a power plant cooling system on copepod and meroplankton survival (Bahía Blanca estuary, Argentina). Iheringia, Série Zoologia 95:311-318

Omori, M., and Ikeda T., 1984. Methods in marine zooplankton ecology. Wiley

Ruz, P., Hidalgo P., Escribano R., Keister J.E., Yebra L., Franco-Cisterna B., 2018. Hypoxia effects on females and early stages of *Calanus chilensis* in the Humboldt Current ecosystem (23ºS). J. Exp. Mar. Biol. Ecol. 498: 61–71.

Tang, K. W., Freund C. S., Schweitzer C. L., 2006. Occurrence of copepod carcasses in the lower Chesapeake Bay and their decomposition by ambient microbes. Estuar. Coast. Shelf Sci. 68:499-508.

Tang, K.W., Gladyshev, M.I., Dubovskaya, O., Kirillin, G., Grossart H.P., 2014. Zooplankton

carcasses and non-predatory mortality in freshwater and inland sea environments. J. Plankton Res. 36, 597–612.

Tang, K, W., Elliott D, T. 2014. Copepod carcasses: Occurrence, fate and ecological importance. Copepods: Diversity, Habitat and Behaviour, Pages: 255 – 278.

Vinogradov, M. E., Shushkina E. A., Vedernikov V. I., Nezlin N. P., Gagarin V. I., 1997. Primary production and plankton stocks in the Pacific Ocean and their seasonal
variation according to remote sensing and field observations. Deep-Sea Res. II 44:1979-2001.

———, Nezlin, N. P., Arnautov G. N., 1998. Vertical distribution of zooplankton in the frontal zone of the Gulf Stream and Labrador Current. J. Plank. Res. 20:85-103.

Yáñez, S., 2009. Tasa de mortalidad y desarrollo de *Paracalanus* cf. *indicus* (Copepoda: Calanoida) (Wolfender, 1905) en la zona Centro-Sur de Chile (36°S) asociada con la zona de mínimo de oxígeno. Seminario de título, Facultad de Ciencias Naturales y Oceanográficas, Universidad de Concepción, Concepción, 65 pp.

Yañez, S., Hidalgo, P., Escribano, R., 2012. Mortalidad natural de *Paracalanus indicus* (Copepoda, Calanoida) en áreas de surgencia asociada a la zona de mínimo oxígeno en el Sistema de Corrientes de Humboldt: implicancias en el transporte pasivo del flujo de carbono. Rev. Biol. Mar. Oceanogr. 47, 295–310.

Table 1: Summary sources of samples

Date	**Location**	**Nets**	**Number of sampling**	**Funding**
May − August 2009	Concepcion	Multinet − Tucker trawl	36	FONDECYT Project number 1080037
January − December 2012	Mejillones	Wp − 2	33	FONDECYT project number 11090146
March − December 2013	Mejillones	Wp − 2	48	CONICYT Collaborative Project CHILE–USA No. USA2012–0006
March 2015	Mejillones	Wp − 2	24	CONICYT Collaborative Project CHILE–USA No. USA2012–0006
Total			141	

Table 2: Neutral red staining protocol

Neutral red staining
Stock
(i) Neutral red 0.5% p/v (1:1000) (diluting 0.5 g of neutral red powder in 1000 mL of deionized water) (ii) Formalin stock: 40% w/v (iii) Buffered formalin stock: 0.4% w/v Sodium Acetate (NaOH, diluting 4.0 g of NaOH in 1000 ml of 40% of formalin solution) (iv) Acetic acid ($C_2H_4O_2$) 1M (v) After preparation, the stock solution should be stored in the dark at room temperature in a sealed amber borosilicate glass vial.
Staining
The collected sample should be transfer to the staining jar, and neutral red stock solution must be to add at a volume of 2-4 mL per 500 mL of sample (that's depend of sample concentration). After stain addition, incubate the sample for 10 minutes. Wash with filtered sea water to remove the excess of stain.
Storage
Add 5 mL of 4% buffered formalin solution, store in the dark and process within 6 months after collection.
Acidification
Add 0.3 mL of 1M Acetic acid (AcOH) per 15 mL of sample.
Activation time
Please, the sample should be analyzed during the limit time of 4-6 months. After that, the color of sample could begin to fade.

Table 3**:** Results of staining efficiency across the range of time and stain concentration tested for *Paracalanus* cf. *indicus* (all copepodite and adults).

Date	Depth (m)	Neutral red concentration (mL)	Stain time (minutes)	Activation time (days)	Comments
9 March 2009	80 − 40 80 − 50 40 − 20 40 − 0	2	20 10 20 10	7	Red Weak pink Red Weak pink
17 March 2009	80 − 40 80 − 50 40 − 20 40 − 0	2	20 10 20 10	15	Weak pink Not active Weak pink Not active
12 May 2009	80 − 50 80 − 0 50 − 0	4	10	14	Red Red Red
12 May 2009	80 − 50 80 − 0 50 − 0	2	10	14	Red Red Weak pink
2 June 2009	80 − 50 80 − 0 50 − 0	4	10	35	Red Weak pink Red
2 June 2009	80 − 50 80 − 0 50 − 0	2	10	35	Red Red Weak pink
9 June 2009	80 − 50 80 − 0 50 − 0	4	10	42	Red Weak pink Weak pink
9 June 2009	80 − 50 80 − 0 50 − 0	2	10	42	Red Weak pink Not active
16 June 2009	80 − 50 80 − 0 50 − 0	4	10	49	Red Weak pink Weak pink
16 June 2009	80 − 50 80 − 0 50 − 0	2	10	49	Red Weak pink Not active
21 August 2009	80 − 50 80 − 0 50 − 0	4	10	115	Red Weak pink Weak pink
21 August 2009	80 − 50 80 − 0 50 − 0	2	10	115	Weak pink Not active Not active

Table 4: Results of staining efficiency test for the various zooplankton groups

Group	**Number of sample**	**% live expected**	**% live observed**	**Staining efficiency**
Copepoda				
A. tonsa	23	98.6	98.5	99.8
	20	40.6	40.4	99.7
	22	60.4	60.2	99.6
	17	81.0	81.5	100.6
P. cf. *indicus*	21	70.2	70.0	99.7
	21	65.8	65.7	99.8
	27	100	99.8	99.8
	38	67.6	67.8	100.2
Appendicularian	6	65.8	65.5	99.5
	11	72.3	72.0	99.5
Ctenophores	20	75.0	71.0	94.6
Salpa	22	50.8	50.4	99.2
Chaetognatha	21	80.8	80.6	99.7
Hydromedusae	15	74.6	74.5	99.9
Siphonophora	18	78.9	78.6	99.7
Crab larvae	25	100	0	0
Fish larvae	15	100	0	0

Figure captions

Figure 1: Appareance neutral red–treated zooplankton under a stereomicroscope (Zeiss Discovery V8) with dark-field. Adults of copepod (A), copepod nauplii and egg (B), and the live and dead individuals of crustacean larvae (C), Appendicularean (D), Siphonophores (E), Chaetognatha (F), Fish larvae and eggs (H). Photo credit: Braulio Fernandez. The camera used was a ZEISS Axiocam ERc 5s model.

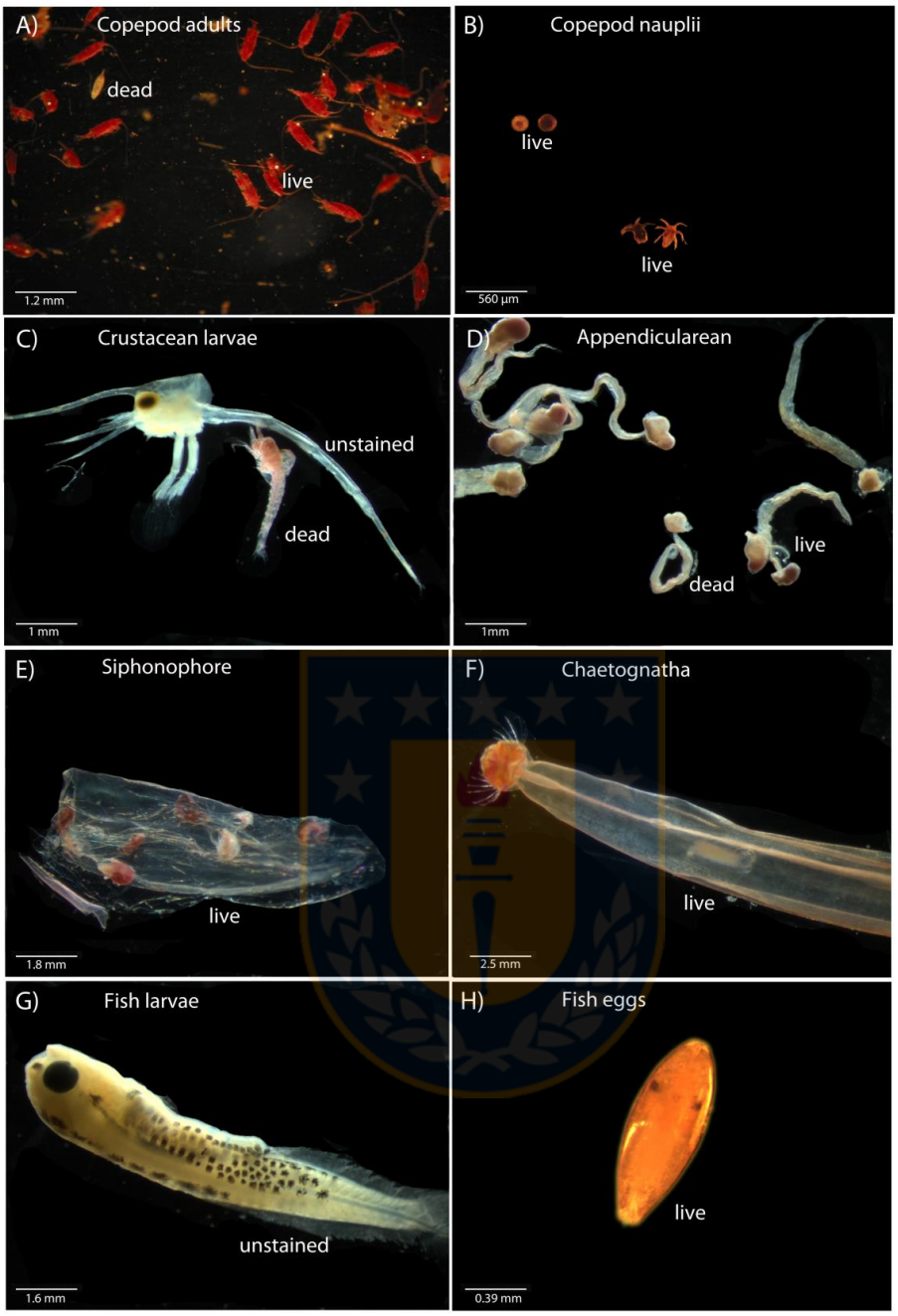
A)
Copepod adults
dead
live
1.2 mm
B)
Copepod nauplii
live
live
560 µm
C)
Crustacean larvae
unstained
dead
1 mm
D)
Appendicularean
live
dead
1mm
E)
Siphonophore
live
1.8 mm
F)
Chaetognatha
live
2.5 mm
G)
Fish larvae
unstained
1.6 mm
H)
Fish eggs
live
0.39 mm

Figure 1

4.1.2. Predatory and non-predatory mortality in dominant copepod species in the northern Chile (23ºS) Humboldt Current Ecosystem

Artículo en preparación

Sonia Yañez

Doctorado en Oceanografía

Universidad de Concepción

Resumen

Las tasas de mortalidad, es un parámetro clave en la biología poblacional de copépodos, sin embargo, rara vez se mide en estudios de campo y, por lo tanto, a menudo es "parámetro inferido" en los modelos de dinámica poblacional. Sumado a este problema, también existe una falta de obsersación de las causas de mortalidad *in situ*. La mortalidad depredatoria representa una transferencia trófica ascendente de la biomasa de copépodos, mientras que la mortalidad no-depredatoria representa un potencial desvío de la producción de copépodos hacia el anillo microbiano o a flujos de sedimentación de materia organica. Usando datos de abundancia de copepoditos vivos y muertos, junto con la duración de estadíos y las tasas de muda, obtuvimos tasas de mortalidad depredatoria y no-depredatoria de las tres especies principales de copépodos marinos dentro del Sistema de Corriente de Humboldt (HCS) de Chile: *Paracalanus* cf. *indicus*, *Acartia tonsa*, y *Calanus chilensis*, y examinamos por primera vez su relación con factores ambientales. Las tasas de mortalidad total aumentaron con los estadíos de desarrollo en las tres especies. Las tasas de mortalidad total de C5 fueron 3-4 veces más altas que las de C1. En promedio, la depredación representó 53,7 de la mortalidad total en *P.* cf. indicus, 56,4% en *A. tonsa* y hasta un 65,2% en *C. chilensis*. Mientras tanto, la mortalidad no depredadora representa entre 34.8 al 46.3% de la mortalidad total, y esto refleja la importancia del estrés ambiental sobre el control de la dinámica poblacional de copépodos en el HCS. Futuros ajustes a esta aproximación son necesarios, particularmente para estimar el tiempo de residencia de las carcasas (τ) en nuestro ambiente. No obstante, esta aproximación podría permitir que los investigadores comiencen estudios de mortalidad no-depredatoria de copépodos, estimulando la posibilidad de futuras discusiones e investigaciones sobre este tópico

Palabras claves: Mortalidad no-depredatoria, carcasas de copépodos, Sistema de Corrientes de Humboldt, Ecuación de Bèlehràdek

Predatory and non-predatory mortality in dominant copepod species in the northern Chile (23ºS) Humboldt Current Ecosystem

Sonia Yáñez[1,2], Pamela Hidalgo[2] and Kam W. Tang[3]

1. Doctoral Program in Oceanography, Department of Oceanography, Faculty of Natural Science and Oceanography, University of Concepcion, P.O. Box 160 C, Concepción, Chile
2. Department of Oceanography and Millennium Institute of Oceanography, Faculty of Natural Science and Oceanography, University of Concepcion, P.O. Box 160 C, Concepción, Chile.
3. Department of Biosciences, Swansea University, Swansea, SA2 8PP, U.K.

Corresponding author: P. Hidalgo (pahidalg@udec.cl)

Abstract

Mortality rate, as a key parameter in copepod population biology, is rarely measured in field studies, and consequently it is often treated as a 'closure term' in population dynamics models. Compounding this problem, there is also a general lack of appreciation of non-predatory mortality causes *in situ*. Predatory mortality represents an upward trophic transfer of copepod biomass, whereas non-predatory mortality represents a potential diversion of copepod production to the microbial loop or sinking fluxes. Using detailed data of live/dead compositions, along with stage durations and molting rates, we derived both predatory and non-predatory mortality rates of the three main copepod species, *Paracalanus* cf. *indicus*, *Acartia tonsa* and *Calanus chilensis*, within the Chilean Humboldt Current System (HCS), and examined their relations with the environmental factors for the first time. Total mortality rates, calculated as the sum of average predatory and non-predatory mortality rates over the two annual cycles, increased with developmental stages in all three species. The total mortality rates of C5 were 3-4 times higher than those of C1. On average, predation accounted for 53.7 of the total mortality in *P.* cf. *indicus*, 56.4% in *A. tonsa*, and up to 65.2% in *C. chilensis*. Meantime, non-predatory mortality accounts for 34.8 to 46.3 % of the total mortality, and this reflects the importance of environmental stresses in controlling the copepod population dynamics within the HCS. Further improvements to this approach are needed, particularly for estimating carcass turnover time (τ) in our environment. Nonetheless, this approach will allow researchers to begin to study non-predatory copepod mortality in greater details. This is a welcomed progress and would likely stimulate further discussion and research into this topic

Keywords: Copepods mortality, Neutral red stain, copepod carcasses, VLT approach, Chilean Humboldt Current System.

Introduction

Mortality is one of the most critical, but poorly quantified, parameters of copepod population dynamics (Ohman & Wood 1995). The main cause of copepod mortality is generally assumed to be predation (Verity & Smetacek 1996), but many non-predatory factors can also cause mortality, such as diseases (Delgado & Alcaraz 1999), parasites (Kimmerer & McKinnon 1990, Burns 1985, Ohtsuka et al. 2004, Duffy et al. 2005), physical and chemical stresses (Carpenter et al. 1974, Roman et al. 1993; Bickel et al. 2011), starvation (Tsuda 1994), and senescence (Ceballos & Kiørboe 2011, Saiz et al. 2015), all of which may leave carcasses behind. Zooplankton carcasses have been observed around the world, at times in high abundances, and most of which are copepod carcasses (Elliott and Tang 2009, Tang et al. 2014, Yañez et al. 2012, 2018). Indeed, a meta-analysis suggests that up to one-third of the mortality in marine pelagic copepods cannot be explained by predation (Hirst & Kiørboe 2002).

Ignorance of carcass occurrences causes errors to many population parameters as well because dead copepods obviously do not molt, grow or reproduce. Recent studies have shown that ignoring even a small magnitude of carcass abundance and non-predation mortality could lead to large errors in population growth and secondary production estimates (Elliott and Tang 2011a, Yañez et al. 2018). As such, proper quantification and separation of predatory and non-predatory components of mortality is critical to a more accurate understanding of the pelagic food web. In this regard, the recent advances in the Neutral Red staining method allow researchers to distinguish between live and dead zooplankton in field samples, thereby providing a means to quantify predatory and non-predatory mortalities directly (Elliott and Tang 2009;Yañez et al. 2012, 2018).

The Humboldt Current System (HCS) is among the most productive pelagic ecosystems, where copepods dominate the metazooplankton communities and play an important role in the transfer of matter and energy to the higher trophic levels (Hidalgo et al. 2010, Pino-Pinuer 2014). In northern Chile, Mejillones Bay (23°S) is one of the most important upwelling centers within the HCS (Marín et al. 1993). The presence of shallow cold-water masses with low oxygen concentration (Equatorial Subsurface Water, ESSW) associated with the Oxygen Minimum Zone (OMZ) are present due to upwelling events that occur year-round (Marín and Olivares 1999). The ESSW supports a high diversity of zooplankton, with at least 107 species of copepods (Hidalgo et al. 2010), nine of which are numerically dominant (Escribano et al. 2012). The abundance and biomass of the copepod community in Mejillones Bay are influenced by the vertical distribution of dissolved oxygen (Yañez et al. 2012), the upwelling intensity (Escribano

et al. 2009, 2012), the upwelling shadow and advection (Giraldo et al. 2002). These studies suggest that the copepods are highly sensitive to environmental variability, which is reflected by changing abundance of copepod carcasses in the surface water of coastal areas in response to changes in upwelling intensity that reduces or expands the oxygenated surface layer in HCS (Yañez et al. 2012)

In this study, we used the Neutral Red staining method to measure the stage-specific live/dead compositions of the three major copepod species (*Acartia tonsa*, *Paracalanus*. cf. *indicus* and *Calanus chilensis*) in the Mejillones Bay over two annual cycles; from these data we then calculated and compared their predatory and non-predatory mortality rates and examined their relationship with the environmental conditions.

Materials and methods

Field sampling

The study was conducted in Northern Chile (Mejillones Bay) within the Humboldt Current System (HCS). Monthly sampling was performed in 2010 and 2011 at three stations along a coastal transect: St-1 (23º 04.2'S, 70º 25.8'W; maximum station depth (z_{max}) = 60 m), St-2 (23º 02.4'S, 70º 27.0'W; z_{max} = 90 m) and St-3 (23º 0.2'S, 70º 28.2'W; z_{max} = 120 m) (Fig.1). Water temperature, salinity, and dissolved oxygen (DO) were measured at each station by autonomous profiler SeaBird SBE-19. Water samples were collected at 10 m depth (within the mixed layer) using a 5-L Niskin bottle, and their chlorophyll-*a* contents were analyzed fluorometrically (Morales & Anabalon 2012, Anabalon et al. 2014). Intensity of upwelling was estimated by Ekman transport using the equation described by Mann & Lazier (1991):

$$MX = \frac{\tau y}{f}$$

Where MX is Ekman transport ($m^3\ s^{-1}\ km^{-1}$), f is the Coriolis parameter and τy is along-shore wind stress (Pa). τy was estimated by the following equation:

$$\tau y = \rho a \times cd \times (vi|vi|)$$

Where ρa is air density (1.2 kg m^{-3}), cd is the empirical constant of drag coefficient (0.00014), and vi is the along-shore wind velocity (m s^{-1}). Ekman transport was averaged monthly from daily estimates based on wind data from the meteorological station in Cerro Moreno airport (http://164.77.222.61/climatologia/)

Copepods were collected by vertical hauls through 0-30 m during the day using a WP-2 net (200 µm mesh and a 50-cm mouth diameter) equipped with a flowmeter. Our target copepod species are concentrated in this upper layer and do not exhibit diel vertical migration in this

region (Escribano et al. 2009). Upon retrieval of the net, the samples were transferred to a chilled thermal box and immediately treated with the vital stain Neutral Red (Elliott and Tang 2009, modified by Yanez 2009 and Yanez et al. 2012 for local conditions). Briefly, each sample was incubated with 2-4 mL of Neutral Red stock solution (0.5% w/v) for 10 min. Afterward, the stained samples were concentrated and briefly rinsed with filtered seawater to remove excess stain, then preserved in 4% neutralized formalin solution in the dark, and processed further in the laboratory within 3-6 months. In the laboratory, the stained samples were concentrated and briefly rinsed with filtered seawater, then acidified by 0.3 mL of 1M acetic acid to develop the stain's color. Under a stereo-microscope (20–40 X), the dominant copepod species *Paracalanus* cf. *indicus*, *Acartia tonsa* and *Calanus chilensis* were counted and identified to developmental stages. Individuals that were alive at the time of sampling appeared red, whereas dead ones remained unstained.

Stage durations and molting rates

Calculations of mortality rate require estimates of stage durations (D_i for stage i, d), which can vary by stage, temperature, food availability and quality (Kimmerer & McKinnon 1989, Peterson 2001, Giraldo et al. 2002, Escribano 1998, Vargas et al., 2010). In this study, stage durations were estimated using the temperature-dependent equation of Belehrádek (1935) (equation (3) in Table S1) and the relevant environmental data from the field sampling. Details of molting rate experiments are reported in Yañez et al. (2018).

Predatory and non-predatory mortality rates

We estimated the predatory and non-predatory components of mortality using the Vertical Life Table (VLT) approach as modified by Elliott and Tang (2011a) by including both the abundances of live copepods and carcasses (Table S1). In this method, both live copepods and intact carcasses are treated as survivors of predatory mortality, but only live individuals proceed to the next life stages. Non-predatory mortality was then calculated as the difference between total mortality rate and predatory mortality rate. This approach was applied only to samples that showed positive values of predatory mortality.

Statistics

Normality was tested by the Kolmogorov-Smirnov test (Zar 1984). When necessary, the data

were log transformed (n+1) to meet the requirement of normal distribution. Seasonal and annual differences in the oceanographic conditions, differences in stage duration and non-predatory mortality rates among development stages and between years were tested with a two-factor nested General Linear Model (GLM) ($\alpha = 0.05$) after checking that the data met the parametric assumptions. Pearson correlations were conducted to test for linear relationships between parameters ($\alpha = 0.05$).

Results

General oceanographic conditions

Oceanographic conditions for both years are summarized in Table 1. Water column temperature ranged between 11.9 °C and 17.3 °C during the sampling period. Temperature did not show significant seasonal differences (spring, summer, fall and winter). We found two significantly different periods (Two samples t-test, $T = 3.15$, $DF = 14$, $P < 0.05$) (Table 2): a warmer period in the summer/fall and a cold period of winter/spring months (Fig. 2a).

The water column was strongly thermally stratified, with the isotherm of 16 °C at 10 m depth most of the time. The lowest temperature values were recorded in water deeper than 50 m. The shoaling of the 14 °C isotherm to near 20 m between July 2010 and March 2011 and in September 2011 was caused by intrusion of cold upwelled water into the bay.

Salinity was rather stable between 34.9 and 34.8 in both years (Fig. 2b) and without significant changes between seasons ($F_{2,36}$, $P > 0.05$) (Table 2). Dissolved oxygen concentration showed similar seasonal patterns between years (Fig. 2c). Dissolved oxygen concentration in the upper 10 m was at 2–6 ml O_2 L^{-1}. The oxycline was located at 10–20 m depth, while the OMZ was characterized by the low oxygen concentrations (< 1 ml O_2 L^{-1}) between 30 and 90 m. In 2010, the average upper boundary of the OMZ (1 ml O_2 L^{-1}) was at 22.0 ± 8.8 m ($n = 24$) and a very deep OMZ was observed in August. In 2011, the upper limit of the OMZ was at an average depth of 26.0 ± 17.0 m ($n = 24$), and was deeper than the 2010 OMZ between June and September. Chlorophyll-*a* concentration showed significant statistical differences throughout the years ($F_{2,74}$, $P < 0.05$) (Table 2). Also, chlorophyll-*a* concentration at 50 m showed significant variations during the study period ($F_{3,48}$, $P < 0.05$) and was highly correlated to that at 10 m depth (Spearman rank correlation, $rs = 0.61$, $N=23$, $P < 0.001$).

During the study period, the Ekman transport was positive most of the time, indicating prevailing upwelling conditions (Fig. 4). Although Mejillones Bay has been suggested as having a weak seasonality of upwelling index compared to other coastal areas

of Chile (Sobarzo et al. 2007), it was possible to observe a seasonal cycle of significant fluctuations ($F_{4.08}$, $P < 0.05$) (Table 2), with the strongest Ekman transport occurring in late winter and early spring, reaching 700 m^3 s^{-1} km^{-1} in October 2010 and 941 m^3 s^{-1} km^{-1} in September 2011, whereas the lowest values were found in the fall.

Copepod stage durations

Figure 5 illustrates development patterns for *Paracalanus* cf. *indicus*, *Acartia tonsa* and *Calanus chilensis*. All three copepod species showed significant differences in stage duration between stages ($P < 0.05$) (Table 3). For *A. tonsa*, a pattern different from the other patterns is seen. *P.* cf. *indicus* closely resemble *C.chilensis*. Development times of three copepod species increase with each developmental stage: development progresses with approximately equal stage durations through the early copepodite stages (C1–C3), then slows through the fourth and/or fifth copepodite. Higher temperatures (14–17°C) resulted in shorter individual stage durations (3–5 days), whereas lower temperatures (10–2°C) led to longer stage durations (13–15 days) (Fig. 5).

Predatory and non-predatory mortality rates

There were significant ontogenetic and temporal differences in predatory mortality rate of *P.* cf. *indicus*, *A. tonsa* and *C. chilensis* (Table 4). The estimated predatory mortality rate of *P.* cf. *indicus* was highest in stages C3–C5, especially in January, June and December of 2011, and lowest in C1–C2 (February, October and December of 2010 and May and September of 2011) (Fig. 6 a,b). The predatory mortality rate of *A. tonsa* had its highest value in C2–C5 in the winter-spring period (September–December) in both years, and lowest in the summer period (January–March) (Fig. 6 c,d). Likewise, the predatory mortality rate of *C. chilensis* was lowest in the summer and fall, and was very high in stages C2–C5, especially in November (Fig 6 d, e). Predatory mortality was positively correlated with dissolved oxygen for all three species, negatively with chlorophyll *a* for *A. tonsa*, and negatively with temperature for *C. chilensis* (Table 5).

Similarly, there were significant ontogenetic, but not temporal, differences in non-predatory mortality rate of *P.* cf. *indicus* and *C. chilensis*, and the rate also varied significantly between months in *A. tonsa* (Table 4). The estimated non-predatory mortality rate of *P.* cf. *indicus* was the highest in stage C5, especially in April, July and October of 2011, and the lowest in

copepodites C1–C2 (February, July of 2010 and August of 2011) (Fig. 7 a,b). The non-predatory mortality rate of *A. tonsa* had its highest value in C1–C4 in the spring period (September–December) in both years, and in C5 in the fall–winter period (April–July), and lowest in the summer period (January–March) (Fig. 7 c,d). Likewise, the non-predatory mortality rate of *C. chilensis* was lowest in the summer, and was high in the spring especially for C5 (Fig 7 d, e). Non-predatory mortality was negatively correlated with dissolved oxygen ($r = -0.596$, $P = 0.000$; $r = -0.574$, $P = 0.000$) and chlorophyll-*a* ($r = -0.374$, $P = 0.000$; $r = -0.175$, $P = 0.001$) in *P.* cf. *indicus* and *A. tonsa*, respectively; whereas it positively correlated with temperature ($r = 0.532$, $P = 0.002$) in *C. chilensis* (Table 5).

Total mortality rates, calculated as the sum of average predatory and non-predatory mortality rates over the two annual cycles, increased with developmental stages in all three species (Table 6, Fig.8). The total mortality rates of C5 were 3-4 times higher than those of C1. The partition of mortality between predatory and non-predatory sources, however, remained rather constant across the developmental stages for each species, with predation accounted for a larger portion of the total mortality. On average, predation accounted for 53.7 of the total mortality in *P. cf. indicus*, 56.4% in *A. tonsa*, and up to 65.2% in *C. chilensis* (Table 6, Fig.8).

Discussion

The Humboldt Current System, which includes the coastal upwelling areas off Chile, is among the most productive marine systems (Thiel et al. 2007). Copepods dominate the zooplankton communities within the HCS, which in turn support large fisheries in the region (Espinoza & Bertrand 2008). Copepod population abundances within the HCS can be highly variable (Hidalgo et al. 2010, 2012, Pino-Pinuer 2014). To understand what controls the dynamics of the copepod populations, past studies have focused on upwelling intensity, food availability, copepod growth and reproduction (Escribano 1998, Escribano et al. 2012, 2016), whereas investigation of copepod mortality rates within the HCS has been lacking. To our knowledge, the present study is the first attempt to measure mortality rates of the three major copepod species in Mejillones Bay in northern Chile and examined their relationships with the environmental conditions.

During this study, the chlorophyll concentration was variable but it was generally at levels not considered to be limiting to zooplankton (Escribano et al. 2016), except in the winter months when the water column was more well mixed and the OMZ was restricted to the deeper depths, and when chlorophyll-*a* was nearly depleted. The water column was thermally stratified with low

DO for much of the years. (Escribano et al. 2004, Ruz et al. 2015, 2017).

An interesting observation from this study is that mortality rate increased with developmental stages in all three species. Elliott and Tang (2011a) showed that over an annual cycle in the Chesapeake Bay, copepodite mortality rates were generally higher than naupliar mortality rates. In Lurefjorden, Norway, where predatory copepods were abundant, the mortality rate of *Calanus* spp. decreased substantially as the copepod developed through the naupliar stages, but subsequently increased slightly between C1 and CV (Eiane et al. 2002). A similar ontogenetic change (from nauplii to CV) in mortality rate was also observed in *Calanus finmarchicus* in the North Sea (Eiane & Ohman 2004). While we do not have mortality rate data on the nauplii, the increased mortality rates between copepodite stages seem to be consistent with the previous studies, and suggest that the higher mortality rates in the later copepodite stages may impose a stronger constraint on population growth. The estimated mortality rates of C1 were comparable to the global average values (ca. 0.10–0.15 d^{-1}; Hirst & Kiørboe 2002) for the observed temperature range, but were much higher for the later stages (up to 0.55 d^{-1}). Nevertheless, similarly high mortality rates have been reported elsewhere, such as the Chesapeake Bay (Elliott & Tang 2010) and the English Channel (Maud et al. 2018).

Using the Neutral Red staining method and the modified VLT approach, we were able to partition the mortality rate into predatory and non-predatory sources. Predatory mortality rates of all three species increased linearly with developmental stages, hence body sizes (Fig. 8). For non-visual predators such as predatory copepods and chaetognaths, their predation success is largely limited by their gape size such that the larger copepodite sizes would offer better protection from these predators (Pearre 1980, Yen 1983). Conversely, larger body sizes may make the copepodites more apparent to visual predators such as planktivorous fish, which often prefer the larger prey (Brooks 1968, O'Brien et al. 1976). Within the HCS, the major planktivores include sardines and anchovies within the oxygenated layer (Espinoza & Bertrand 2008), which may explain the observed positive relationship of predatory mortality rates with the copepodite stage (i.e. body size), as well as with DO in two of the three species.

Intermittent intrusion of oxygen-poor water associated with coastal upwelling is a common feature in the region (Marín et al. 1993), which could cause episodic hypoxia and copepod mortality (Yañez et al. 2012, Elliott et al. 2010, 2013). In our study, low DO was associated with high non-predatory mortality rates of *P. cf. indicus* and *A. tonsa*, consistent with earlier reports (Yáñez et al. 2012, Ruz et al. 2015). In contrast, low DO did not have a significant effect on *C. chilensis*, reflecting the latter species' better ability to cope with low oxygen environment

(Hirche et al. 2014, Ruz et al. 2018).

Chlorophyll concentration was negatively correlated with non-predatory mortality rates of *P. cf. indicus* and *A. tonsa*, indicating food limitation effects. Of the three species, only *A. tonsa* showed a significant, negative correlation in predatory mortality with chlorophyll-*a*. Both *P. cf. indicus* and *C. chilensis* are primarily suspension feeders, whereas *A. tonsa* is known to switch from suspension feeding mode to ambush feeding mode when phytoplankton concentration is low (Kiørboe et al. 1996), and an ambush feeding mode perceivably generates stronger hydrodynamic disturbances that may alert planktivores, leading to a higher predatory mortality rate (Kiørboe et al. 2010).

Interestingly, temperature correlated positively with non-predatory mortality rate, but negatively with predatory mortality rate of *C. chilensis*. This species is endemic to the coastal upwelling system (Escribano & Rodriguez, 1994,1995, Escribano 1998, Torres and Escribano 2003). Increasing water column temperature reflects the weakening of the upwelling condition, which may lead to lower food availability and thence higher non-predatory mortality rate. Meanwhile, a less stratified condition may allow the copepod to migrate deeper diurnally to avoid predation, resulting in lower predatory mortality rate.

Overall, the relative proportions of predatory vs. non-predatory mortality rates remain fairly consistent across developmental stages within a species. On average, non-predatory mortality accounts for 34.8 to 46.3 % of the total mortality. This is higher than the global average for pelagic adult copepods (Hirst & Kiørboe 2002), but similarly high proportions of non-predatory mortality have been observed for *Calanus helgolandicus* in the English Channel (Maud et al. 2018), and this reflects the importance of environmental stresses in controlling the copepod population dynamics within the HCS (Pino-Pinuer et al. 2014, Escribano et al. 2012, Medellin-Mora, 2016).

Conclusions

Mortality rate, as a key parameter in copepod population biology, is rarely measured in field studies, and consequently it is often treated as a ‘closure term’ in population dynamics models (Runge et al. 2004). Compounding this problem, there is also a general lack of appreciation of non-predatory mortality causes *in situ* (Elliott et al.2010, Elliott & Tang 2011b). Predatory mortality represents an upward trophic transfer of copepod biomass, whereas non-predatory mortality represents a potential diversion of copepod production to the microbial loop (Tang et al. 2006, 2009, Bickel & Tang 2010) or sinking fluxes (Sampei et al. 2009, 2012). Using detailed

data of live/dead compositions, along with stage durations and molting rates, we derived both predatory and non-predatory mortality rates of the three main copepod species within the Chilean HCS, and examined their relations with the environmental factors for the first time. We showed that non-predatory mortality rates accounted for considerable fractions of the total mortality rates throughout the year and among all copepodite stages.

In the Southwest Pacific, climate change is expected to intensify upwelling in the HCS (Echevin et al. 2012), with potential corresponding changes in hydrography, water chemistry, species diversity and phenology (Hays et al. 2005). Increase in coastal upwelling events could promote chained diatom blooms and alter the quality of food sources (Vargas et al. 2006, Poulet et al. 2007). Strong upwelling could also promote extreme shoaling of the OMZ. The shoaling of OMZs diminishes the extent of the usable habitat of zooplankton (Manríquez et al.2009) and small-pelagic (Bertrand et al. 2010) that prey on zooplankton and also that have been shown to decrease their diving depths (Stramma et al. 2011), thus possibly increasing their exposure to predator because of their shallower distribution. Based on our present findings, these future events will likely increase non-predatory mortality rates of the copepod populations. It is therefore pertinent that researchers consider both predatory and non-predatory mortality causes in order to fully understand copepod population dynamics within this important ecosystem.

Acknowledgements

This work was supported by the CONICYT-FONDECYT No. 11090146 (P. Hidalgo) and CONICYT Collaborative Project CHILE–USA No. USA2012–0006 (P. Hidalgo). Yañez was supported by the Scholarship of CONICYT-PCHA/Doctorado Nacional/2013-21130213 and by Red Doctoral en Ciencia, Tecnología y Ambiente, REDOC CTA, University of Concepcion. The authors thank Dr. David Elliott and Benjamin Glasner for helping with data analysis, Captain Juan Menares and the crew of R/V Menachos for assistance in the field. This work is a contribution by Millennium Institute of Oceanography ICM 120019.

References

Anabalón V, Arísteguia J, Morales CE, Andrade I, Benavides M, Correa-Ramírez MA, Espino M, Ettahiri O, Hormazabal S, Makaoui A, Montero MF, Orbi A (2014) The structure of planktonic communities under variable coastal upwelling conditions off Cape Ghir (31°N) in the Canary Current System (NW Africa). Progr Oceanogr 120: 320–339.

Belehrádek J (1935). Temperature and living matter. Protoplasma Monogr. 8:1–277.

Bertrand A, Ballón M, Chaigneau A (2010) Acoustic observation of living organisms reveals the upper limit of the oxygen minimum zone. PLoS One 5, e10330.
Bickel S, Tang K (2010) Microbial decomposition of proteins and lipids in copepod versus rotifer carcasses. Mar Biol 157:1613–1624.
Bickel SL, Hammond JDM, Tang KW (2011) Boat-generated turbulence as a potential source of mortality among copepods. J Exp Mar Biol Ecol 401:105–109.
Brooks LJ (1968). The effects of prey size selection by lake planktivores. Systematic Biology, 17(3): 273–291.
Burns CW (1985) Fungal parasitism in a copepod population: the effects of Aphanomyces on the population dynamics of *Boeckella dilatata* Sars. J Plankton Res 7: 201–205.
Carpenter EJ, Peck BB, Anderson SJ (1974) Survival of copepods passing through a nuclear power station on north-eastern Long Island Sound, USA. Mar Biol 24: 49–55.
Ceballos S, Kiørboe T (2011) Senescence and sexual selection in a pelagic copepod. PLoS One 6(4):18870. doi:10.1371/journal. pone.0018870.
Daneri G, Dellarossa V, Quiñonez R, Jacob B, Montero P, Ulloa O (2000) Primary production and community respiration in the Humboldt Current System off Chile and associated oceanic areas. Mar Ecol Prog Ser 97: 41–49.
Delgado M, Alcaraz M (1999) Interactions between red tide microalgae and herbivorous zooplankton: the noxious effects of *Gyrodinium corsicum* (Dinophyceae) on *Acartia grani* (Copepoda: Calanoida). J Plankton Res 21: 2361–2371.
Duffy MA, Hall SR, Tessier A and others (2005) Selective predators and their parasitized prey: are epidemics in zooplankton under top–down control? Limnol Oceanogr 50: 412–420.
Dorazio RM (1984) The contribution of longevity to population death rates. Hydrobiologia, 108: 239–243.
Echevin V, Goubanova K, Belmadani A, Dewitte B (2012) Sensitivity of the Humboldt Current system to global warming: a downscaling experiment of the IPSL-CM4 model. Climate Dynam 38: 761–774.
Eiane K, Aksnes DL, Ohman MD, Wood S, Martinussen MB (2002) Stage-specific mortality of *Calanus spp.* under different predation regimes. Limnol. Oceanogr 47:636-645.
Eiane K, Ohman MD (2004) Stage-specific mortality of *Calanus finmarchicus, Pseudocalanus elongates* and *Oithona similis* on Fladen Ground, North Sea, during a spring bloom. Mar Ecol Prog Ser 268:183-193.
Elliott DT, Tang KW (2009) Simple staining method for differentiating live and dead marine

zooplankton in field samples. Limnol Oceanogr Methods 7: 585–594.
Elliott DT, Harris CK, Tang KW (2010). Dead in the water: The fate of copepod carcasses in the York River estuary, Virginia. Limnol Oceanogr 55: 1821–1834.
Elliott DT, Tang KW (2011a). Influence of carcass abundance on estimates of mortality and assessment of population dynamics in *Acartia tonsa*. Mar Ecol Prog Ser 427: 1–12.
Elliott DT, Tang KW (2011b) Spatial and temporal distributions of live and dead copepods in the lower Chesapeake Bay (Virginia, USA). Estuar Coasts 34: 1039–1048.
Elliott DT, Pierson JJ, Roman M (2013) Copepods and hypoxia in Chesapeake Bay: abundance, vertical position and non-predatory mortality. J Plankton Res 0: 1-8.
Escribano R and Rodriguez L (1994). Life cycle of Calanus chilensis Brodsky in northern Chile. In: Ecology and Morphology of Copepods. F.D. Ferrari & B.P. Bradley (eds). Kluwer Academic Publishers, Boston. pp. 289-294.
Escribano R, Rodriguez L (1995) Seasonal size variation and growth of Calanus chilensis Brodsky in northern Chile. Revista Chilena de Historia Natural. 68: 373-382.
Escribano R (1998) Population dynamics of Calanus chilensis in the Chilean Eastern Boundary Humboldt Current. Fish Oceanogr 7(3/4): 245-251.
Escribano R, Hidalgo P, Krautz C (2009) Zooplankton associated with the oxygen minimum zone system in the northern upwelling region of Chile during March 2000. Deep-Sea Res. II 56: 1083–1094.
Escribano R, Hidalgo P, Fuentes M, Donoso K (2012) Zooplankton time series in the coastal zone off Chile: Variation in upwelling and responses of the copepod community. Progr Oceanogr 97: 74–186.
Espinoza P, Bertrand A, (2008) Revisiting Peruvian anchovy (*Engraulis ringens*) trophodynamics provides a new vision of the Humboldt Current system. Progr Oceanogr 79: 215–227.
Genin A, Gal G, Haury L (1995) Copepod carcasses in the ocean. II. Near coral reefs. Mar Ecol Prog Ser 123: 65–71.
Giraldo A, Escribano R, Marin VH (2002) Spatial distribution of Calanus chilensis off Mejillones Peninsula (northern Chile): ecological consequences upon coastal upwelling. Mar Ecol Progr Ser 230: 225–234.
Hall LW, Alden RW (1997) A review of concurrent ambient water column and sediment toxicity testing in the Chesapeake Bay watershed: 1990–1994. Environ Toxicol Chem 16: 1606–1617.
Harris R, Wiebe P, Lenz J, Skjoldal HR, Huntley M (2000) ICES Zooplankton Methology

Manual. Academic Press. San Diego, USA.
Hays G, Richardson A, Robinson C (2005) Climate change and marine plankton. Trends Ecol Evol 20: 337–344.
Hidalgo P, Escribano R, Morales CE (2005) Ontogenetic vertical distribution and diel migration of the copepod *Eucalanus inermis* in the oxygen minimum zone off northern Chile. J of Plank Res 27: 519–529.
Hidalgo P, Escribano R (2008) The life cycles of two coexisting copepods, *Calanus chilensis* and *Centropages brachiatus*, in the upwelling zone off northern Chile (23°S). Mar Biol 155: 429–442.
Hidalgo P, Escribano R, Vergara O, Jorquera E, Donoso K, Mendoza P (2010) Patterns of copepod diversity in the Chilean coastal upwelling system. Deep-Sea Res Part II 57: 2089–2097.
Hirche HJ, Barz K, Ayon P, Schulz J (2014) High resolution vertical distribution of the copepod Calanus chilensis in relation to the shallow oxygen minimum zone off northern Peru using LOKI, a new plankton image system. Deep Sea Res. Part I 188: 63–73.
Hirst AG, Kiørboe T (2002) Mortality of marine planktonic copepods: global rates and patterns. Mar Ecol Prog Ser 230: 195–209.
Kimmerer WJ, McKinnon D (1987) Growth, mortality, and secondary production of the copepod *Acartia tranteri* in Westernport Bay, Australia. Limnol Oceanogr 32: 14–28.
Kimmerer WJ, McKinnon D (1989) Zooplankton in a marine bay. III. Evidence for influence of vertebrate predation on distributions of two common copepods. Mar Ecol Prog Ser 3: 21–35.
Kiørboe T, Saiz E, Viitasalo M (1996) Prey switching behaviour in the planktonic copepod *Acartia tonsa*. Mar Ecol Prog Ser 143: 65–75.
Kiørboe T, Jiang H, Colin SP (2010) Danger of zooplankton feeding: the fluid signal generated by ambush-feeding copepods. Proceedings of the Royal Society of London B: Biological Sciences 277(1698): 3229–3237.
Ohman MD, Wood SN (1995) The inevitability of mortality. ICES J Mar Sci 52: 517–522.
Pearre Jr S (1980) Feeding by Chaetognatha: the relation of prey size to predator size in several species. Mar Ecol Prog Ser 3: 125–134.
Mann KH, Lazier JNR (1991) Dynamics of marine ecosystems: biological-physical interactions in the oceans. Blackwell Scientific Publications, Oxford, United Kingdom. 394 pp.
Manríquez K, Escribano R, Hidalgo P (2009) The influence of coastal upwelling on the mesozooplankton community structure in the coastal zone off Central/Southern Chile as assessed by automated image analysis. J Plankton Res 31(9): 1075 – 1088.

Marín V, Rodríguez L, Vallejo L, Fuenteseca J, Oyarce E (1993) Efectos de la surgencia costera sobre la productividad primaria primavera de la Bahía Mejillones de Sur (Antofagasta, Chile). Rev Chil Hist Nat 66: 479–491.

Marín V, Olivares G (1999) Estacionalidad de la productividad primaria en Bahía Mejillones del Sur (Chile): una aproximación proceso-funcional. Rev. Chil. Hist. Nat. 72, 629–641.

Morales CE, Lange BC (2004) Oceanographic studies in the Humboldt current system off Chile: an introduction. Deep-Sea Research II. 51, 2345–2348.

Morales CE, Anabalon V (2012) Spatio-temporal distribution of chlorophyll-a, picoplankton, and nanoplankton during the spring upwelling season in the coastal area off Concepción, central-southern Chile. Progr. Oceanogr. special volume.

Medellín-Mora J, Escribano R, Schneider W (2016) Community response of zooplankton to oceanographic changes (2002–2012) in the central/southern upwelling system of Chile. Prog. Oceanogr. 142:17–29.

O'Brien WJ, Slade, NA, Vinyard G L (1976) Apparent size as the determinant of prey selection by bluegill sunfish (Lepomis macrochirus). Ecology 57(6): 1304–1310.

Ohtsuka S, Hora M, Suzaki T, Arikawa M, Omura G, Yamada K (2004) Morphology and host-specificty of the apostome ciliate *Vampyrophrya pelagica* infecting pelagic copepods in the Seto Inland Sea, Japan. Mar Ecol Prog Ser 282: 129–142.

Peterson WT (2001) Patterns in stage duration and development among marine and freshwater calanoid and cyclopoid copepods: a review of rules, physiological constraints, and evolutionary significance. Hydrobiologia. 453/454: 91–105.

Pino-Pinuer P, Escribano R, Hidalgo P, Riquelme-Bugueño R, Schneider W (2014) Copepod community response to variable upwelling conditions off central-southern Chile during 2002−2004 and 2010−2012. Mar Ecol Progr Ser 515: 83–95.

Poulet SA, Escribano R, Hidalgo P, Cueff A, Wichardc T, Aguilera V, Vargas CA, Pohnert G (2007) Collapse of Calanus chilensis reproduction in a marine environment with high diatom concentration. J Exp Mar Bio Ecol 352: 187–199.

Roman MR, Gauzens AL, Rhinehart WK, White JR (1993) Effects of low oxygen waters on Chesapeake Bay zooplankton. Limnol Oceanogr 38: 1603–1614.

Rodríguez-Graña L, Calliari D, Tiselius P, Hansen BW, Skold HM (2010) Gender-specific ageing and non-Mendelian inheritance of oxidative damage in marine copepods. Mar Ecol Progr Ser 401:1–13.

Runge JA, Franks PJS, Gentleman WC, Megrey BA, Rose KA, Werner FE, Zakardjian B (2004)

Diagnosis and prediction of variability in secondary production and fish recruitment processes: developments in physical-biological modeling. In: Robinson AR, Brink KH (eds) The sea, Vol 13. Harvard University Press, Cambridge, MA, p 413–473.

Ruz PM, Hidalgo P, Yáñez S, Escribano R, Keister JE (2015) Egg production and hatching success of Calanus chilensis and Acartia tonsa in the northern Chile upwelling zone (23°S), Humboldt Current System. J Marine Syst 148: 200–212.

Ruz P, Hidalgo P, Escribano R, Keister JE, Yebra L, Franco-Cisterna B (2018). Hypoxia effects on females and early stages of Calanus chilensis in the Humboldt Current ecosystem (23ºS). J Exp Mar Biol Ecol 498: 61–71.

Ruz PM, Hidalgo P, Riquelme-Bugueño R, Franco-Cisterna B, Cornejo M (2017) Vertical distribution of copepod eggs in the oxygen minimum zone off Mejillones Bay (23°S) in the Humboldt Current System. Mar Ecol Progr Ser doi: 10.3354/meps12117

Ruz PM, Hidalgo P, Escribano R, Keister JE, Yebra L, Franco-Cisterna B (2018) Hypoxia effects on females and early stages of Calanus chilensis in the Humboldt Current ecosystem (23°S). J Exp Mar Biol Ecol 498: 61–71.

Saiz E, Calbet A, Grifell K, Guilherme J, Bersano F, Isari S, Solé M, Peters J, Alcaraz M (2015) Ageing and caloric restriction in a marine planktonic copepod. Sci Rep 5:14962.

Sampei M, Sasaki H, Hattori H, Forest A, Fortier L (2009) Significant contribution of passively sinking copepods to the downward export flux in Arctic waters. Limnol Oceanogr 54: 1894–1900.

Sampei, M, Sasaki H, Forest A, Fortier L (2012). A substantial export flux of particulate organic carbon linked to sinking dead copepods during winter 2007-2008 in the Amundsen Gulf (southeastern Beaufort Sea, Arctic Ocean). Limnol Oceanogr 57: 90–96.

Sherman K (1990) Productivity, perturbations and options for biomass yield in large marine ecosystems. In Sherman, K, Alexander, L.M. and Gold, B.D: (eds) Large marine ecosystems: Patterns, Progress and yield. American Association for the Advancement of Sci. 206–219.

Stramma LS, Schmidtko LA Levin, Jonhson GC (2010) Ocean oxygen minima expansions and their biological impacts. Deep-Sea Res I 57: 587–595.

Tang, KW, Freund, CS, Schweitzer CL (2006) Occurrence of copepod carcasses in the lower Chesapeake Bay and their decomposition by ambient microbes. Estuarine, Coastal and Shelf Science 68: 499–508.

Tang K W, Bickel SL, Dziallas C, Grossart HP (2009) Microbial activities accompanying decomposition of cladoceran and copepod carcasses under different environmental conditions.

Aquatic Microbial Ecology 57: 89–100.
Tang KW, Gladyshev MI, Dubovskaya OP, Kirillin G, Grossart HP (2014) Zooplankton carcasses and non-predatory mortality in freshwater and inland sea environments. J Plankton Res 36: 597–612. doi:10.1093/plankt/fbu014.
Tang K W, Elliott D T (2014) Copepod carcasses: Occurrence, fate and ecological importance. Copepods: Diversity, Habitat and Behaviour, Pages: 255 – 278.
Thiel M, Macaya EC, Acuña E, Arntz WE and others (2007) The Humboldt Current System of Northern and Central Chile: oceanographic processes, ecological interactions and socioeconomic feedback. Oceanogr Mar Biol Ann Rev 45: 195–344.
Tsuda A (1994). Starvation tolerance of a planktonic marine copepod *Pseudocalanus newmani* frost. J Exp Mar Biol Ecol 181: 81–89.
Vargas CA, Escribano R, Poulet S (2006) Phytoplankton diversity determines time windows for successful zooplankton reproductive pulses. Ecol 87: 2992–2999.
Vargas CA, Martínez RA, Escribano RE, Lagos NA (2010) Seasonal relative influence of food quantity, quality, and feeding behaviour on zooplankton growth regulation in coastal food webs. J Mar Biol Assoc UK 90:1189–1201.
Wetzel RG (1995) Death, detritus, and energy flow in aquatic ecosystems. Fresh Biol 33: 83-89.
Yañez S, Hidalgo P, Escribano R (2012) Natural mortality of *Paracalanus indicus* (Copepoda: Calanoida) in coastal upwelling areas associated with oxygen minimum zone in the Humboldt current system: implications for the passive carbon flux. Rev Biol Mar Oceanogr 47: 295–310.
Yañez S, Hidalgo P, Ruz P, Tang K (2018) Copepod secondary production in the sea: assessing errors associated with the molt rate method and incidence of carcasses. Progr Oceanogr 165: 257-267. https://doi.org/10.1016/j.pocean.2018.06.008.
Yen, J (1983) Effects of prey concentration, prey size, predator life stage, predator starvation, and season on predation rates of the carnivorous copepod *Euchaeta elongata*. Mar Biol 75(1): 69-77.
Zar JH (1984) Biostatistical Analysis. Prentice-Hall International Inc., New Jersey, 718 pp.

Table 1: Summary table for oceanographic variables in Mejillones bay during 2010 − 2011.

Variable	**2010**				**2011**			
	Mean	Max.	Min.	SD	Mean	Max.	Min.	SD
Temperature at 10 m (°C)	13.39	14.37	12.62	0.72	13.19	14.10	12.63	0.38
Temperature at 50 m (°C)	14.55	15.52	13.09	0.78	14.55	15.52	13.31	0.77
Salinity at 10 m	34.75	34.83	34.62	0.07	34.78	34.83	34.77	0.02
Salinity at 50 m	34.80	34.85	34.75	0.03	34.80	34.83	34.75	0.03
Dissolved oxygen at 10 m (mL L^{-1})	2.86	5.42	1.22	1.30	0.98	3.02	0.00	0.99
Dissolved oxygen at 50 m (mL L^{-1})	0.47	3.02	0.00	0.98	3.37	1.24	5.42	1.22
Chlorophyll-a at 10 m [mg m^{-3}]	24.03	102.0	0.60	31.22	4.19	10.08	0.93	2.85
Chlorophyll-a at 50 m [mg m^{-3}]	25.20	116.8	0.02	36.21	1.56	9.98	0.04	2.74

Table 2: General Lineal Model (GLM) performed on oceanographic variables at the coastal upwelling zone of northern Chile during 2010 − 2011.

Variable		**F**	***P***
Chlorophyll-a	Seasons	2.77	< 0.05
	Years	2.74	< 0.05
Ekman transport	Seasons	4.08	< 0.05
	Years	0.28	0.626
Salinity	Seasons	2.36	0.055
	Years	0.24	0.626
Dissolved oxygen	Seasons	6.63	< 0.05
	Years	0.82	0.374

Table 3: Two factor nested General Lineal Model (GLM) to test differences among months and stages as a function of stage duration in *P.* cf. *indicus*, *A.tonsa* and *C. chilensis* at the coastal upwelling zone of northern Chile during 2010 − 2011. * indicates significant difference at $p < 0.05$.

Variable		**Stage duration**		
		df	**F**	***P***
P. cf. *indicus*	Months	23	2.77	0.000*
	Stages	4	1.73	0.000*
A. tonsa	Months	23	1.18	0.000*
	Stages	4	2.41	0.000*
C.chilensis	Months	23	7.45	0.000*
	Stages	4	5.78	0.000*

Table 4: Two factor nested General Lineal Model (GLM) to test differences among months and stages as a function of predatory and non-predatory mortality rates (d^{-1}) in *P.* cf. *indicus, A.tonsa* and *C. chilensis* at the coastal upwelling zone of northern Chile during 2010 − 2011. * indicates significant difference at $p < 0.05$.

Variable		**Predatory mortality rates**			**Non- predatory mortality rates**		
		df	**F**	***P***	**df**	**F**	***P***
P. cf. *indicus*	Months	23	10.35	0.001*	23	2.18	0.140
	Stages	4	21.68	0.000*	4	18.56	0.000*
A. tonsa	Months	23	43.53	0.000*	23	5.69	0.000*
	Stages	4	42.74	0.000*	5	12.97	0.000*
C. chilensis	Months	23	11.31	0.001*	23	3.30	0.070
	Stages	4	9.82	0.000*	4	4.21	0.002*

Table 5: Spearman rank order correlation were run in predatory and non-predatory mortality rates (d^{-1}) of three copepod species among oceanographic variables: temperature (T), salinity (S), dissolved oxygen (DO) and chlorophyll-a (Chla). * indicates significant difference at $p < 0.05$.

Variable		**Predatory mortality rates**				**Non-predatory mortality rates**			
		T	**S**	**DO**	**Chla**	**T**	**S**	**DO**	**Chla**
P. cf. *indicus*	r	0.117	0.143	0.236	-0.099	-0.083	0.317	-0.596	-0.374
	P	0.202	0.120	0.009*	0.291	0.117	0.117	0.000*	0.000*
A. tonsa	r	0.132	0.074	0.352	-0.226	0.022	0.065	-0.574	-0.175
	P	0.151	0.420	0.006*	0.013*	0.676	0.219	0.000*	0.001*
C. chilensis	r	-0.290	-0.102	0.127	0.127	0.532	0.077	0.112	-0.161
	P	0.001*	0.269	0.165	0.058	0.002*	0.143	0.702	0.102

Table 6. Average prosome length (μm), stage-specific total mortality rate (d^{-1}) and its partition between predatory (PM) and non-predatory (NPM) sources (%).

	Paracalanus cf. *indicus*				*Acartia tonsa*				*Calanus chilensis*			
Stage	Prosome length	Total mortality	% PM	% NPM	Prosome length	Total mortality	% PM	% NPM	Prosome length	Total mortality	% PM	% NPM
C1	350.0	0.15	53.3	46.7	528.0	0.15	60.0	40.0	940.0	0.11	63.6	36.4
C2	426.7	0.18	55.6	44.4	596.7	0.17	58.8	41.2	1126.0	0.29	69.0	31.0
C3	592.6	0.24	54.2	45.8	657.9	0.22	54.5	45.5	1278.3	0.32	68.8	31.2
C4	724.7	0.35	54.3	45.7	730.0	0.32	56.3	43.7	1491.7	0.42	66.7	33.3
C5	844.0	0.55	50.9	49.1	870.4	0.46	52.2	47.8	1812.0	0.45	57.8	42.2
		avg	*53.7*	*46.3*		*avg*	*56.4*	*43.6*		*avg*	*65.2*	*34.8*

Figure Captions

Figure 1: Upwelling zone off Mejillones bay (23°S) where samples were collected.

Figure 2: Oceanographic conditions (average of three station samples: a) temperature, b) salinity and c) dissolved oxygen found off Mejillones (northern Chile) during 2010-2011.The black line represents the isoline of 1 ml L^{-1} (upper OMZ boundary)

Figure 3: Annual variation of phytoplankton biomass, measured as Chlorophyll-a, in the upper 50 m layer of Mejillones during 2010-2011.

Figure 4: Temporal variability of Upwelling index ($m^3\ s^{-1}\ km^{-1}$) based on Ekman transport ($m^3\ s^{-1}\ km^{-1}$) calculated monthly from daily estimated wind data obtained from a meteorological station at Cerro Moreno airport in Antofagasta during 2010-2011.

Figure 5: The copepodid stage duration as a function of temperature (from Bèlehràdek equation) at Mejillones bay: a) *P. cf. indicus,* b) *A.tonsa* and c) *C.chilensis*.

Figure 6: Changes of predatory mortality rates (d^{-1}) through year-round at Mejillones Bay: a), b) *P. cf. indicus;* c), d) *A.tonsa* and e), f) *C.chilensis*.

Figure 7: Changes of non-predatory mortality rates (d^{-1}) through year-round at Mejillones Bay: a), b) *P. cf. indicus;* c), d) *A.tonsa* and e), f) *C.chilensis*.

Figure 8: Total mortality rate vs. copepodite stage.

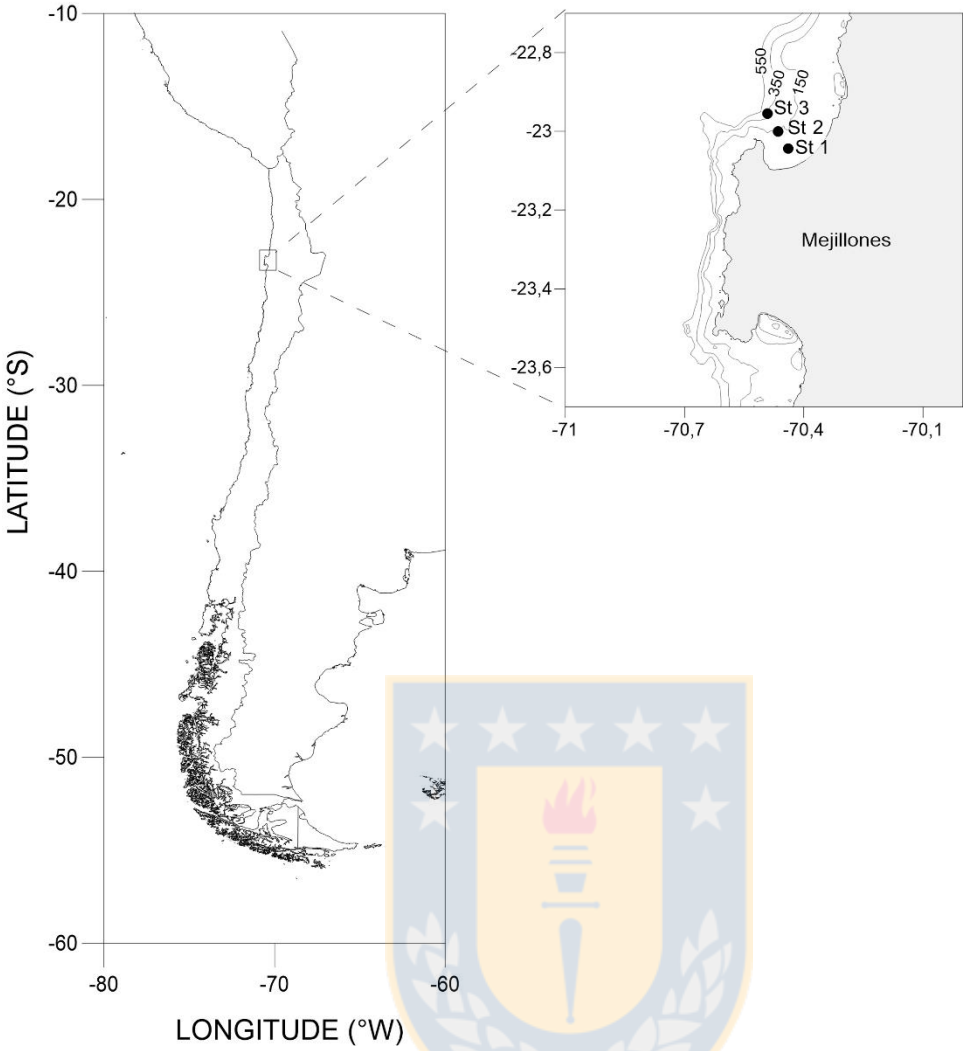
-10
-20
-30
-40
-50
-60
LATITUDE (°S)
-80
-70
-60
LONGITUDE (°W)
-22,8
-23
-23,2
-23,4
-23,6
-71
-70,7
-70,4
-70,1
550
350
150
St 3
St 2
St 1
Mejillones

Figure 1

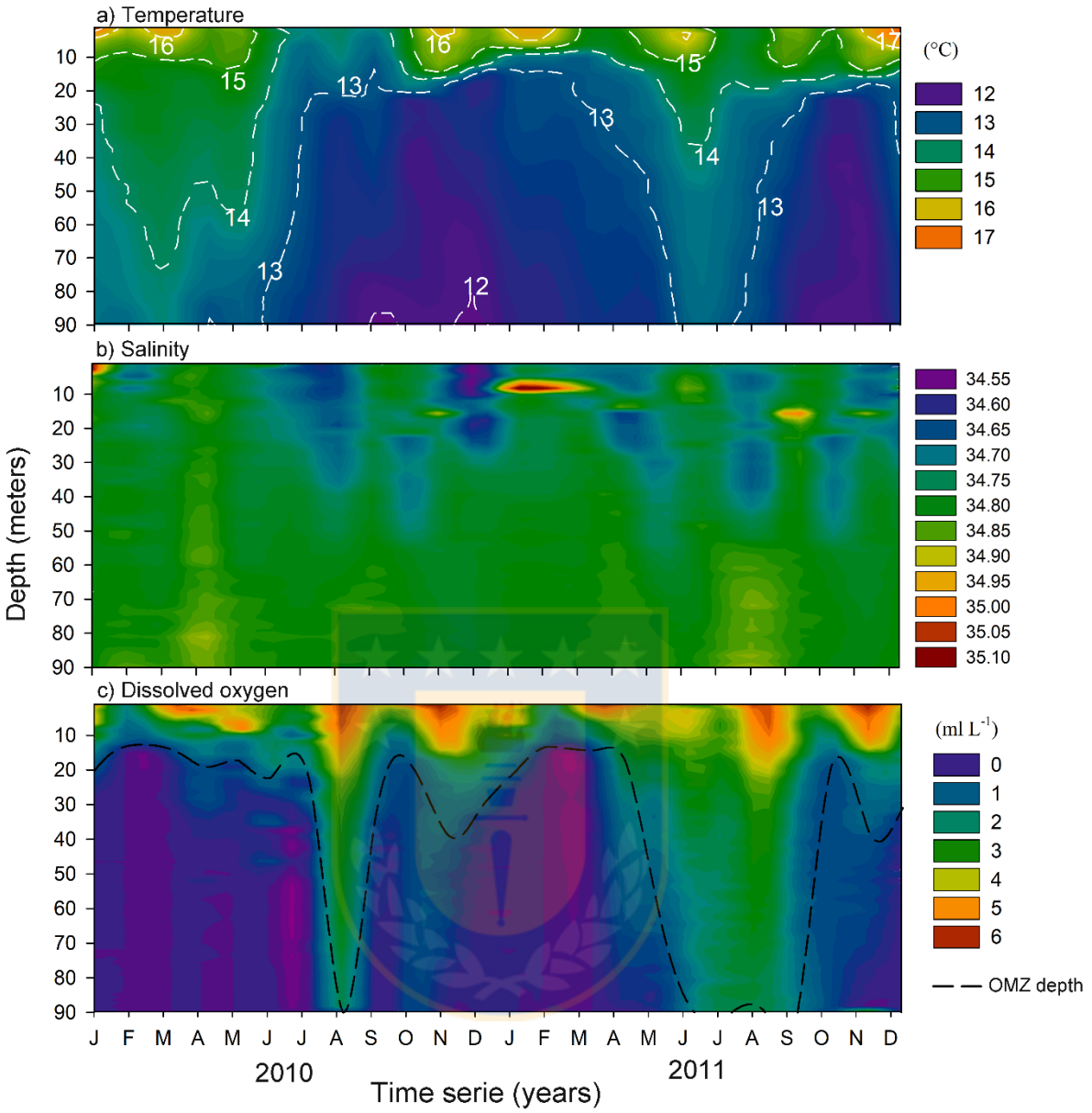
a) Temperature
(°C)
12
13
14
15
16
17
b) Salinity
34.55
34.60
34.65
34.70
34.75
34.80
34.85
34.90
34.95
35.00
35.05
35.10
c) Dissolved oxygen
(ml L-1)
0
1
2
3
4
5
6
OMZ depth
Depth (meters)
10
20
30
40
50
60
70
80
90
J F M A M J J A S O N D J F M A M J J A S O N D
2010
2011
Time serie (years)

Figure 2

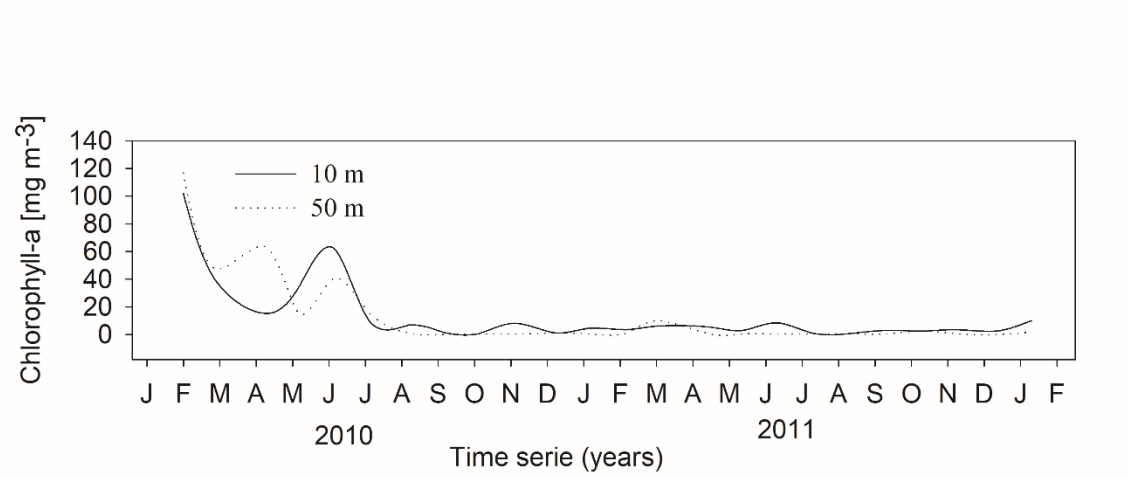
Chlorophyll-a [mg m-3]
140
120
100
80
60
40
20
0
10 m
50 m
J F M A M J J A S O N D J F M A M J J A S O N D J F
2010
2011
Time serie (years)

Figure 3

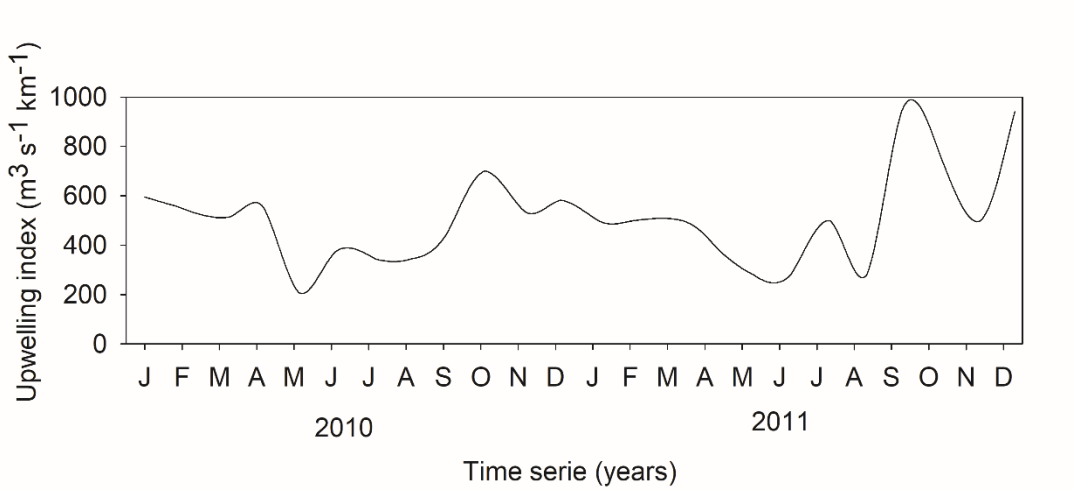
Upwelling index (m3 s-1 km-1)
1000
800
600
400
200
0
J F M A M J J A S O N D J F M A M J J A S O N D
2010
2011
Time serie (years)

Figure 4

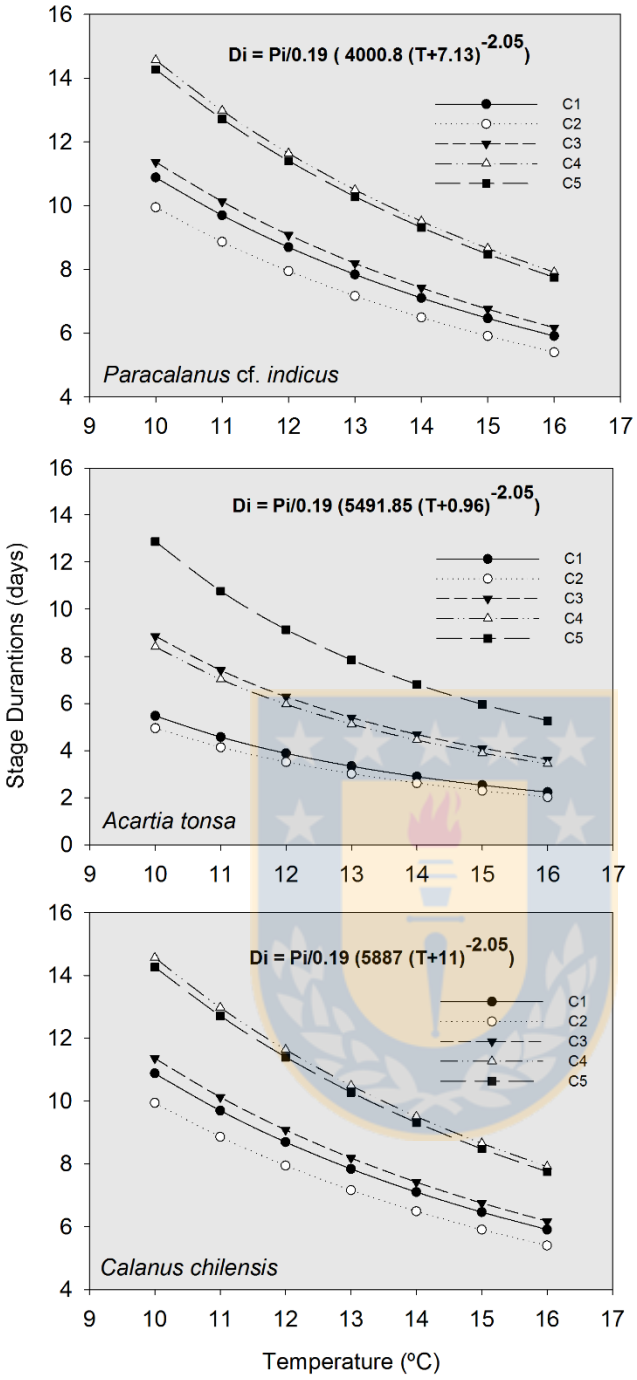
Di = Pi/0.19 (4000.8 (T+7.13)-2.05)
C1
C2
C3
C4
C5
Paracalanus cf. indicus
Di = Pi/0.19 (5491.85 (T+0.96)-2.05)
Acartia tonsa
Di = Pi/0.19 (5887 (T+11)-2.05)
Calanus chilensis
Stage Durantions (days)
Temperature (ºC)

Figure 5

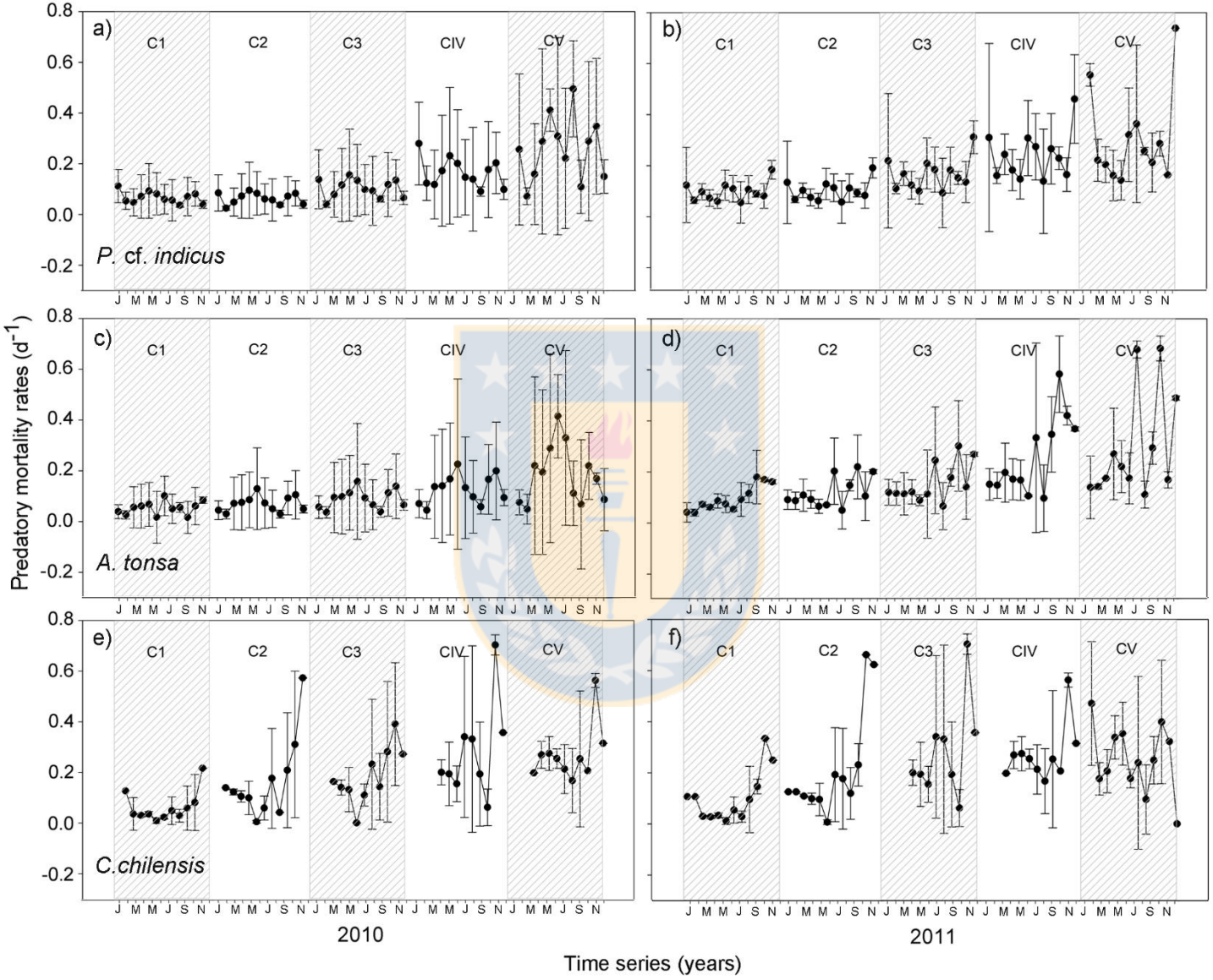
a)
b)
c)
d)
e)
f)
C1
C2
C3
CIV
CV
P. cf. indicus
A. tonsa
C.chilensis
Predatory mortality rates (d-1)
0.8
0.6
0.4
0.2
0.0
-0.2
J M M J S N J M M J S N J M M J S N J M M J S N J M M J S N
2010
2011
Time series (years)

Figure 6

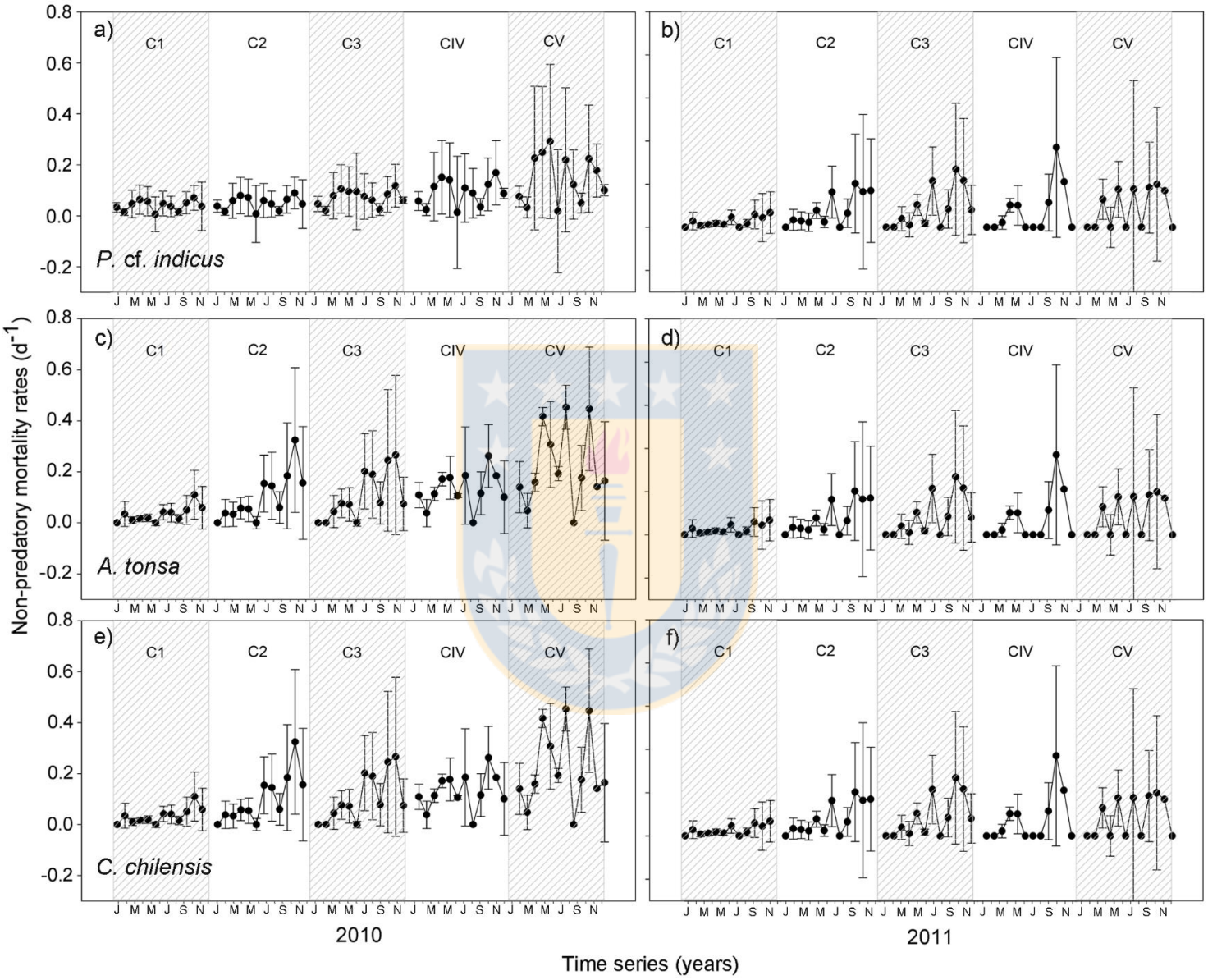
a)
b)
c)
d)
e)
f)
C1
C2
C3
CIV
CV
P. cf. indicus
A. tonsa
C. chilensis
Non-predatory mortality rates (d-1)
0.8
0.6
0.4
0.2
0.0
-0.2
J M M J S N J M M J S N J M M J S N J M M J S N J M M J S N
2010
2011
Time series (years)

Figure 7

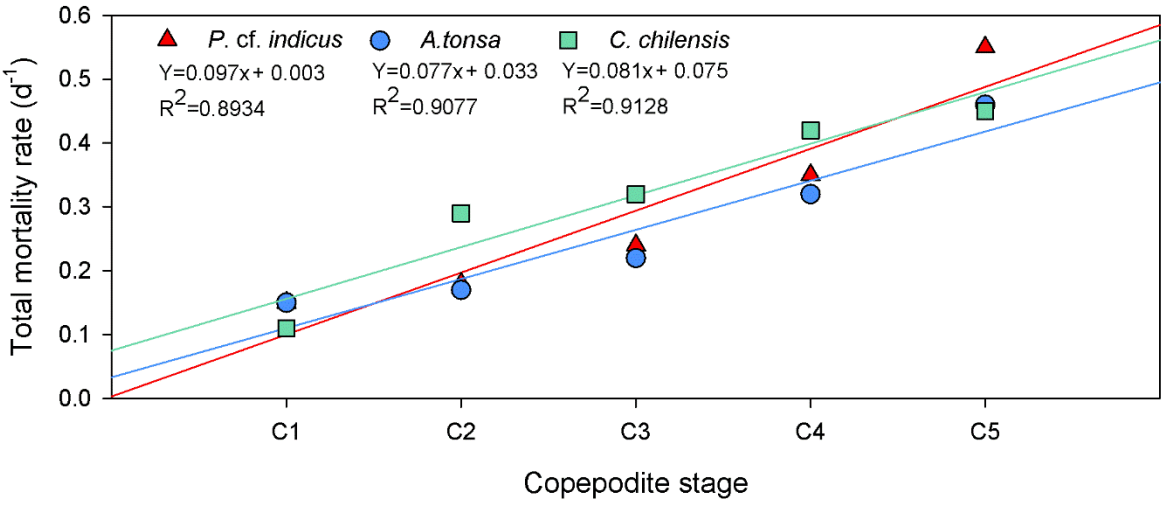
P. cf. indicus
Y=0.097x+ 0.003
R2=0.8934
A.tonsa
Y=0.077x+ 0.033
R2=0.9077
C. chilensis
Y=0.081x+ 0.075
R2=0.9128
Total mortality rate (d-1)
0.0
0.1
0.2
0.3
0.4
0.5
0.6
C1
C2
C3
C4
C5
Copepodite stage

Figure 8

4.1.3. Copepod secondary production in the sea: errors due to uneven molting and growth patterns and incidence of carcasses

Artículo aceptado en Progress in Oceanography
https://doi.org/10.1016/j.pocean.2018.06.008

Sonia Yañez

Doctorado en Oceanografía

Universidad de Concepción

Resumen

La producción secundaria (PS) de copépodos es uno de los parámetros básicos que controlan la estructura y función de la cadena trófica pelágica, y es comúnmente estimada como el incremento de biomasa acumulativa basada sobre experimentos de tasas de muda (MR). La exactitud de este método depende de dos supuestos fundamentales: (1) No existe crecimiento ni desarrollo inter-estadio; (2) Todos los copépodos *in situ* están vivos. Nosotros desarrollamos un estudio anual en una bahía costera dentro de Sistema de Corrientes de Humboldt con el objetivo de evaluar los errores en estimaciones de PS cuando estos supuestos son ignorados. Las abundancias de individuos vivos y muertos de las especies dominantes: *Paracalanus* cf. *indicus, Acartia tonsa* y *Calanus chilensis* fueron muestreadas mensualmente. Simultáneamente, fueron realizados experimentos de tasas de muda para obtener la PS de copépodos. Una ecuación modificada de MR fue utilizada para corregir errores en la estimación de producción secundaria asociada al supuesto (1). Ignorar los supuestos fundamentales provocó un error en la estimación de producción secundaria, más severamente en *P.* cf. *indicus.* El error no fue igualmente distribuido a través de los meses, y en el caso de *C. chilensis*, este fue cambiando entre sobre y sub- estimaciones, repetidamente. El promedio anual fue -39,2% en *P.* cf. *indicus*, 3,1% en *A.tonsa*, y 5,2% en *C.chilensis*. Los errores también variaron en magnitud y signo a través de los estadios de desarrollo, con algunos estadios con un error de un 70% sobrestimado. Para algunas especies de copépodos con tiempos generacionales cortos, aunque el error sea pequeño, este se podría propagar y resultar en proyecciones de producción secundaria altamente sesgadas. Por lo

tanto, para obtener estimaciones de producción secundaria es necesario una cuidadosa evaluación de la duración de estadios y crecimiento entre estadios al aplicar el método de MR, y la cuantificación de individuos muertos en terreno.

Palabras claves: Producción secundaria, copépodos, mortalidad no-depredatoria, carcasas, método de rojo neutro, surgencia costera

Progress in Oceanography 165 (2018) 257–267

Contents lists available at ScienceDirect

Progress in Oceanography

journal homepage: www.elsevier.com/locate/pocean

Copepod secondary production in the sea: Errors due to uneven molting and growth patterns and incidence of carcasses

Sonia Yáñez[a,b], Pamela Hidalgo[b,*], Paula Ruz[b,c], Kam W. Tang[d]

[a] Doctoral Program in Oceanography, Department of Oceanography, Faculty of Natural Science and Oceanography, University of Concepcion, P.O. Box 160 C, Concepción, Chile
[b] Department of Oceanography and Millennium Institute of Oceanography, Faculty of Natural Science and Oceanography, University of Concepcion, P.O. Box 160 C, Concepción, Chile
[c] Escuela de Ciencias del Mar, Pontificia Universidad Católica de Valparaíso, Valparaiso, Chile
[d] Department of Biosciences, Swansea University, Swansea SA2 8PP, UK

ARTICLE INFO

Keywords:
Secondary production
Copepods
Non-predatory mortality
Carcasses
Molting rate method
Coastal upwelling

ABSTRACT

Secondary production of copepods is one of the basic parameters that govern the structure and function of the marine pelagic food web, and it is commonly estimated as cumulative biomass increase through consecutive molting based on short-term molting rate (MR) incubation experiments. The accuracy of the method depends on two underlying assumptions: (1) Even stage duration and inter-molt growth; (2) All copepods *in situ* are alive. We conducted a year-long study in a coastal bay within the Humboldt Current System to assess the errors in copepod secondary production estimation when these assumptions are violated. Abundances of live and dead individuals of the dominant species: *Paracalanus* cf. *indicus*, *Acartia tonsa* and *Calanus chilensis* were measured monthly. Concurrent molting rate experiments were conducted to derive copepod secondary production. A modified MR formulation was used to correct the secondary production estimates for error in assumption (1), and the live/dead copepod data were used to correct the estimates for error in assumption (2). Violation of the underlying assumptions caused error in secondary production estimation, most severely in *P.* cf. *indicus*. The error was not evenly distributed across the months, and in the case of *C. chilensis*, it switched between over- and under-estimation repeatedly. The annual average error was −39.2% in *P.* cf. *indicus*, 3.1% in *A. tonsa*, and 5.2% in *C. chilensis*. The errors also varied in magnitude and in sign among developmental stages, with some stages yielding nearly 70% over-estimation. For copepod species with short generation times, even small errors could quickly propagate and result in highly skewed secondary production projection. Reliable secondary production measurements therefore require careful assessment of species-specific stage duration and between-stage growth when applying the MR method, and quantification of stage-specific live and dead individuals in the field.

1. Introduction

The population dynamics of copepods—the dominant metazoan zooplankton—is governed by three fundamental processes: Reproduction, growth, and mortality. Of these, reproduction is the most frequently measured as egg production by adult copepods (Mauchline, 1998). Somatic growth of adult copepods is often assumed to be negligible, whereas growth of younger stages can be challenging to measure, and in the absence of relevant data, it is often (incorrectly) assumed to be equal to adult reproduction rate (Hirst and Bunker, 2003). As the younger stages develop, they molt and increase somatic mass between stages. This characteristic allows scientists to conduct short-term incubation experiments and measure molting and biomass change between consecutive stages, from which they derive the growth rate—this is the commonly used molting rate (MR) method for estimating copepod secondary production (Runge et al., 1985; Kimmerer and McKinnon, 1987). Theoretical study and meta-analysis of literature data, however, suggest that the MR method is subject to errors when researchers fail to account for uneven stage duration and uneven somatic growth between stages (Hirst et al., 2005, 2014). Nevertheless, direct evaluation of errors associated with the MR method in the field has not been attempted.

The final parameter, mortality, is perhaps the least constrained in copepod population dynamics (Runge et al., 2004). Traditional research for convenience assumes that mortality is driven solely by predation and therefore can be derived from changes in population abundances. A

* Corresponding author.
E-mail address: pahidalg@udec.cl (P. Hidalgo).

https://doi.org/10.1016/j.pocean.2018.06.008
Received 20 July 2017; Received in revised form 8 May 2018; Accepted 20 June 2018
Available online 21 June 2018

corollary to this practice is that field sampling simply ignores the live/dead status of the animals. It is, however, illogical to believe all copepods *in situ* are alive. Copepods and other zooplankton can suffer non-predation mortality that leaves behind carcasses (Tang et al., 2014). A meta-analysis of literature data suggests that up to one-third of *in situ* copepod mortality cannot be explained by predation (Hirst and Kiørboe, 2002). Ignorance of carcass occurrences also causes errors to other population parameters because dead copepods obviously do not molt, grow or reproduce. A modelling study showed that ignoring even a small magnitude of carcass abundance and non-predation mortality could lead to unrealistic projection of population growth (Elliott and Tang, 2011).

Here we report a year-long field study where we measured and compared the secondary production of different copepod species, and assessed the errors due to uneven molting and growth patterns and occurrence of carcasses. Our results showed that error in secondary production estimation varied among co-existing species, and switched between over-and under-estimation according to months or developmental stages. Reliable secondary production measurements therefore require careful assessment of species-specific stage duration, between-stage growth and stage-specific live/dead composition in the field, especially for species with a short generation time.

2. Materials and methods

2.1. In situ live/dead copepod compositions

The study was conducted in northern Chile (Mejillones Bay) within the Humboldt Current System (HCS). This region is known for its active and intermittent coastal upwelling (Marín et al., 1993) that brings in shallow, oxygen-poor cold water masses associated with the Oxygen Minimum Zone (OMZ) (Marín and Olivares, 1999), and supports high levels of primary production (Daneri et al., 2000) and fish yield (Alheit and Bernal, 1993; Arcos et al., 2001).

Its metazooplankton community is dominated by copepods (Hidalgo et al., 2010; Escribano et al., 2012; Pino-Pinuer et al., 2014). Monthly sampling was performed in 2010 at three stations along a coastal transect: St–1 (23°04.2′S, 70°25.8′W; maximum station depth (z_{max}) = 60 m), St–2 (23°02.4′S, 70°27.0′W; z_{max} = 90 m) and St–3 (23°0.2′S, 70°28.2′W; z_{max} = 120 m). Water temperature, salinity, and dissolved oxygen (DO) were measured at each station by an autonomous profiler SeaBird SBE–19. Water samples were collected at 10 m (within the mixed layer) using a 5-L Niskin bottle, and their chlorophyll-*a* contents were analyzed fluorometrically (Morales and Anabalon, 2012; Anabalón et al., 2014).

Copepods were collected by vertical hauls through 0–30 m during the day using a WP–2 net with a non-filtering cod (200 μm mesh and 50-cm mouth diameter) equipped with a flowmeter. Our target copepod species are concentrated in this upper layer and do not exhibit diel vertical migration in this region (Escribano et al., 2009). Upon retrieval of the net, the samples were transferred to a chilled thermal box and immediately treated with the vital stain Neutral Red (Elliott and Tang, 2009; modified by Yáñez (2009) and Yáñez et al. (2012) for local conditions). Briefly, each sample was incubated with 2–4 mL of Neutral Red stock solution (0.5% w/v) for 10 min. Afterward, the stained samples were concentrated and briefly rinsed with filtered seawater to remove excess stain, then preserved in 4% neutralized formalin solution in the dark, and processed further in the laboratory within 3–6 months. In the laboratory, the stained samples were concentrated and briefly rinsed with filtered seawater, then acidified by 0.3 mL of 1 M acetic acid to develop the stain's color. Under a stereo-microscope (20–40×), the dominant copepod species *Paracalanus* cf. *indicus*, *Acartia tonsa* and *Calanus chilensis* were counted and identified to developmental stages. Individuals there were alive at the time of sampling appeared red, whereas dead ones remained unstained.

2.2. Molting rate experiments

Molting rate experiments were conducted with the three dominant copepod species in the region: *P.* cf. *indicus*, *A. tonsa*, and *C. chilensis*. Copepods were collected by oblique tows of a WP–2 net with a non–-filtering cod end from the upper 50 m at St–2 and St–3. The samples were immediately diluted in seawater and transported to the laboratory within 1–2 h. Additionally, seawater was collected with Niskin bottles at 10 m for the incubation. Upon return to the laboratory, live copepods were sorted by stage. Thirty individuals of each copepodid stage were randomly selected to measure prosome length, mean dry mass, carbon and nitrogen contents.

To determine mass–at–entry and mass–at–exit of each stage, stage C4, C5 and adult male and adult female individuals were each incubated in 23 μm-filtered seawater in 500 mL containers. A total of 45 individuals of C4, 40 C5, 80 adult male and 80 adult female were incubated at 15 °C for 24 h. Afterward, the animals were checked for stage and condition; those that had molted to the next stage were measured for prosome length, dry mass, carbon and nitrogen contents.

To set up the molting rate experiments, copepods were sorted in a temperature-controlled room set at near *in situ* temperature at 10-m depth. Groups of 10 individuals for each copepodid stage, in triplicate, were incubated in 200 mL vials containing 23-μm filtered seawater. Every 24 h, the initial stage, subsequent stage, molts and carcasses were counted. Dry masses of C1 and C2 were calculated from body lengths based on published conversion factors (Chisholm and Roff, 1990 for *P.* cf. *indicus* and *A. tonsa*; Escribano, 1998 for *C. chilensis*). For C3, C4 and C5 stages, dry masses were measured on a Cahn C-32 microbalance (0.001 mg precision) after being dried at 60 °C for 24 h; body C and N contents were measured with a Thermo Scientific Flash EA 1112 HT Elemental Analyzer at the Universidad de Concepcion. We present all masses as geometric means for the specific stages. In total, we conducted 29 experiments with *P.* cf. *indicus* in February, March, and April; 42 experiments with *A. tonsa* in February, April, August, September, and November, and 31 experiments with *C. chilensis* in August and September.

2.3. In situ copepod live/dead abundances

The mesh size we used was not appropriate for capturing the small nauplii; therefore, we only presented the data for copepodid stages (C1 to adult). To account for possible under-sampling of the small copepodid stages with the 200 μm mesh, we derived correction factors by comparing the abundances of all stages of each species caught by a 200 μm mesh vs. a 100 μm mesh (see Eqs. (1) and (2) in Table 1; also Supplementary Material). Additionally, abundances were examined with a sensitivity analysis to assess their effect on the estimates of secondary production. The model responds accurately despite variation in the correction factor (between low and high values), suggesting it is a robust model (Fig. S1 in Supplementary Material). Then we applied the correction factors only for C1–C3 of *Acartia tonsa* and *Paracalanus* cf. *indicus*, and C1 and C2 of *Calanus chilensis*, as there were no differences between mesh sizes for the later stages (Tables S1 and S2 in Supplementary Material).

2.4. Secondary production calculations

Secondary productions of the three copepod species were calculated in different ways (Table 1). Firstly, we used the conventional MR equations to calculate the stage-specific secondary production, and the summation of all stages in each month gave the monthly secondary production for each species (NSP_{MR}). Next, we used the modified MR equations of Hirst et al. (2005) to calculate the monthly secondary production (NSP_H) by accounting for uneven stage duration and uneven between-stage growth. Lastly, we corrected both secondary production estimates by accounting for the occurrence of carcasses (CSP_{MR} and

Table 1
Parameters and formulations for calculating copepod secondary production.

Parameter	Symbol	Unit	Note
Molting rate	MR	d^{-1}	Stage-specific MR is indicated by subscript *i*
Number of individuals in molting rate experiment	N		Consecutive stages are indicated by subscripts *i* and *i + 1*
Time	T	h	
Mean weight of stage *i*	W_i	mg	
Mean weight of stage *i + 1*	W_{i+1}	mg	
Total biomass *in situ*	B_i	mg C m^{-2}	No differentiation of live and dead individuals
Biomass of live individuals *in situ*	B_{i_a}	mg C m^{-2}	
Numerical abundance *in situ*	n_i	m^{-2}	No differentiation of live and dead individuals
Numerical abundance of live individuals *in situ*	n_{i_a}	m^{-2}	
Abundances Correction Factor	CFn_i	no unit	Abundances of dead individuals
Abundances Correction Factor	CFn_{i_a}	no unit	Abundances of live individuals
Stage-specific growth rate estimated from MR method	g_{i_MR}	d^{-1}	
Non-corrected secondary production from MR method	NSP_{MR}	mg C m^{-2} d^{-1}	No differentiation of live and dead individuals
Corrected secondary production from MR method	CSP_{MR}	mg C m^{-2} d^{-1}	NSP_{MR} estimates corrected for occurrence of carcasses
Proportion of animals which molted during incubation	M		Stage-specific M is indicated by the subscript *i*
Incubation period	L	d	
Stage duration	D	d^{-1}	Calculated as D = 1/MR
Mortality rates during incubation	B	d^{-1}	Calculated from proportion of carcasses according to Elliott and Tang (2011); stage specific β is indicated by subscript *i*
Actual development time of stage *i*	D_{i_actual}	d^{-1}	Calculated from stage-specific β_i and M_i
Actual development time of stage *i + 1*	D_{i+1_actual}	d^{-1}	Calculated from stage-specific β_{i+1}, and M_{i+1}
Geometric mean weight of stage *i*	$\hat{W}_i$	mg	Including the weight of molt lost between stages
Geometric mean weight of stage *i + 1*	$\hat{W}_{i+1}$	mg	Including the weight of molt lost between stages
Growth rate g_i from the mid-point of stages *i* to *i + 1*	$g_{i\rightarrow i+1}$	d^{-1}	For C1-C4 stages
Growth rate g_i calculated based on W_{i_entry} and W_{i_exit}	g_{i_corr}	d^{-1}	For C5 where the following stage (*i + 1*) does not molt (Hirst et al., 2005)
Mass at entry	W_{i_entry}	mg	Arithmetic mean weights at point of entry to C5
Mass at exit	W_{i_exit}	mg	Arithmetic mean weights at point of exit from C5
Non-corrected secondary production from modified MR method	NSP_H	mg C m^{-2} d^{-1}	No differentiation of live and dead individuals
Corrected secondary production from modified MR method	CSP_H	mg C m^{-2} d^{-1}	NSP_H estimates corrected for the occurrence of carcasses

Calculations of correction factor

$$CF_i = \frac{n_{i(100\mu m)}}{n_{i(200\mu m)}} \quad (1)$$

$$CF_{i\_a} = \frac{n_{i\_a(100\mu m)}}{n_{i\_a(200\mu m)}} \quad (2)$$

Calculations of secondary production

MR method (NSP_{MR}) (Runge et al., 1985; Kimmerer and McKinnon, 1987)

$$MR = \left(\frac{N_i + N_{i+1}}{N_i}\right) \times t \quad (3)$$

$$g_{i\_MR} = \ln\left(\frac{W_{i+1}}{W_i}\right) \times MR_i \quad (4)$$

$B_i = \sum_{i=1}^{N} (W_i n_i) \times 0.4$ where 0.4 is the factor to convert dry weight to carbon (Escribano et al. 2007, 2016) (5)

$$NSP_{MR} = \sum_{i=1}^{N} (B_i g_{i\_MR}) \quad (6)$$

MR method corrected for carcasses (CSP_{MR}). To correct NSP_{MR} for the occurrence of carcasses, Eqs. (3) and (4) are changed to

$$B_{i\_a} = \sum_{i=1}^{N} (W_i n_{i\_a}) \times 0.4 \quad (7)$$

$$CSP_{MR} = \sum_{i=1}^{N} (B_{i\_a} g_{i\_MR}) \quad (8)$$

Modified MR method (NSP_H) (Hirst et al., 2005)

$$M = \exp(-\beta D)[\exp(\beta L) - 1]/[1 - \exp(-\beta D)] \quad (9)$$

$$D_{i\_actual} = \ln\{1 + [\exp(\beta_i L) - 1]/M_i\}/\beta_i \quad (10)$$

$$g_{i\rightarrow i+1} = \ln\left(\frac{\hat{W}_{i+1}}{\hat{W}_i}\right) \div [(D_{i\_actual} + D_{i+1\_actual})/2] \quad (11)$$

$$g_{i\_corr} = \ln\left(\frac{W_{i\_exit}}{W_i}\right) \times MR_i \quad (12)$$

$$B_i = \sum_{i=1}^{N} (W_i n_i) \times 0.4 \quad (13)$$

$$NSP_H = \sum_{i=1}^{N} (B_i g_i) \quad (14)$$

Modified MR method corrected for carcasses (CSP_H). To correct NSP_H for the occurrence of carcasses, Eqs. (11) and (12) are changed to

$$B_{i\_a} = \sum_{i=1}^{N} (W_i n_{i\_a}) \times 0.4 \quad (15)$$

$$CSP_H = \sum_{i=1}^{N} (B_{i\_a} g_i) \quad (16)$$

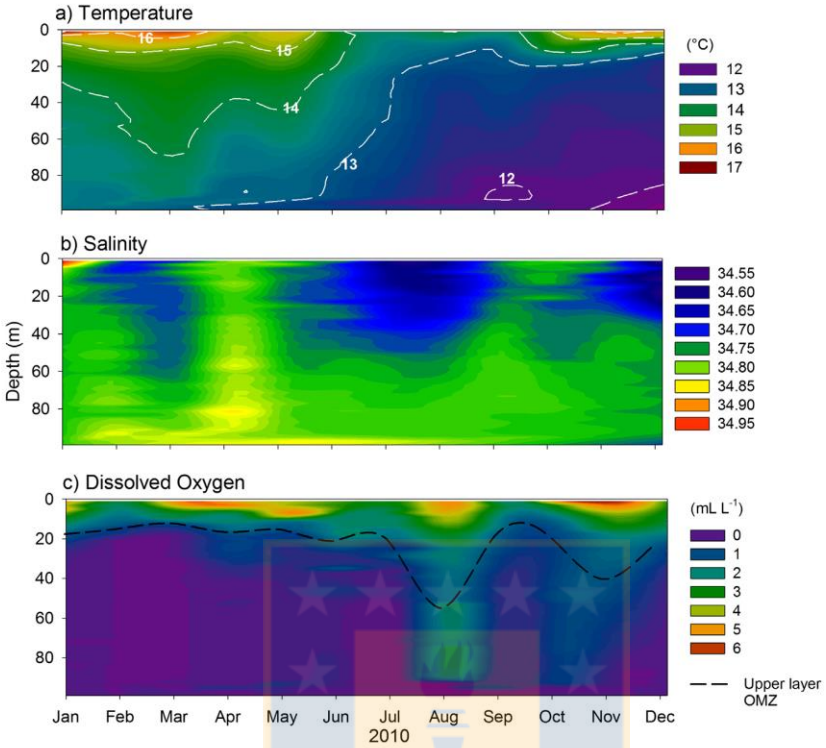

Fig. 1. Oceanographic conditions off Mejillones Bay, northern Chile, in 2010 (average of three stations): (a) Temperature, (b) Salinity and (c) Dissolved oxygen.

CSP_H).

2.5. Statistics

Normality was tested by the Kolmogorov-Smirnov test (Zar, 1984). When necessary, the data were log transformed (n + 1) to meet the requirement of normal distribution. Spatial (by stations) and temporal (by months) differences in the abundances of live and dead copepods were compared by ANOSIM pairwise comparisons. Seasonal growth rates (all stages combined) were grouped into Spring/Summer season (September–March) and Autumn/Winter season (April–August), and were then compared by *t*-test. Stage-specific growth rates (all months combined) were compared by ANOVA followed by Tukey's post–hoc test.

3. Results

3.1. General oceanographic conditions

The water column was thermally stratified except between July and September (Fig. 1a). The depth-average temperature ranged from 12.5 to 13.5 °C. Slightly less saline water masses were present in the upper 40 m for parts of the year (Fig. 1b). The depth-average salinity was 34.7–34.8 across the three stations. Well-oxygenated water was mostly limited to the upper 20 m (Fig. 1c). The upper limit of the OMZ (defined by DO = 1 mL O_2 L^{-1}) was at *ca.* 20 m during most of the year, except in August and November when it descended to ≥40 m, coinciding with the weakening of thermal stratification and intrusion of less saline waters. Chlorophyll-*a* concentrations within the mixed layer were considerably higher in the austral summer/autumn months than in the winter/spring months, opposite to the DO trend (Fig. 2).

3.2. In situ copepod live/dead abundances

There were significant spatial, but not temporal, differences in live copepod abundances of *P.* cf. *indicus*, and the opposite for *A. tonsa* and *C. chilensis* (Table 2). The abundances of live copepods were generally higher closer to shore (St–1 and St–2) than offshore (St–3). Copepod carcasses were present throughout the year for all three species, and at times were comparable or even exceeding live copepod abundances (Figs. 3–5). Contrary to live individuals, carcass abundances varied significantly between months, but not between stations for *P.* cf. *indicus*, and the opposite for *A. tonsa* and *C. chilensis* (Table 2). Carcasses of *P.* cf. *indicus* were dominated by the younger copepodites (C1–C3), and their percentages peaked in April and July/August. *A. tonsa* carcasses showed peak percentages in April and August, and were dominated by older stages (C4–adult). In contrast, *C. chilensis* carcasses showed peak percentages in June and October, consisting of mostly C1–C4, and a smaller November peak of adult carcasses.

3.3. Copepod molting and growth experiments

The stage duration ranged between 2.1 and 16 d for the different copepodid stages (C1–C5) of *P.* cf. *indicus*, whereas it was 1.2–10 d for *A. tonsa*, and 1.2–8 d for *C. chilensis*. None of the copepod species showed significant seasonal differences in growth rates ($P > 0.05$) (Table 3). Stage-specific growth rates of *P.* cf. *indicus*, *A. tonsa* and *C. chilensis* ranged from 0.15 to 0.23 d^{-1}, 0.14 to 0.20 d^{-1} and 0.10 to 0.27 d^{-1}, respectively (Table 3). Only *C. chilensis* showed significant variations in stage-specific growth rates ($P = 0.008$), caused by the significantly higher growth rate in C4 (Table 3).

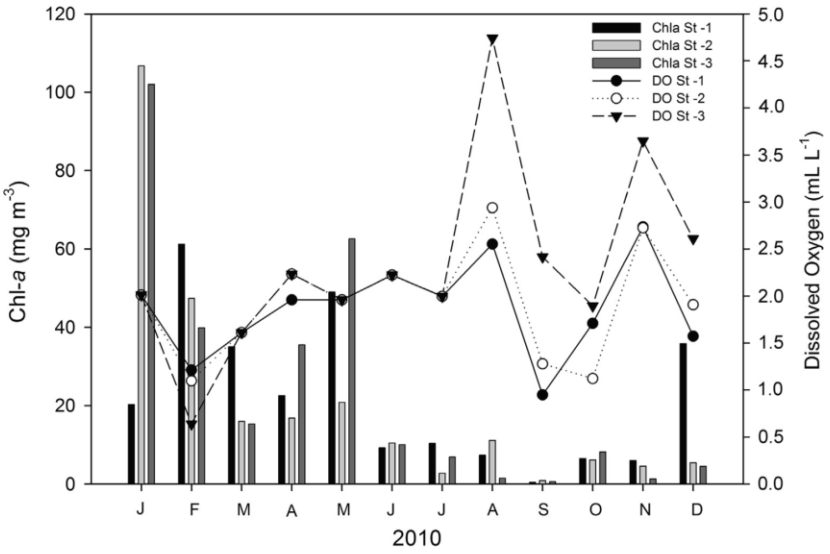

Fig. 2. Chlorophyll-*a* (at 10 m) and average DO (0–30 m) at St–1, St–2 and St–3 in different months during this study.

Table 2
ANOSIM pairwise comparisons of abundances of live and dead individuals of *Paracalanus* cf. *indicus*, *Acartia tonsa* and *Calanus chilensis* at different stations and months in the Mejillones Bay during 2010. *r* value is the strength of the factors on the samples (number of levels in each factor as stations = 3, Months = 12.

Source of variance		*P.* cf. *indicus*		*A. tonsa*		*C. chilensis*	
		Live	Dead	Live	Dead	Live	Dead
Stations	*r*	0.643	−0.029	0.047	−0.059	0.002	−0.015
	p	0.001*	0.828	0.143	0.057	0.410	0.634
Months	*r*	−0.155	0.328	218	0.244	0.357	0.480
	p	0.960	0.001*	0.006*	0.011*	0.010*	0.010*

* Significant difference at $p < 0.05$.

3.4. Secondary production estimations

The estimated secondary production (sum of all stages; averaged across the three stations) of *P.* cf. *indicus* showed the highest value in February and the lowest value in September (Fig. 6a). The production of *A. tonsa* had its highest value in March and lowest in July, whereas the production of *C. chilensis* was concentrated in the autumn–winter period (May–August) (Fig. 6b, c). The modified MR method produced substantially different secondary production values for *P.* cf. *indicus* (6a), and the CSP_H values were 33–96% higher than CSP_{MR}. In contrast, the CSP_H values were comparable to CSP_{MR} for *A. tonsa* (within 1–13%) and *C. chilensis* (within 1–20%; Fig. 6b, c).

Presence of carcasses introduced relatively small errors to the conventional MR method (CSP_{MR} vs. NSP_{MR}) and lowered the estimation by an average of 2.3% (*P.* cf. *indicus*), 0.8% (*A. tonsa*) and 2.6% (*C. chilensis*) (data not shown). Likewise, presence of carcasses led to an average of 0.7–3.7% discrepancy between CSP_H and NSP_H (data not shown).

By considering CSP_H as the "true" secondary production values, we estimated the error associated with conventional MR method as $[(NSP_{MR} - CSP_H)/CSP_H] \times 100\%$ (Table 4). The error was negative (i.e. underestimation) for *P.* cf. *indicus* throughout the year, with a mean of 39.2% (SD 6.6%). The error was small and consistently positive for *A. tonsa* (mean ± SD; 3.1 ± 2.8%). In contrast, the error switched sign repeatedly for *C. chilensis*, and was concentrated in January, July and November (mean ± SD; 5.2 ± 14.9%) (Table 4).

Similarly, we calculated the stage-specific production and examined how the error was distributed among the different stages (Fig. 7a,b,c). For *P.* cf. *indicus*, most of the error was associated with C1, C5 (*ca.* +65%) and C4 (−56%). For *A. tonsa*, the error was concentrated in C4 and C5 (+61 to +69%). The largest error for *C. chilensis* was found in C2 (+66%), followed by C3 (+48%) and C4 (−38%).

4. Discussion

The HCS, as a part of the larger upwelling system off the west coast of South America, is a well–known, highly productive area for sardines and anchovies, which in turn support many predatory fish and bird species (Thiel et al., 2007). As both sardines and anchovies rely on zooplankton for food (Espinoza and Bertrand, 2008); much research effort has been dedicated to measuring the compositions, abundances, growth and production rates of the zooplankton, including copepods, within the HCS.

The water column of Mejillones Bay was characterized by thermal stratification and low DO for much of the year, except in winter months when the water column was more well mixed and the OMZ was restricted to the deeper depths, and when chlorophyll-*a* was nearly depleted. Previous studies have shown that changes in upwelling intensity (Escribano et al., 2012), the presence of thermal fronts, upwelling shadows acting as retention areas (Marín et al., 1993; Giraldo et al., 2002), and a shallow OMZ could aggregate and increase copepod diversity in the food–rich photic zone (Hidalgo and Escribano, 2008; Hidalgo et al., 2010). These factors, in addition to seasonal changes in food concentrations, affect the growth and development of copepods (Escribano, 1998; Poulet et al., 2007), and may explain the high temporal and spatial variabilities in copepod abundances in this study.

In past studies, copepod growth rates were estimated by fitting dry weight data to an exponential growth model (Escribano et al., 1997); alternatively, the MR method was used to resolve stage-specific growth rates (Vargas et al., 2007). The so–estimated growth rates were then applied to *in situ* biomass data to derive secondary production (Escribano and McLaren, 1999; Vargas et al., 2007). These and other approaches, however, suffer a fundamental oversight by ignoring the *in*

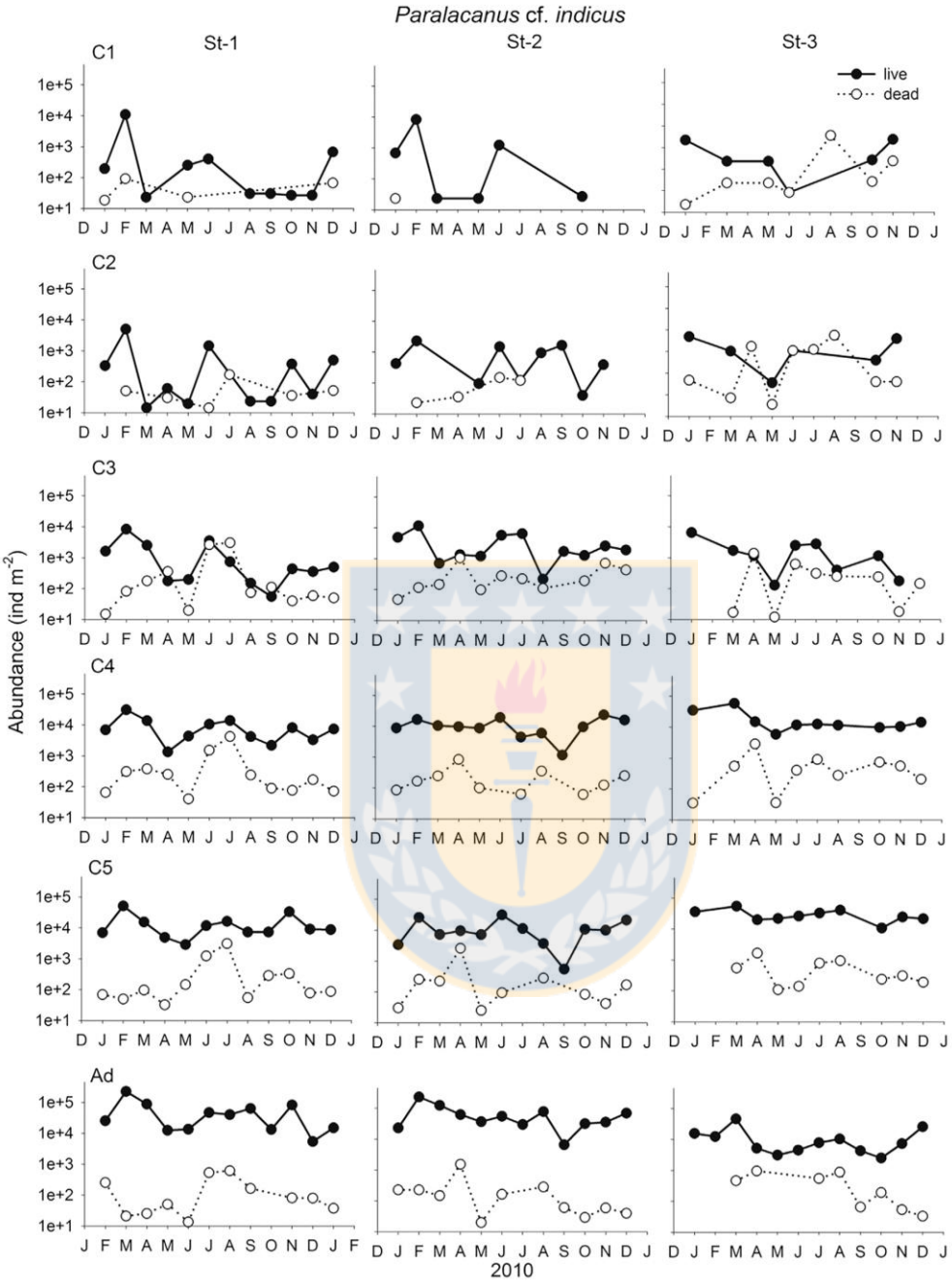

Fig. 3. Abundances of live and dead copepodid stage C1, C2, C3, C4, C5, and adults (Ad) of *Paracalanus* cf. *indicus* at the three stations in different months.

situ live/dead status of the copepods. It remains a common practice in field sampling where scientists simply preserve and count all copepods as 'live' (Harris et al., 2000). This has been partly due to the lack of methods for identifying live and dead individuals in the samples, and partly due to the ingrained perception that copepods only die of predation in the field (Hirst and Kiørboe, 2002). Recent advances in staining methods for distinguishing between live and dead individuals in field samples open the opportunities to make detailed quantification of copepod carcasses in the HCS, as well as to access the error they introduce into the secondary production estimation.

The total abundances of the three copepod species were higher closer to shore, similar to earlier observations (Escribano and Hidalgo,

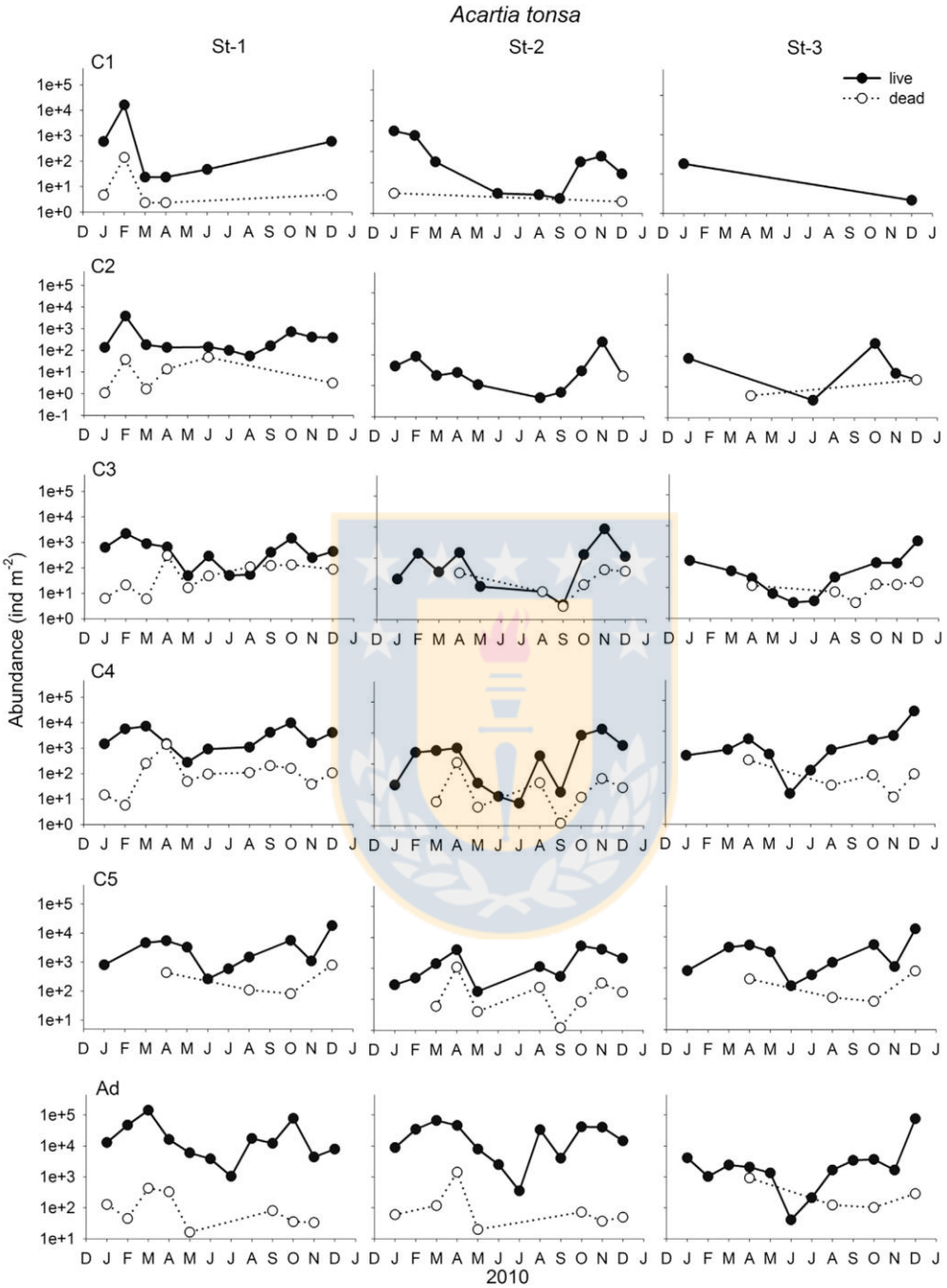

Fig. 4. Abundances of live and dead copepodid stage C1, C2, C3, C4, C5, and adults (Ad) of *Acartia tonsa* at the three stations in different months.

2000; Giraldo et al., 2006). The abundances of both live and dead copepods varied considerably across stations, months and stages, reflecting the highly dynamic and heterogeneous environments in the region (Escribano, 1998; Giraldo et al., 2002; Escribano et al., 2012). Elliott and Tang (2009, 2011) observed higher percentages of carcasses and higher non-predation mortality rates in nauplii than in the older stages. Although we did not include nauplii in this study, we also found that the high carcass percentages were principally composed of young

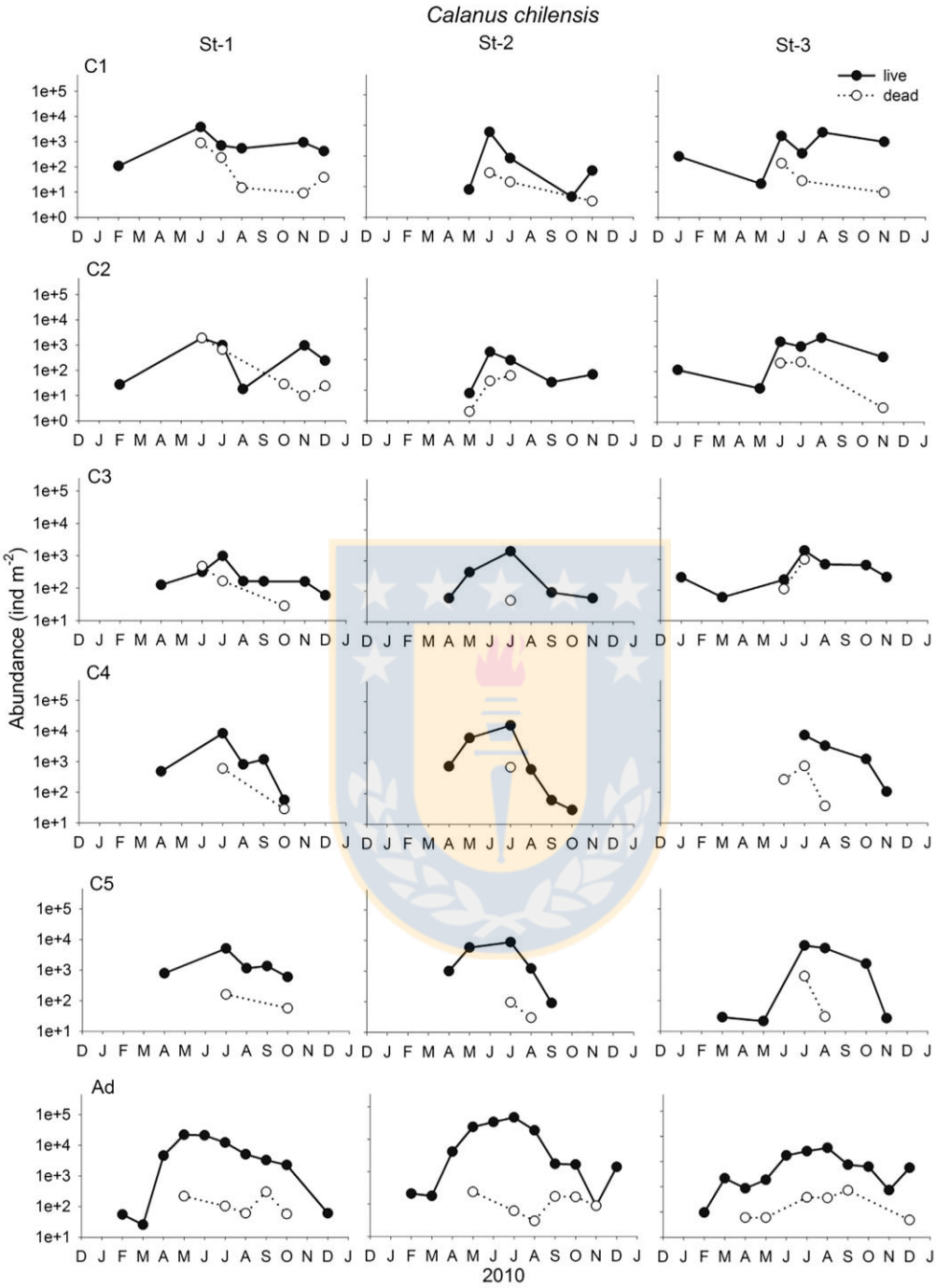

Fig. 5. Abundances of live and dead copepodid stage C1, C2, C3, C4, C5, and adults (Ad) of *Calanus chilensis* at the three stations in different months.

copepodites, suggesting that the younger stages were more susceptible to environmental stresses in this dynamic region, one of which could be the low DO. Intermittent intrusion of oxygen-poor water associated with coastal upwelling is a common feature in the region (Marín et al., 1993), which could cause episodic hypoxia and copepod mortality, similar to other studies (Yañez et al., 2012; Elliott et al., 2010, 2013).

Copepod carcasses are not necessarily lost from the food web. Some of them can be eaten by planktivores (Elliott et al., 2010), or be

Table 3
Summary of seasonal and stage−specific growth rates (g; d^{-1}) (mean ± SD) of *Paracalanus* cf. *indicus*, *Acartia tonsa* and *Calanus chilensis*. (n = number of measurements).

	P. cf. *indicus*		*A. tonsa*		*C. chilensis*	
Spring/Summer	0.21 ± 0.07	(n = 140)	0.12 ± 0.06	(n = 60)	0.21 ± 0.05	(n = 60)
Autumn/Winter	0.20 ± 0.07	(n = 150)	0.18 ± 0.10	(n = 260)	0.21 ± 0.08	(n = 250)
C1	0.22 ± 0.02	(n = 30)	0.20 ± 0.01	(n = 30)	0.22 ± 0.08	(n = 50)
C2	0.19 ± 0.06	(n = 30)	0.16 ± 0.03	(n = 30)	0.10 ± 0.05	(n = 40)
C3	0.21 ± 0.07	(n = 100)	0.14 ± 0.03	(n = 60)	0.18 ± 0.05	(n = 50)
C4	0.23 ± 0.06	(n = 60)	0.15 ± 0.06	(n = 180)	0.27 ± 0.07	(n = 70)
C5	0.15 ± 0.01	(n = 70)	0.17 ± 0.04	(n = 120)	0.19 ± 0.06	(n = 100)

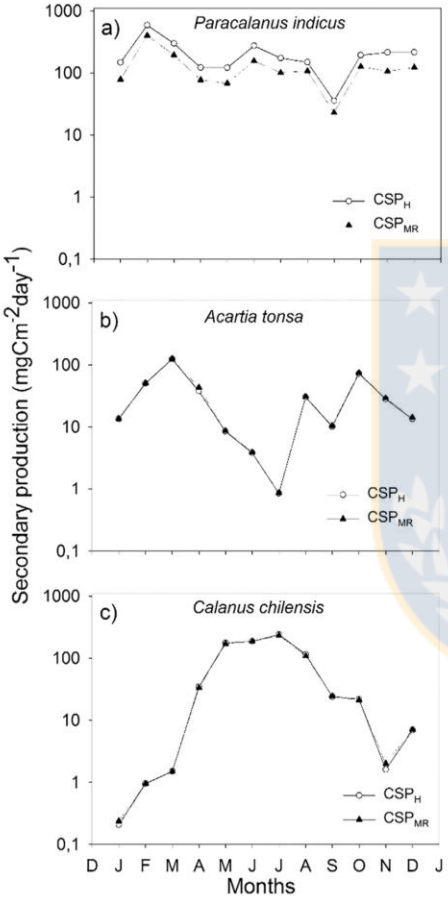

Fig. 6. Secondary production estimates and stage-specific errors for *Paracalanus* cf. *indicus* (a), *Acartia tonsa* (b), and *Calanus chilensis* (c). CSP_{MR} is secondary production estimates (sum of all stages; averaged across stations) based on conventional MR method after correction for carcasses. CSP_H is secondary productions based on modified MR method after correction for carcasses.

incorporated into the microbial food web (Tang et al., 2009; Bickel and Tang, 2010), with the remainder contributing to the sinking flux (Sampei et al., 2009, 2012; Ivory et al., 2014). Nevertheless, a dead copepod obviously "behaves" very differently than a live copepod, and understanding the fate of the carcasses will improve our knowledge of how they influence the ecosystem. More importantly, because dead individuals do not contribute to population growth, appropriate corrections are required for secondary production estimation.

Table 4
Errors in secondary production estimates. By considering CSP_H as the "true" secondary production values, we estimated the error associated with conventional MR method as $[(NSP_{MR} - CSP_H)/CSP_H] \times 100\%$. Negative and positive values represent the underestimated and overestimated secondary production, respectively.

	Paracalanus cf. *indicus*	*Acartia tonsa*	*Calanus chilensis*
January	−46.3	1.2	14.9
February	−31.6	1.7	−0.5
March	−34.9	1.5	6.2
April	−22.6	6.2	−4.4
May	−37.0	4.0	−3.6
June	−43.8	1.2	6.6
July	−43.0	1.1	16.9
August	−42.1	0.8	−5.4
September	−27.9	2.8	−5.5
October	−35.7	1.9	−7.8
November	−50.4	5.1	45.2
December	−43.1	10.1	0.1
Mean	**−39.2**	**3.1**	**5.2**
S.D.	**6.6**	**2.8**	**14.9**

While the MR method has been widely used to estimate secondary production (Runge and Roff, 2000), it is not without flaw (Rey-Rassat et al., 2002; Hirst et al., 2005, 2014). In this study, we quantified the errors in secondary production caused by the negligence of uneven stage duration and uneven between-stage growth, and the failure to differentiate live vs. dead copepods. Overall, our calculated range of errors based on field data was comparable to that derived from literature meta-analysis (Hirst et al., 2005, 2014). More importantly, our results showed that both the extent and sign of the error varied among the co–existing copepod species, and it was an order of magnitude higher in *P.* cf. *indicus* than in *A. tonsa* and *C. chilensis* (Table 4). *P.* cf. *indicus* is highly abundant throughout the HCS and plays major roles in the region's ecology (Escribano et al., 2012, 2016; Pino-Pinuer et al., 2014). This species is more likely to contribute carcasses than the other species, providing their greater abundance and potentially higher mortality. *P.* cf. *indicus* may rapidly respond to environmental variations (e.g. increased growth and development rates), and thus increasing the non-predatory mortality, as we observed in this study with the presence of carcasses. Our findings suggest that the secondary production estimation of this species is particularly error-prone, and extra caution is required when considering the regional food web dynamics and fisheries involving this species. The average errors for *A. tonsa* and *C. chilensis*, despite their lower values, are still important for consideration because even a small initial error, when propagating through generations, would result in a large error over time (Elliott and Tang, 2011). This is particularly important for copepod species with short generation times, such as those in the HCS (Hidalgo and Escribano, 2008; Escribano et al., 2014). Equally important is the observation that, within species, the error distribution was not uniform across months or across stages (Table 4, Fig. 6). Knowing when and where most of the error occurs may help scientists to design more

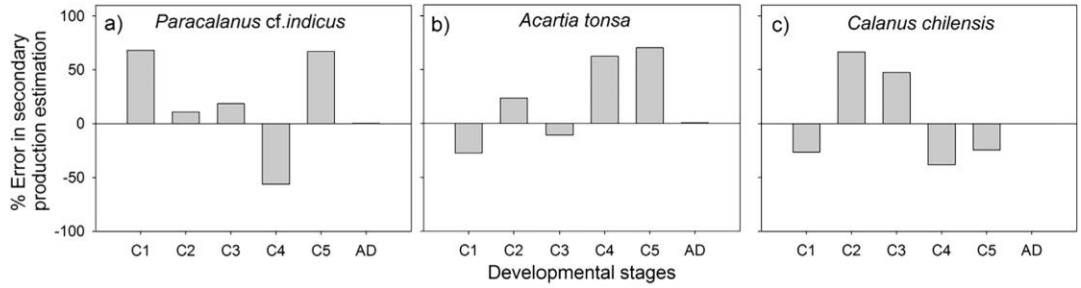

Fig. 7. Stage-specific errors for *Paracalanus* cf. *indicus* (a), *Acartia tonsa* (b), and *Calanus chilensis* (c) in secondary production estimation calculated based on average (n = 12) stage-specific NSP_{MR} and CSP_{H} (see text for explanation).

appropriate sampling and modelling strategies to minimize bias.

The Southwest Pacific region is strongly influenced by El Nino Southern Oscillation (ENSO). It is expected that climate change will intensify upwelling within the HCS (Echevin et al., 2012), with corresponding changes in hydrography, water chemistry, species diversity, and phenology (Hays et al., 2005). The potential increase in coastal upwelling events could promote blooms of chained diatoms that adversely affect the food supply for copepods (Vargas et al., 2006; Poulet et al., 2007). Stronger upwelling may also increase the shoaling of the OMZ and intensify hypoxia-related stresses. These projected changes may all lead to increasing incidents of non-predation mortality among the copepods. In future studies, efforts should be made to differentiate and quantify live and dead copepods *in situ*, and apply the appropriate corrections when estimating secondary production.

5. Conclusion

Copepod secondary production is a key parameter in ecology linking primary production to fishery yield, but reliable measurement of it remains challenging. This study used the first detailed quantitative data set of copepod live/dead compositions within the Chilean HCS, along with molting rate measurements, to evaluate errors associated with copepod secondary production estimation. We showed that (1) copepod carcasses were ubiquitous in the region; (2) without proper corrections for uneven molting and growth patterns and carcass occurrence, there could be substantial errors in secondary production estimation; and (3) the magnitude and sign of the errors varied among months, species, and life stages; (4) carcass presence resulted in a relatively small % error when compared to choice of models (MR vs H), but even small % error caused by the ignorance of live/dead composition may lead to a large error in production projection (Elliott and Tang, 2011), especially for species with a short generation time.

Acknowledgements

This work was supported by the CONICYT-FONDECYT No. 11090146 (P. Hidalgo) and CONICYT Collaborative Project CHILE–USA No. USA2012–0006 (P. Hidalgo). Yañez was supported by the Scholarship of CONICYT-PCHA/Doctorado Nacional/2013-21130213 and by Red Doctoral en Ciencia, Tecnología y Ambiente, REDOC CTA, University of Concepcion. Ruz was supported by the Scholarship of CONICYT-PCHA/Doctorado Nacional/2011-21110560. The authors thank Dr. David Elliott for helping with data analysis, Captain Juan Menares and the crew of R/V Menachos for assistance in the field, and Dr. Andrew Hirst and Prof. Thomas Kiørboe for valuable comments and suggestions on earlier drafts of the manuscript. This work is a contribution by Millennium Institute of Oceanography ICM 120019.

Appendix A. Supplementary material

Supplementary data associated with this article can be found, in the online version, at https://doi.org/10.1016/j.pocean.2018.06.008.

References

Alheit, J., Bernal, P., 1993. Effects of physical and biological changes on the biomass yield of the Humboldt current ecosystem. In: Sherman, K., Alexander, L.M., Gold, B.D. (Eds.), Large Marine Ecosystems. American Association for the Advancement of Science Press, Washington, DC, pp. 53–58.

Anabalón, V., Arísteguia, J., Morales, C.E., Andrade, I., Benavides, M., Correa-Ramírez, M.A., Espino, M., Ettahiri, O., Hormazabal, S., Makaoui, A., Montero, M.F., Orbi, A., 2014. The structure of planktonic communities under variable coastal upwelling conditions off Cape Ghir (31°N) in the Canary Current System (NW Africa). Progr. Oceanogr. 120, 320–339.

Arcos, D.F., Cubillos, L.A., Nuñez, S.P., 2001. The jack mackerel fishery and El Niño 1997–98 effects of Chile. Progr. Oceanogr. 49, 597–617.

Bickel, S.L., Tang, K.W., 2010. Microbial decomposition of proteins and lipids in copepod versus rotifer carcasses. Mar. Biol. 157, 1613–1624.

Chisholm, L., Roff, J., 1990. Size-weight relationships and biomass of tropical neritic copepods off Kingston, Jamaica. Mar. Biol. 106, 71–77.

Daneri, G., Dellarossa, V., Quiñones, R., Jacob, B., Montero, P., Ulloa, O., 2000. Primary production and community respiration in the Humboldt Current System off Chile and associated oceanic areas. Mar. Ecol. Prog. Ser. 97, 41–49.

Echevin, V., Goubanova, K., Belmadani, A., Dewitte, B., 2012. Sensitivity of the Humboldt Current system to global warming: a downscaling experiment of the IPSL-CM4 model. Clim. Dyn. 38, 761–774.

Elliott, D.T., Tang, K.W., 2009. Simple staining method for differentiating live and dead marine zooplankton in field samples. Limnol. Oceanogr. Methods 7, 585–594.

Elliott, D.T., Harris, C.K., Tang, K.W., 2010. Dead in the water: The fate of copepod carcasses in the York River estuary, Virginia. Limnol. Oceanogr. 55, 1821–1834.

Elliott, D.T., Tang, K.W., 2011. Influence of carcass abundance on estimates of mortality and assessment of population dynamics in *Acartia tonsa*. Mar. Ecol. Prog. Ser. 427, 1–12.

Elliott, D.T., Pierson, J.J., Roman, M., 2013. Copepods and hypoxia in Chesapeake Bay: abundance, vertical position and non-predatory mortality. J. Plankton Res. 1–8.

Escribano, R., Irribarren, C., Rodriguez, L., 1997. Influence of food quantity and temperature on development and growth of the marine copepod *Calanus chilensis* from northern Chile. Mar. Biol. 128, 281–288.

Escribano, R., 1998. Population dynamics of *Calanus chilensis* in the Chilean eastern boundary Humboldt Current. Fish. Oceanogr. 7, 241–251.

Escribano, R., McLaren, I., 1999. Production of *Calanus chilensis* in the upwelling area of Antofagasta, northern Chile. Mar. Ecol. Progr. Ser. 177, 147–156.

Escribano, R., Hidalgo, P., 2000. Spatial distribution of copepods in the north of the Humboldt Current region off Chile during coastal upwelling. J. Mar. Biol. Assoc. UK 80, 283–290.

Escribano, R., Hidalgo, P., Krautz, C., 2009. Zooplankton associated with the oxygen minimum zone system in the northern upwelling region of Chile during March 2000. Deep-Sea Res. II 56, 1083–1094.

Escribano, R., Hidalgo, P., Fuentes, M., Donoso, K., 2012. Zooplankton time series in the coastal zone off Chile: Variation in upwelling and responses of the copepod community. Progr. Oceanogr. 97, 74–186.

Escribano, R., Hidalgo, P., Valdes, V., Frederick, L., 2014. Temperature effects on development and reproduction of copepods in the Humboldt Current: the advantage of rapid growth. J. Plankton Res. 36, 104–116.

Escribano, R., Bustos-Ríos, E., Hidalgo, P., Morales, C.E., 2016. Non-limiting food conditions for growth and production of the copepod community in a highly productive upwelling zone. Cont. Shelf Res. 126, 17–114.

Espinoza, P., Bertrand, A., 2008. Revisiting Peruvian anchovy (*Engraulis ringens*) trophodynamics provides a new vision of the Humboldt Current system. Progr. Oceanogr. 79, 215–227.

Giraldo, A., Escribano, R., Marin, V.H., 2002. Spatial distribution of *Calanus chilensis* off

Mejillones Peninsula (northern Chile): ecological consequences upon coastal upwelling. Mar. Ecol. Progr. Ser. 230, 225–234.
Giraldo, A., Escribano, R., Marin, V.H., 2006. A field test of temperature effects on ecophysiological responses of copepodid *Calanus chilensis* during coastal upwelling in northern Chile. Cont. Shelf Res. 26, 1307–1315.
Harris, R., Wiebe, P., Lenz, J., Skjoldal, H.R., Huntley, M., 2000. ICES Zooplankton Methology Manual. Academic Press, San Diego, USA.
Hays, G., Richardson, A., Robinson, C., 2005. Climate change and marine plankton. Trends Ecol. Evol. 20, 337–344.
Hidalgo, P., Escribano, R., 2008. The life cycles of two coexisting copepods, *Calanus chilensis* and *Centropages brachiatus*, in the upwelling zone off northern Chile (23°S). Mar. Biol. 155, 429–442.
Hidalgo, P., Escribano, R., Vergara, O., Jorquera, E., Donoso, K., Mendoza, P., 2010. Patterns of copepod diversity in the Chilean coastal upwelling system. Deep-Sea Res. Part II 57, 2089–2097.
Hirst, A.G., Bunker, A.J., 2003. Growth of marine planktonic copepods: global rates and patterns in relation to chlorophyll a, temperature, and body weight. Limnol. Oceanogr. 48, 1988–2010.
Hirst, A.G., Kiørboe, T., 2002. Mortality of marine planktonic copepods: global rates and patterns. Mar. Ecol. Progr. Ser. 230, 195–209.
Hirst, A.G., Peterson, W.T., Rothery, P., 2005. Errors in juvenile copepod growth rate estimates are widespread: problems with the Moult Rate method. Mar. Ecol. Progr. Ser. 296, 263–279.
Hirst, A.G., Keister, J.E., Richardson, A.J., Ward, P., Shreeve, R.S., Escribano, R., 2014. Re-assessing copepod growth using the Moult Rate Method. J. Plankton Res. 36, 1224–1232.
Ivory, J.A., Tang, K.W., Takahashi, K., 2014. Use of Neutral Red in short-term sediment traps to distinguish between zooplankton swimmers and carcasses. Mar. Ecol. Progr. Ser. 505, 107–117.
Kimmerer, W.J., McKinnon, D., 1987. Growth, mortality, and secondary production of the copepod *Acartia tranteri* in Westernport Bay. Australia. Limnol. Oceanogr. 32, 14–28.
Marín, V., Rodríguez, L., Vallejo, L., Fuenteseca, J., Oyarce, E., 1993. Efectos de la surgencia costera sobre la productividad primaria primavera de la Bahía Mejillones de Sur (Antofagasta, Chile). Rev. Chil. Hist. Nat. 66, 479–491.
Marín, V., Olivares, G., 1999. Estacionalidad de la productividad primaria en Bahía Mejillones del Sur (Chile): una aproximación proceso-funcional. Rev. Chil. Hist. Nat. 72, 629–641.
Mauchline, J., 1998. The Biology of Calanoid Copepods. Advances in Marine Biology. Academic Press.
Morales, C.E., Anabalon, V., 2012. Spatio-temporal distribution of chlorophyll-a, picoplankton, and nanoplankton during the spring upwelling season in the coastal area off Concepción, central-southern Chile. Oceanogr. Progr (special volume).
Pino-Pinuer, P., Escribano, R., Hidalgo, P., Riquelme-Bugueño, R., Schneider, W., 2014. Copepod community response to variable upwelling conditions off central-southern Chile during 2002–2004 and 2010–2012. Mar. Ecol. Progr. Ser. 515, 83–95.
Poulet, S.A., Escribano, R., Hidalgo, P., Cueff, A., Wichardc, T., Aguilera, V., Vargas, C.A., Pohnert, G., 2007. Collapse of *Calanus chilensis* reproduction in a marine environment with high diatom concentration. J. Exp. Mar. Bio. Ecol. 352, 187–199.
Rey-Rassat, C., Irigoien, X., Harris, R., Head, R., Carlotti, F., 2002. Growth and development of *Calanus helgolandicus* reared in the laboratory. Mar. Ecol. Progr. Ser. 238, 125–138.
Runge, J.A., McLaren, I.A., Corkett, C.J., Koslow, J.A., 1985. Molting rates and cohort development of *Calanus finmarchicus* and *Calanus glacialis* in the sea southwest Nova Scotia. Mar. Biol. 86, 241–246.
Runge, J.A., Roff, J.C., 2000. The measurement of growth and reproductive rates. In: Harris, R. (Ed.), ICES Zooplankton Methodology Manual. Academic, New York, pp. 401–454.
Runge, J.A., Franks, P.J., Gentleman, W.C., Megrey, B.A., Rose, K.A., Werner, F.E., Zakardjian, B., 2004. Diagnosis and prediction of variability in secondary production and fish recruitment processes: developments in physical-biological modelling. In: Robinson, A.R., Brink, K.H. (Eds.), The Sea. Harvard University Press, pp. 413–473.
Sampei, M., Sasaki, H., Hattori, H., Forest, A., Fortier, L., 2009. Significant contribution of passively sinking copepods to downward export flux in Arctic waters. Limnol. Oceanogr. 54, 1894–1900.
Sampei, M., Sasaki, H., Forest, A., Fortier, L., 2012. A substantial export flux of particulate organic carbon linked to sinking dead copepods during winter 2007–2008 in the Amundsen Gulf (southeastern Beaufort Sea, Arctic Ocean). Limnol. Oceanogr. 57, 90–96.
Tang, K.W., Bickel, S.L., Dziallas, C., Grossart, H.P., 2009. Microbial activities accompanying decomposition of cladoceran and copepod carcasses under different environmental conditions. Aquat. Microb. Ecol. 57, 89–100.
Tang, K.W., Gladyshev, M.I., Dubovskaya, O., Kirillin, G., Grossart, H.P., 2014. Zooplankton carcasses and non-predatory mortality in freshwater and inland sea environments. J. Plankton Res. 36, 597–612.
Thiel, M., et al., 2007. The Humboldt current system of northern and central Chile. Oceanogr. Mar. Biol.: Annu. Rev. 45, 195–344.
Vargas, C.A., Escribano, R., Poulet, S., 2006. Phytoplankton diversity determines time windows for successful zooplankton reproductive pulses. Ecology 87, 2992–2999.
Vargas, C.A., Martínez, R.A., Cuevas, L.A., Pavez, M.A., Cartes, C., González, H.E., Escribano, R., Daneri, G., 2007. The relative importance of microbial and classical food webs in a highly productive coastal upwelling area. Limnol. Oceanogr. 52, 1495–1510.
Yáñez, S., 2009. Tasa de mortalidad y desarrollo de Paracalanus cf. indicus (Copepoda: Calanoida) (Wolfender, 1905) en la zona Centro-Sur de Chile (36°S) asociada con la zona de mínimo de oxígeno. Seminario de título, Facultad de Ciencias Naturales y Oceanográficas, Universidad de Concepción, Concepción 65 pp.
Yañez, S., Hidalgo, P., Escribano, R., 2012. Mortalidad natural de *Paracalanus indicus* (Copepoda, Calanoida) en áreas de surgencia asociada a la zona de mínimo oxígeno en el Sistema de Corrientes de Humboldt: implicancias en el transporte pasivo del flujo de carbono. Rev. Biol. Mar. Oceanogr. 47, 295–310.
Zar, J.H., 1984. Biostatistical Analysis. Prentice-Hall International Inc., New Jersey, pp. 718.

4.2. CAPÍTULO 2: Degradación y composición bacterianan de carcasas de copépodos en aguas de bajo contenido de oxígeno: potenciales impactos en el ciclo del N y C

4.2.1. Bacterial community and decomposition of copepod carcasses associated to oxic and anoxic conditions

Artículo en preparación

Sonia Yañez

Doctorado en Oceanografía

Universidad de Concepción

Resumen

Los copépodos marinos forman uno de los grupos más abundantes del zooplancton en los océanos y han sido relacionados con varios grupos de diferentes especies de bacterias. Desde experimentos de laboratorio, nosotros seguimos el curso de la degradación de carcasas del copépodo marino *Acartia tonsa*. En condiciones óxicas, la degradación del cuerpo de los copépodos comenzó rápidamente hasta las 18 hrs de incubación, luego entre 18-24 hrs esta se observó relativamente estable, y se incrementó lentamente, alrededor del 20 % del cuerpo de las carcasas fue observado en las últimas 6 horas de incubación. En contraste, el proceso de degradación fue mucho más lento en condiciones anóxicas durante las primeras 18 hrs, luego este incrementó enormemente y más del 50% del cuerpo fue degradado alrededor de las 24 hrs, así continúo aumentando rápidamente durante las últimas 6 horas de incubación. Distintas comunidades bacterianas fueron observadas entre los diferentes tratamientos desde los experimentos de degradación, además de cambios y sucesión de estas comunidades a través de ambas incubaciones. Usando la secuenciación masiva Illumina del gen 16S fueron identificados los miembros de la comunidad bacteriana asociada a la degradación de carcasas del copépodo marino *A.tonsa*. Desde los análisis filogenéticos, podemos concluir que las carcasas de *A.tonsa* están asociados con tres phyla: Proteobacteria, Bacteroidetes y Verrucomicrobia. Vibrionaceae, Pseudoalteromonadaceae, Rhodobacteraceae, Flavobacteriaceae and Verrucomicrobiaceae fueron las familias de bacterias más abundantes. Mientras que, la presencia de genes marcadores

de desnitrificación *nirK* y *nosZ,* (producción N_2 y N_2O, respectivamente) fueron encontrados bajo condiciones anóxicas, principalmente asociados con el estadio final de degradación. Entonces, la investigación de carcasas de copépodos asociados a bacterias es importante debido a la función de estas carcasas y su degradación bacteriana como *hotspots* pelágicos que tienen implicancias biogeoquímicas en el ciclo del nitrógeno, a través de la desnitrificación. Sin embargo, se requieren más estudios para evaluar cuantitativamente la contribución de estas comunidades a los ciclos biogeoquímicos globales.

Palabras claves: Carcasas de copépodos, degradación bacteriana, comunidad bacteriana, Illumina secuenciación masiva, genes funcionales, ciclos biogeoquímicos.

Bacterial community and decomposition of copepod carcasses associated to oxic and anoxic conditions

Sonia Yáñez[1,2], Pamela Hidalgo[1,2], Nicole Trefault[3], Osvaldo Ulloa[2], Rodrigo De la Iglesia[4]

[1] Doctoral Program of Oceanography, Department of Oceanography, University of Concepción, P.O. Box 160C, Concepción, Chile.
[2] Millenium Institute of Oceanography, University of Concepción, P.O. Box 160C, Concepción, Chile.
[3] GEMA Center for Genomics, Ecology & Environment, Universidad Mayor. Camino La Pirámide 5750, Santiago, Chile.
[4] Department of Molecular Genetics and Microbiology, Pontificia Universidad Católica de Chile.

Corresponding author: pahidalg@udec.cl

Abstract

Marine copepods form one of the most abundant mesozooplankton groups in the oceans and are associated with various numbers of different bacterial species. By the use of laboratory experiments, we followed the course of decomposition of the carcass of the marine copepod *Acartia tonsa*. In oxic conditions, copepod bodies begun to degrade rapidly at the initial 18 h, with a slow increased during the rest of the experiment of incubation, later between 18 − 24h it remained relatively stable, and then slowly increased, about 20% of bodies of carcasses was measured during the 6 last hours. In contrast, the decomposition process was much slower in the anoxic conditions during the 18 first hours, and then a high increase of >50% was observed over 24 hours of incubation, increasing greatly and quickly over the last 6 hours. Using Illumina sequencing of the 16S rRNA gene we identified members of the bacterial community associated with carcass decomposition of *A. tonsa*. Different bacterial communities were found between the different treatments of the decomposition experiments. From the phylogenetic analysis, it could be concluded that the investigated marine copepod carcass was associated with bacteria of three phyla: Proteobacteria, Bacteroidetes and Verrucomicrobia. Whereas, Vibrionaceae, Pseudoalteromonadaceae, Rhodobacteraceae, Flabobacteriaceae and Verrucomicrobiaceae were the most abundant bacterial families. Detection of *nirK* and *nosZ* marker genes for denitrification (N_2 and N_2O production, respectively) were detected under anoxic conditions and showed an increase with time, mainly associated with the late stage of decomposition. Then, the investigation of bacteria associated to decomposition of copepod carcasses is very important, because the functioning of those carcasses as pelagic hotspots for bacterial decomposition may have implications in nitrogen cycling via denitrification. However, further studies to quantitatively assess the contribution of these communities to the global biogeochemical cycles are required.

Keywords: Copepod carcasses, bacterial decomposition, bacterial communities, llumina sequencing, functional genes, biochemical cycles.

Introduction

The study of the relationship between zooplankton and microorganisms in the pelagic environment of the ocean has focused, historically, on the indirect link via the microbial food web (Tang et al. 2009). These two components of the marine food web are generally treated as separate entities only connected through the trophic cascades, albeit, microbes and zooplankton are dynamically linked at different ecological levels (Azam and Malfatti, 2007; Tang et al., 2010). However, recent studies have shown that their occurrence and ecological functions can be closely linked (e.g. Møller et al. 2007 and Tang et al. 2009a). The bacterial abundance associated with copepods can even be orders of magnitude higher than that in the free-living bacteria on a per volume base, indicating active bacterial colonization and growth in these microenvironments (Tang et al., 2006b; Tang et al., 2010; Tang et al., 2011; Schmidt et al., 2016). The investigation of the bacterial communities associated with marine planktonic copepods is therefore highly relevant. The fact that marine copepods may constitute up to 80 % of the mesozooplankton biomass (Verity and Smetacek 1996) underlines this.

Copepods also are key components of the food web as grazers of primary production and as food for fish (Cushing 1989; Møller and Nielsen 2001). Similarly, their molts and carcasses can be populated and decomposed by bacteria (Tang et al. 2006a; Tang et al. 2006b; Tang et al. 2009b). This disintegration and decomposition of copepod carcasses provide an alternative pathway for nutrient regeneration, elemental recycling and microbial production (Harding, 1973; Lee and Fisher, 1992; Reinfelder et al., 1993). Thus, rapid decomposition and remineralization by microbes will channel carcass materials to the microbial food web within the pelagic zone. Then, to understand the direct association between both groups could give information about the functioning of the pelagic environment from an ecologic and biogeochemical point of view.

Marine copepods contributes significantly to the transport of carbon and nitrogen from the euphotic to the mesopelagic zone through both the sinking of particles and vertical migration (Steinberg et al., 2000; Steinberg, Goldthwait and Hansell 2002; Escribano et al., 2009; Yañez et al., 2012). The copepod body has a higher relative C:N ratio than the phytoplankton biomass due to the lack of a carbohydrate storage, which makes them attractive bacterial habitats (Bickel and Tang 2010). In the un-poisoned treatment, the

leached carbon appeared to be rapidly consumed and the total carbon loss rate was also higher, indicating direct bacterial decomposition (Lee and Fisher, 1992). In addition to organic carbon, trace elements were also being remineralized during bacterial decomposition of copepod carcasses (Reinfelder et al., 1993). Consequently, the carcasses are hydrolyzed and mineralized at high rates (Lundgaard, 2016).

The elevated bacterial activity and the eventually already established anoxic microenvironment, depending on the food remains in the gut, makes them possible microhabitats for anaerobic N- cycling. Recent investigations into copepod microbiomes have revealed a number of recurring bacterial groups, such as Vibrio sp., Bacteroidetes, Firmicutes, Actinobacteria, and Pseudoalteromonas sp., that are associated with different copepod species from different ecosystems (Gerdts et al., 2013; De Corte et al., 2014, 2018; Moisander et al., 2015; Scavotto et al., 2015; Shoemaker and Moisander, 2015). Separating out the microbial communities that colonize the gut or the exoskeleton of zooplankton is challenging though (Møller et al., 2007; De Corte et al., 2014; Skovgaard et al., 2015). Additionally, the metabolic functions of copepod-associated bacteria remain largely unknown, unlike those of microorganisms associated with benthic invertebrates (Dubilier et al., 2001; Martinez-Garcia et al., 2008; Hoffmann et al., 2009; Stief et al., 2009). Globally, OMZs are responsible for up to 50% of the oceanic fixed nitrogen loss (N-loss) via denitrification and anammox (DeVries et al., 2013). Copepod carcasses may directly contribute to this N-loss via denitrification and possibly anammox (Glud et al., 2015). Associations between copepods and N_2-fixing and denitrifying bacteria had been founded (Zehr et al., 1998; Glud et al., 2015; Scavotto et al., 2015). Meantime, in small marine zooplankton from an oxygen-depleted coastal basin, DNRA and denitrification were the most active pathways of anaerobic N-cycling, whereas anammox was the dominant pathway in the ambient anoxic seawater (Stief et al. 2017). This finding underlines that N-cycling associated with sinking carcasses can significantly differ from N-cycling in the surrounding water, probably owing to distinctive microbial communities that colonize and develop on zooplankton carcasses (Stief et a., 2018).

The present study investigated the bacterial communities of the marine calanoid copepod specie, *Acartia tonsa*. Here, we measured the bacterial community and decomposition directly associated with the copepod carcasses, in an upwelling zone with anoxic bottom

water (Mejillones bay, Chile). This coastal marine OMZ is an environmental showcase for pelagic N loss through anammox and denitrification activity.

Materials and Methods

Study area and sampling strategy

The study was conducted in northern Chile at Mejillones Bay (23°S), within the Humboldt Current System (HCS). This region is known for its active upwelling, and intermittent upwelling throughout the year which supports high levels of primary productivity (Marin et al., 1993; Daneri et al.,2000). Sampling was performed in 2013 at two stations along a coastal transect: St-2 (23º, 02 S - 70º 27 W; zmáx = 90m) y St-3 (23º, 03S - 70º 28 W; zmáx = 120m).

In this area metazooplankton community is dominated by copepods (Hidalgo et al., 2010; Escribano et al., 2012). Copepods were collected by oblique tows through 0-30 m and 30-50 m during the day using a WP–2 net (200 µm mesh and 50-cm mouth diameter) equipped with a flowmeter. Afterward, the samples were immediately diluted in seawater and transported to the laboratory within 1 – 2 h. Upon return to the laboratory, thirty- five adult copepods were randomly selected for decomposition rates experiments and bacterial community assessment associated with this decomposition.

Additionally, water temperature, salinity, and dissolved oxygen (DO) were measured at each station by an autonomous profiler SeaBird SBE–19. 40 L of water samples were collected at 30 m (within the oxygenated layer) and at 50 m (within the anoxic layer) using a 5-L Niskin bottle for experiments of decomposition of copepod carcasses.

Decomposition of copepod carcasses

To set up the decomposition of copepod carcasses experiments, oxic and anoxic controlled environments were set up into the two big bottles of 20 L (see Fig. 1, section B and C). To keep anoxic conditions, sea water was first thoroughly purged with nitrogen gas before use, especially to decrease oversaturation caused by filtering. The DO concentrations were verified with an optical sensor OXY-4 Micro-Optode PreSens, by collecting 20-mL seawater subsamples by overflow using optical sensors that had been calibrated using a two point calibration (100% and 0% oxygen saturation) following the

manufacturer's instructions. The oxygen measurements were carried out in bottles. At the incubation end-points, final oxygen was recorded inside the same bottles initially measured.

Before of the incubations, the zooplankton sample was allowed to stand, so that dead zooplankton settled to the bottom while live zooplankton actively swam near the surface. Live zooplankton were removed from the bottle and concentrated on a nylon mesh. Live zooplankton were immediately killed by brief exposure to acetic acid, rinsed repeatedly with 0.2 µm filtered sea water and transferred to a sterile Petri dish. The carcasses were examined under a dissecting microscope, and adults of the copepod specie *Acartia tonsa* were selected for experiments. To make sure incubation bottles were clean/had no bacteria on the bottle's walls, they were rinsed with acid and MQ water prior to experiments (Kanda 2008). Groups of 35 carcasses, in triplicate, were incubated in 250 mL modified bottles containing 0.2-µm filtered seawater at each treatment. Afterward, all incubations were stored in a cold room at 14 °C, which is the typical mean in situ temperature of the ~30 m layer during non-El Niño years (Ruz et al., 2015).

Bacterial community

Twenty- five fresh carcasses were preserved in a sterile 2 mL Eppendorf vial for DNA extraction and sequencing the 16S gene for determining of the initial bacterial community composition associated with the copepod carcasses. After 6,12,18, 24, 30 and 36 hours of incubation, twenty-five carcasses were preserved in a sterile 2 mL Eppendorf vial and frozen with liquid nitrogen (-196°C) until DNA extraction.

Microscopy

On hours 6,12,18, 24, 30 and 36, three bottles from each series was selected for microscopy. On each of the hours given above, 10 carcasses were randomly selected from each incubation series and transferred onto a glass slide. The carcasses were observed under a microscope; loss of internal tissues was readily visible under dark-field (Tang et al. 2006b). Images of the carcasses were made with the aid of a camera lucida attached to a light microscope (CH2 Olympus).

Bacterial community composition.

On each sampling hours, 25 carcasses were transferred from each incubation series to a sterile 2 mL Eppendorf vial and stored in liquid nitrogen at –196°C until DNA extraction. DNA was extracted with the NucleoSpin Tissue XS kit (Macherey-Nagel®), following the manufacturer's indications. DNA obtained was visualized for integrity in 1% agarose gel electrophoresis, stained with ethidium bromide and visualized in a UV transilluminator. Also, Nanodrop ND-1000 spectrophotometer (Thermo Scientific) and Qubit fluorometer V 1.27 (Invitrogen®) was used to check the concentration and quality of the extracted DNA. Finally, the volume of DNA samples was reduced by concentration with SpeedVac for 2 minutes at 37°C.

Illumina next generation sequencing analysis

For bacterial community identification, general 16S rRNA PCR amplicons (in triplicates) were obtained using primers 349F-806R targeting the V4 region of the 16S SSU rRNA (Caporaso et al.,2011). The amplicons were sequenced using Illumina MiSeq on the Fluidigm platform (https://www.fluidigm.com) at Functional Genomics Laboratory (University of Illinois). The open-source, platform-independent, community-supported software program, mothur (http://www.mothur.org), was used to process and analyze the sequence data. Sequence reads were cleaned and filtered, pre-clustering, and chimera elimination. The high-quality reads were clustered into operational taxonomic units (OTUs) using Mothur. BLASTn of taxonomic classification down to the phylum, class and genus level was then performed using MOTHUR via SILVA132 database with a set confidence threshold of 80%.

To confirm the taxonomical assignation of the 5 most abundant OTUs in each dataset, local alignments against representative sequences were done. Representative sequences were obtained by BLASTn (Altschul et al. 1990) against the GenBank 16S ribosomal RNA sequences (Bacteria) database (release 209, August 2015).

Functional genes

To study the detection of specific genes mainly those involved in denitrification, nitrification processes and mechanism of CO_2 fixation. PCR amplicons were obtained using

the same DNA template used for gene 16S. The primers used for each gene were the following: *nosZ*, 1F-1R, *nirK*, 876F-1040R; *amoA*: 1F-2R; petbf-petbr; RbIIf-RbIIr.

Then, *nosZ* and *nirK* , the genes of nitrous oxide and nitrite reductase, respectively, involved in denitrification processes, *petB*, the gene of electron transfer -cytochrome b6, *amoA* the gene for an ammonium monooxygenase subunit, involved in steps of nitrification and *rbcS*, gene of Ribulosephosphate carboxylase/oxygenase, is the mechanism for CO_2 fixation.

The amplicons also were sequenced using Illumina MiSeq on the Fluidigm platform (https://www.fluidigm.com) at Functional Genomics Laboratory (University of Illinois). To obtain a database of effective sequences for each sample, random sequencing error, low-quality sequences and chimeras were detected, trimmed and removed by MOTHUR Software (http://sourceforge.net/projects/seqclean/ and http://www.mothur.org/wiki/MainPage).

Results

Decomposition of copepod carcasses

We followed the course of decomposition of the carcass of the marine copepod *Acartia tonsa*. by dark-field microscopy. In oxic conditions, copepod bodies begun to degrade rapidly, seemed transparent with intact internal tissues at initial 18 h, with a slow increased during the rest of the experiment of incubation (Fig.2A). Later, between 18 − 24 h it remained relatively stable, and the slowly increased. Between 24 − 30 h carapace begun to fracture (Fig.2A). Most of the internal tissues and had disappeared and mainly the carapace remained with a little bit of internal tissue inside, about 20% of bodies of carcasses was measured during the 6 last hours (Fig. 2 A,B). In contrast, the decomposition process was much slower in the anoxic conditions during the first 18 hours, the copepod carcasses remained intact (Fig. 2A). Then, a heavy break-down of internal tissue and high increase of >50% was observed during the 24 h of incubation (Fig.2A,B), increasing greatly and quickly over the last 6 hours, the copepod carcasses contained no internal tissue, but beared undamaged setae and intact copepod exoskeleton (<10% in bodies of

carcasses was measured) (Fig. 2A,B).

Community composition determined by NGS

Detailed taxonomic characterization of the bacterial communities' changes during decomposition of copepod carcasses (*A. tonsa*) in Mejillones bay was accomplished using Next-generation sequencing (NGS) of 13 samples that were taken from decomposition experiments described above.

Bacterial 16S rRNA gene sequencing produced 728807 reads and 470312 OTUs, after clustering at 97% similarity. Community composition was >50% similar between samples based on Bray- Curtis similarities (Fig. 3B). In anoxic conditions, taxonomic identification indicates a dominance of Gammaproteobacteria (27% of total relative abundance). Meantime, in oxic contitions a dominance of Alphaproteobacteria (16%) followed by Gammaproteobacteria and Verrucomicrobia (10%) (Table 1).

Most abundant taxa in oxic conditions included members of the families Rhodobacteraceae (14%, phylum Alphaproteobacteria) and Verrucromicrobiaceae (10%, phylum Verrucomicrobia). Meanwhile, in anoxic conditions were oberved Rhodobacteraceae (16%, phylum Alphaproteobacteria), Vibrionaceae (16%, phylum Gammaproteobacteria), and Pseudoalteromonadaceae (7%, phylum Gammaproteobacteria) (Fig.3A). Subsequently, the classes Bacilli and Clostridia (phylum Firmicutes), and Sphingobacteria (phylum Bacteroidetes) have also been found in both of two conditions, to occur in low abundance (Fig.3A).

Treatments clustered show rows that are closely together (have small dissimilarity) linked near the right side (oxic conditions) and left side (anoxic conditions) of the plot. Rows that link up near the left side are very different. T0 (environmental sample) appears to be quite different from any of the other samples (Fig. 3B). The similarities between the two different O_2 treatments were assessed with ANOSIM and the significant R-score for the grouping anoxic vs. oxic treatments was 0.60 and P-value was 0.006 indicating that the two clusters were indeed different. Together with the results of the environmental incubation, this indicates that the carcasses-associated degradation processes were mainly driven by carcasses-specific bacterial communities and not by the communities originally found in

the seawater.

The temporal development in the microbial communities in both treatments was also evidenced by relative abundances of the OTUs responsible for the observed difference between treatments during the course of the experiment, based on SIMPER analysis (Fig.4). Overall, we observed a total of OTU 0001 and 00007 responsible for the difference between treatments and most exhibited opposite dynamics in the two parallel O_2 treatments, with exception of OTU 00019 (Fig. 4 A,B). In oxic conditions, OTUs 0001 and 00007 increased more than threefold and twofold in relative abundance over the 18 − 30 h and 30 − 36 h, respectively. Meantime, OTUs concurrently were reduced ½ or more in relative abundance over the 24 and 30 h. Of those, OTU 00019 were completely lost in the oxic treatment (Fig 4A), meantime this increased more than twofold in relative abundance over the 36 hours in anoxic treatment Fig. 4B). Overall, shifts in the microbial community dynamics as expressed by an extreme increase or decrease in relative abundance of given OTUs were thus most explicit in the oxic treatment.

Functional genes

Genes associated with nitrification and denitrification, such as *amoA, nirK, nosZ* (Fig.5) were also found in the experiments of the bacterial decomposition of copepods carcasses. These genes were evident in incubation with seawater from the anoxic water layer, mainly associated with the late stage of the *A. tonsa* carcasses decomposition (Fig. 5B).

Furthermore, a few genes usually associated to oxygen-limited environments and oxygen saturated surface water, such as cytochrome b, nitrite reductase and *rbcS* (Fig. 5), were also detected in the experiments.

Discussion

Copepod carcasses are dense packages of organic matter and their fate therefore has important implications for material and energy fluxes through of the water column. Here

we focused on bacterial decomposition, their community associated and potential implications on N-loss in OMZ.

In laboratory studies, we followed the course of decomposition of the carcass of the marine copepod *A. tonsa*. When copepod carcasses were exposed to oxic conditions, decomposition begun rapidly during first 18h, later it remained relatively stable, and slowly increased towards the last 6 h of the incubations. In contrast, the decomposition process was much slower in the anoxic conditions during 18 h, increasing greatly and quickly over the last 6 hours of the incubations. The differences in decomposition observed in this study during the first hours of incubation between treatments: highest percentage of internal tissues loss in oxic than anoxic conditions are comparable to the observation of Tang et al., (2006). Toward the end of the decomposition, most of the tissues have disappear, leaving behind the chitinous exoeskeleton and trace amounts of internal tissues coincident with Tang et al., (2009). Although chitilolytic bacteria are present in ocean, chitin degradation by bacteria in nature tends to be very slow. For example, *in situ* incubation of purified chitin particles showed a loss rate of <1% per day (Hood & Meyers 1977, Kirchner 1995, Kirchman & White 1999, Tang et al., 2009).

Using Illumina sequencing of the 16S rRNA gene we found significant differences between the bacterial communities associated with copepod carcasses.

Rhodobacteraceae, the first most abundant family found in the copepod carcasses - associated bacterial community, have been reported to live associated with marine organisms, such as coral, sponges and microalgae (Ridley et al., 2005; Burke et al., 2011; Roder et al., 2014) and to contribute to biofilm formation (Pujalte et al., 2014), indicating that this group may play a major role in the colonization of the zooplankton exoskeleton.

While, some bacteria typically associated with marine copepods, such as Vibrio spp., Sphingomonas sp., and Pseudoalteromonas spp. express chitinases and are able to utilize chitin as source for carbon and nitrogen (Svitil et al., 1997; Zhu et al., 2007; Tang et al., 2010; Gerdts et al., 2013), there are Vibrionaceae. Sphingomonadaceae and Pseudoalteromonadaceae family, respectively. In this study, Vibrionaceae was the one of more dominant into the decomposition experiments, especially during the early and late stages of decomposition on oxic conditions, when the chitin of copepod carcasses was broken and high degraded. Therefore, it is possible to suggest to this community is the main

responsible of that chitin degradation.

Unexpectedly, we did obtain sequences related to Verrucomicrobiaceae family on copepods carcasses sinking. Members of this family had been reported so far only related as sponge (Thiel et al., 2007) and hydromedusa (Daley et al., 2016) associated bacteria.

In our study, we observed that their abundance was consistently high on copepod carcasses, specially within the treatments with oxic conditions, in contrast to previous studies conducted when the microbiome in marine copepods had been researched (Moinsander et al., 2015).

Otherwise, members of phylum Firmicutes are found in marine particulate matter (Vojvoda et al. 2014). as well as in microbiome of mammals and terrestrial and aquatic invertebrates (Ley et al. 2005; Wust et al. 2011). Moreover, they have major roles in animal digestion previously and have been found in freshwater copepods, while absent in the surrounding water (Grossart et al. 2009; Homonnay et al. 2012). In this study, Clostridiales, Lactobacillales and Bacillales, the members of this Phyllum were found in low abundances but were more abundant under oxic conditions.

The microbial communities associated with copepod carcasses, including those attached to the exoskeleton, are exposed to the low ambient O_2 levels and will likely changes and will be dominate for anaerobic or facultative anaerobic organisms, compared to oxic ones, when exposed to environments with low oxygen levels. This will reinforce the functioning of copepod carcasses as O_2-depleted, pelagic hotspots with possible large-scale biogeochemical implications.

In this research, the detection of *nirK* and *nosZ* (N_2 and N_2O production, respectively) were found to occur under anoxic conditions and showed an increase with time, mainly associated with the late stage of decomposition. Similar to the other studies when expression of *nirS*, *nirK* and *nosZ* were documented in arctic copepods (Glud et al. 2015) and in the north Atlantic Ocean (De Corte et al. 2018).

Thus, the investigation of bacteria associated to decomposition of copepod carcasses is very important, because the functioning of those carcasses as pelagic hotspots for bacterial decomposition, they may have implications in nitrogen cycling via denitrification. However, the quantitative importance as a sink for bioavailable nitrogen is strongly dependent on the ambient O_2 level. The importance of carcass associated denitrification

could be highly significant in O_2 depleted environments such as Oxygen Minimum Zones (OMZ).

Conclusion

Marine copepods form one of the most abundant mesozooplankton groups in the oceans and are associated with various numbers of different bacterial species. We showed that 1) from laboratory experiments, following the course of decomposition of the carcass of the marine copepod *A. tonsa*. In oxic conditions, decomposition begun rapidly, later it remained relatively stable, and slowly increased towards the last hours of the incubations. In contrast, the decomposition process was much slower in the anoxic conditions, increasing greatly and quickly over the last hours of the incubations; 2) Different bacterial communities among different treatments of decomposition experiments were found, whereas changes were observed throughout both incubations; and 3) further studies to quantitatively assess the contribution of these communities to the global biogeochemical cycles are required.

Acknowledgements

This work was supported by Millennium Institute of Oceanography ICM 120019. Yañez was supported by the Scholarship of CONICYT-PCHA/Doctorado Nacional/2013-21130213. The authors thanks Captain Juan Menares and the crew of R/V Menachos for assistance in the field, Benjamin Glasner and Leslie Daille for helping data analysis. Thanks to the Laboratorio de Microbiología marina at the Pontificia Universidad Católica de Chile for helped me on the molecular part, analysis, collaboration, and sharing ideas for useful discussions. This work is a contribution by Millennium Institute of Oceanography ICM 120019.

References

Azam F, Malfatti F. 2007. Microbial structuring of marine ecosystems. Nat. Rev. Micro. 5: 782-791.

Bickel, S.L., Tang, K.W. 2010. Microbial decomposition of proteins and lipids in copepod versus rotifer carcasses. Mar. Biol. 157 (3), 1613–1624.

Burke, C., Thomas, T., Lewis, M., Steinberg, P., and Kjelleberg, S. 2011. Composition, uniqueness and variability of the epiphytic bacterial community of the green alga *Ulva australis*. ISME J 5, 590–600.

Caporaso, J. G., Lauber, C. L., Walters, W. A., Berg-Lyons, D., Lozupone, C. A., Turnbaugh, P. J., Noah Fierer, N., & Knight, R. (2011). Global patterns of 16S rRNA diversity at a depth of millions of sequences per sample. Proc Natl Acad Sci USA 108, 4516–4522.

Cushing D.H.1989. A difference in structure between ecosystems in strongly stratified waters and in those that are only weakly stratified. J Plankton Res 11, 1-13.

Daley M.C., Urban-Rich J., and Moisander P. 2016. Bacterial associations with the hydromedusa *Nemopsis bachei* and scyphomedusa *Aurelia aurita* from the North Atlantic Ocean. Mar. Biol. Res. 12:10, 1088 –1100.

Daneri, G., Dellarossa, V., Quiñonez, R., Jacob, B., Montero, P., Ulloa, O., 2000. Primary production and community respiration in the Humboldt Current System off Chile and associated oceanic areas. Mar. Ecol. Prog. Ser. 97, 41–49.

De Corte, D., Lekunberri, I., Sintes, E., Garcia, J. A. L., Gonzales, S., and Herndl, G.J. 2014. Linkage between copepods and bacteria in the North Atlantic Ocean. Aquat. Microb. Ecol. 72, 215–225. doi: 10.3354/ame01696.

De Corte, D., Srivastava, A., Koski, M., Garcia, J. A. L., Takaki, Y., Yokokawa, T., Nunoura, T., Elisabeth, N. H., Sintes, E. and Herndl, G. J. 2018. Metagenomic insights into zooplankton-associated bacterial communities. Environ Microbiol, 20: 492–505. doi:10.1111/1462-2920.13944.

DeVries T, Deutsch C, Rafter PA, Primeau F. 2013. Marine denitrification rated determined from a global 3-D inverse model. Biogeosciences. 10, 2481− 2496.

Dubilier, N., Mulders, C., Ferdelman, T., de Beer, D., Pernthaler, A., Klein, M., et al. 2001. Endosymbiotic sulphate-reducing and sulphide-oxidizing bacteria in an oligochaete worm. Nature 411, 298–302.

Escribano, R., Hidalgo, P., Fuentes, M., Donoso, K., 2012. Zooplankton time series in the coastal zone off Chile: Variation in upwelling and responses of the copepod community. Progr. Oceanogr. 97, 74–186.

Grossart, H.P., Dziallas, C., and Tang, K.W. 2009. Bacterial diversity associated with

freshwater zooplankton. Env Microbiol Rep 1: 50-55.

Glud, R. N., Grossart, H. P., Larsen, M., Tang, K. W., Arendt, K. E., Rysgaard, S., et al. 2015. Copepod carcasses as microbial hot spots for pelagic denitrification. Limnol. Oceanogr. 60, 2026–2036.

Gerdts, G., Brandt, P., Kreisel, K., Boersma, M., Schoo, K. L., and Wichels, A. 2013. The microbiome of North Sea copepods. Helgoland Mar. Res. 67, 757–773. doi: 10.1007/s10152-013-0361-4. 3

Harding GCH (1973) Decomposition of marine copepods. Limnol Oceanogr 18, 670-673

Hidalgo P, Escribano R, Vergara O, Jorquera E, Donoso K, Mendoza M. 2010. Patterns of copepod diversity in the Chilean coastal upwelling system. Deep-Sea Research. II, 57: 2089 – 2097.

Hoffmann, F., Radax, R., Woebken, D., Holtappels, M., Lavik, G., Rapp, H. T., et al.2009. Complex nitrogen cycling in the sponge Geodia barretti. Environ. Microbiol. 11, 2228–2243.

Homonnay ZG, Keki Z, Marialigeti K et al. 2012.Bacterial communities in the gut of the freshwater copepod *Eudiaptomus gracilis*. J Basic Microbiol. 52, 86–90.

Lee BG, Fisher NS.1992. Decomposition and release of elements from zooplankton debris. Mar Ecol Prog Ser 88:117–128.

Ley R.E., Backhed F., Turnbaugh P. et al. 2005. Obesity alters gut microbial ecology. P Natl Acad Sci USA.102,11070–5.

Lundgaard, A. S. 2016. Sinking aggregates and copepod carcasses; overlooked anaerobic hotspots in the aquatic nitrogen cycling. Ph.D. thesis. Univ. of Southern Denmark.

Marín, V., Rodríguez, L., Vallejo, L., Fuenteseca, J., Oyarce, E., 1993. Efectos de la surgencia costera sobre la productividad primaria primavera de la Bahía Mejillones de Sur (Antofagasta, Chile). Rev. Chil. Hist. Nat. 66, 479–491.

Martinez-Garcia, M., Stief, P., Diaz-Valdes, M., Wanner, G., Ramos-Espla, A., Dubilier, N., et al. (2008). Ammonia-oxidizing Crenarchaeota and nitrification inside the tissue of a colonial ascidian. Environ. Microbiol. 10, 2991–3001.

Moisander, P. H., Sexton, A. D., and Daley, M. C. 2015. Stable associations masked by temporal variability in the marine copepod microbiome. PLoS ONE 10:e0138967. doi: 10.1371/journal.pone.0138967.

Møller E.F., Nielsen T.G. 2001. Production of bacterial substrate by marine copepods: Effect of phytoplankton biomass and cell size. J Plankton Res 23: 527-536

Møller, E. F., Riemann, L., and Søndergaard, M. 2007. Bacteria associated with copepods, abundance, activity and community composition. Aquat. Microb. Ecol. 47, 99–106. doi: 10.3354/ame047099.

Pujalte, M.J., Lucena, T., Ruvira, M.A., Arahal, D.R., and Macian, M.C. 2014. The family Rhodobacteraceae. In *The Prokaryotes: Alphaproteobacteria and Betaproteobacteria*. Rosenberg, E., DeLong, E.F., Lory, S., Stackebrandt, E., and Thompson, F. (eds). Berlin, Heidelberg: Springer Berlin Heidelberg, pp. 439–512.

Reinfelder JR, Fisher NS, Fowler SW, Teyssié JL (1993) Release rates of trace elements and protein from decomposition of plankton debris. 2. Copepod carcasses and sediment trap particulate matter. J Mar Res 51:423–442

Ridley, C.P., Faulkner, D.J., and Haygood, M.G. 2005. Investigation of Oscillatoria spongeliae-dominated bacterial communities in four dictyoceratid sponges. Appl Environ Microb 71, 7366–7375.

Roder, C., Arif, C., Bayer, T., Aranda, M., Daniels, C., Shibl, A., et al. 2014. Bacterial profiling of White Plague Disease in a comparative coral species framework. ISME J 8, 31–39.

Ruz, P. M., P. Hidalgo, S. Yáñez, R. Escribano, and J. E. Keister. 2015. Egg production and hatching success of Calanus chilensis and Acartia tonsa in the northern Chile upwelling zone (23° S), Humboldt Current System. J. Marine. Syst. 148: 200–212.

Scavotto, R. E., Dziallas, C., Bentzon-Tilia, M., Riemann, L., and Moisander, P. H. 2015. Nitrogen-fixing bacteria associated with copepods in coastal waters of the North Atlantic Ocean. Environ. Microbiol. 17, 3754–3765.doi: 10.1111/1462-2920.12777

Skovgaard, A., Castro-Mejia, J. L., Hansen, L. H., and Nielsen, D. S. 2015. Hostspecific and pH-dependent microbiomes of copepods in an extensive rearing system. PLoS ONE 10: e0132516. doi: 10.1371/journal.pone.0132516.

Schmidt K., Schlosser C., Atkinson A., Fielding S., Venables HJ., Waluda CM., Achterberg EP .2016. Zooplankton Gut Passage Mobilizes Lithogenic Iron for Ocean Productivity Current Biology 26, 2667–2673.

Shoemaker, K. M., and Moisander, P. H. 2015. Microbial diversity associated with

copepods in the North Atlantic subtropical gyre. FEMS Microbiol. Ecol. 91:fiv064. doi: 10.1093/femsec/fiv064.

Svitil AL, Chadhain SMN, Moore JA, Kirchman DL.1997. Chitin degradation proteins produced by the marine bacterium Vibrio harveyi growing on different forms of chitin. Appl Environ Microbiol. 63, 408–13.

Steinberg D.K., Carlson C.A., Bates N.R. et al. 2000. Zooplankton vertical migration and the active transport of dissolved organic and inorganic carbon in the Sargasso Sea. Deep-Sea Res Pt I.47,137–58.

Steinberg, D. K., Goldthwait, S. A., & Hansell, D. A. 2002. Zooplankton vertical migration and the active transport of dissolved organic and inorganic nitrogen in the Sargasso Sea. Deep-Sea Research Part I: Oceanographic Research Papers, 49(8), 1445-1461.

Stief, P., Poulsen, M., Nielsen, L. P., Brix, H., and Schramm, A. 2009. Nitrous oxide emission by aquatic macrofauna. Proc. Natl. Acad. Sci. U.S.A. 106, 4296–4300.

Stief, P., Lundgaard, A.S.B., Morales-Ramirez A et al. 2017. Fixed-nitrogen loss associated with sinking zooplankton carcasses in a coastal oxygen minimum zone (Golfo Dulce, Costa Rica). Front Mar Sci;4:Art.152.

Stief, P., Lundgaard, A.S.B., Treusch A.H., Thamdrup Bo., Grossart H.P., Glud R.N. 2018. Freshwater copepod carcasses as pelagic microsites of dissimilatory nitrate reduction to ammonium. FEMS Microbiology Ecology, 94: 1-12.

Tang, K.W., Freund, C.S., Schweitzer, C.L .2006a. Occurrence of copepod carcasses in the lower Chesapeake Bay and their decomposition by ambient microbes. Estuar Coast Shelf Sci 68: 499-508

Tang, K.W., Hutalle, K.M.L, Grossart H-P. 2006b. Microbial abundance, composition and enzymatic activity during decomposition of copepod carcasses. Aquat Microb Ecol 45: 219-227

Tang K. W., Dziallas C, Hutalle-Schmelzer K, Grossart H.P. 2009a. Effects of food on bacterial community composition associated with the copepod *Acartia tonsa* Dana. Biology letters, doi: 10.1098/rsbl.2009.0076.

Tang K. W., Bickel S.L., Dziallas C., Grossart H.P.2009b. Microbial activities accompanying decomposition of cladoceran and copepod carcasses under different environmental conditions. Aquat Microb Ecol 57: 89–100

Tang, K. W., V. Turk, & Grossart, H. P. 2010. Linkage between crustacean zooplankton and aquatic bacteria. Aquat. Microb. Ecol. 61: 261–277.

Tang, K.W., Glud, R.N., Glud, A., Rysgaard, S., and Nielsen, T.G. 2011. Copepod guts as biogeochemical hotspots in the sea: Evidence from microelectrode profiling of Calanus spp. Limnol Oceanogr *56*, 666-672.

Thiel V., Neulinger S C., Staufenberger T., Schmaljohann R., and Imhoff J. F. 2007. Spatial distribution of sponge-associated bacteria in the Mediterranean sponge *Tethya aurantium*. FEMS Microbiol Ecol. 59, 47–63.

Verity P. G. and Smetacek V.1996. Organism life cycles, predation, and the structure of marine pelagic ecosystems. Mar Ecol Prog Ser 130: 277-293.

Vojvoda J, Lamy D, Sintes E et al. 2014.Seasonal variation in marinesnow-associated and ambient-water prokaryotic communities in the northern Adriatic Sea. Aquat Microb Ecol. 73, 211–24.

Wust P.K., Horn M.A., Drake H.L. 2011. Clostridiaceae and Enterobacteriaceae as active fermenters in earthworm gut content. ISME J. 5, 92–106.

Yañez, S., Hidalgo P., Escribano, R., 2012. Mortalidad natural de Paracalanus indicus (Copepoda, Calanoida) en áreas de surgencia asociada a la zona de mínimo oxígeno en el Sistema de Corrientes de Humboldt: implicancias en el transporte pasivo del flujo de carbono. Rev. de Biol. Mar. Oceanogr. 47,Nº2: 295-310.

Zehr, J. P., Mellon, M. T., and Zani, S. 1998. New nitrogen-fixing microorganisms detected in oligotrophic oceans by amplification of nitrogenase (*nifH*) genes.Appl. Environ. Microbiol. 64, 3444–3450.

Zhu X-f, Zhou Y, Feng J-l .2007. Analysis of both chitinase and chitosanase produced by Sphingomonas sp. Cj-5. J Zhejiang Univ 8: 831-838

Table 1: Variations in abundance (abund, number) and relative abundance (rel. abund.) of operational taxonomic unit (OTU) composition between the microbiomes of *A. tonsa* under oxic (Ox, < 4.6 mL/L), anoxic conditions (An, 0 mL/L) and environment (En).

Phylum	**Clase**	**Abund (n° of OTUs)**			**Rel. abund. (%)**		
		En	**An**	**Ox**	**En**	**An**	**Ox**
Acidobacteria	Solibacteres	0	0	2	0,0	0,0	0,0
Actinobacteria	Actinobacteria	0	53	815	0,0	0,0	0,2
Bacteria_unclassified	Bacteria_unclassified	0	87	499	0,0	0,0	0,1
Bacteroidetes	Bacteroidetes_Incertae_Sedis	0	0	664	0,0	0,0	0,1
Bacteroidetes	Bacteroidetes_unclassified	0	701	251	0,0	0,1	0,1
Bacteroidetes	Flavobacteriia	32	20270	9961	0,0	4,3	2,1
Bacteroidetes	Sphingobacteriia	0	99	5	0,0	0,0	0,0
Chloroflexi	Anaerolineae	0	190	0	0,0	0,0	0,0
Chloroflexi	Chloroflexi_unclassified	0	119	0	0,0	0,0	0,0
Firmicutes	Bacilli	0	86	1719	0,0	0,0	0,4
Firmicutes	Clostridia	0	0	8	0,0	0,0	0,0
Gemmatimonadetes	Gemmatimonadetes	0	0	52	0,0	0,0	0,0
Gracilibacteria	Gracilibacteria_cl	0	177	141	0,0	0,0	0,0
Planctomycetes	Planctomycetacia	0	135	241	0,0	0,0	0,1
Proteobacteria	Alphaproteobacteria	842	76233	63862	0,2	16,2	13,6
Proteobacteria	Betaproteobacteria	627	30	548	0,1	0,0	0,1
Proteobacteria	Deltaproteobacteria	0	0	383	0,0	0,0	0,1
Proteobacteria	Epsilonproteobacteria	11	13634	8687	0,0	2,9	1,8
Proteobacteria	Gammaproteobacteria	43889	124514	47191	9,3	26,5	10,0
Proteobacteria	Verrucomicrobiae	57	5786	47610	0,0	1,2	10,1
Total	470312						

Figure captions

Figure 1: Experimental setup decomposition of copepod carcasses experiments. A) Sampling point, Mejillones Bay, northern Chile. At each point, 40 L seawater (SW) samples were collected at two depths (from oxic and anoxic layer), for zooplankton species collection.; B) Experimental setup for copepod carcasses decomposition in oxic and anoxic controlled environments. Anoxic conditions were reached by purging nitrogen gas into water; and C) Experimental setup under different oxygen conditions, with 3 replicates bottles per each treatment.

Figure 2: A) Decomposition of copepod carcasses (*Acartia tonsa*) as observed by dark-field microscopy. In oxic conditions, the copepod body was transparent with intact internal tissues at the beginning (6-12 hrs), early stage of decomposition during, almost a 30% of total of the copepod carcasses had begun to decompose at first 18 h. Between 24 and 30 h carapace began to fracture. At late 30-36 hrs most of the internal tissues and had disappeared and mainly the carapace remained with a little bit of internal tissue inside. Meantime, during anoxic conditions the decomposition was slower than oxic. At first 18 hours the copepod carcasses remain intact. After 24 hours a heavy break- down of internal tissue was observed. At late 36 hours the copepod carcasses containing no internal tissue but bearing undamaged setae and intact copepod exoskeleton. B) Course of decomposition of copepod carcasses (*Acartia tonsa*) at oxic and anoxic controlled environments. The stage of decomposition is described by a scale of 0 to 4 based on the percentage coverage of body decompose by bacteria: 0, 0% percentage of decomposition; 1 up to 30%; 2 = 30-70%; 3=70-90% and 4 > 90%..

Figure 3: Bacterial community composition changes during decomposition of copepod carcasses experiments based on relative distribution of bacterial 16s rRNA gene sequence. A: Hierarquical cluster analysis based on Bray-Curtis coefficient for the different treatments. Red doted lines indicate statistically supported nodes according to SIMPROF analysis. B: Taxonomic distribution of the assigned. T0: environmental sample for initial incubation time; T1: 6 hours of incubation time; T2: 12h; T3:18h; T4:24h; T5: 30h; T6:36h. OTUs representing less than 2% of total bacteria sequences are included in the group 'Others + unassigned'.

Figure 4: Changes on relative abundances of the OTUs responsible for the observed difference between treatments, based on SIMPER analysis. Gray lines indicate the stage of copepod degradation.

Figure 5: Changes on the number of reads of specific genes responsible for the observed difference between treatments. Gray lines indicate the stage of copepod degradation.

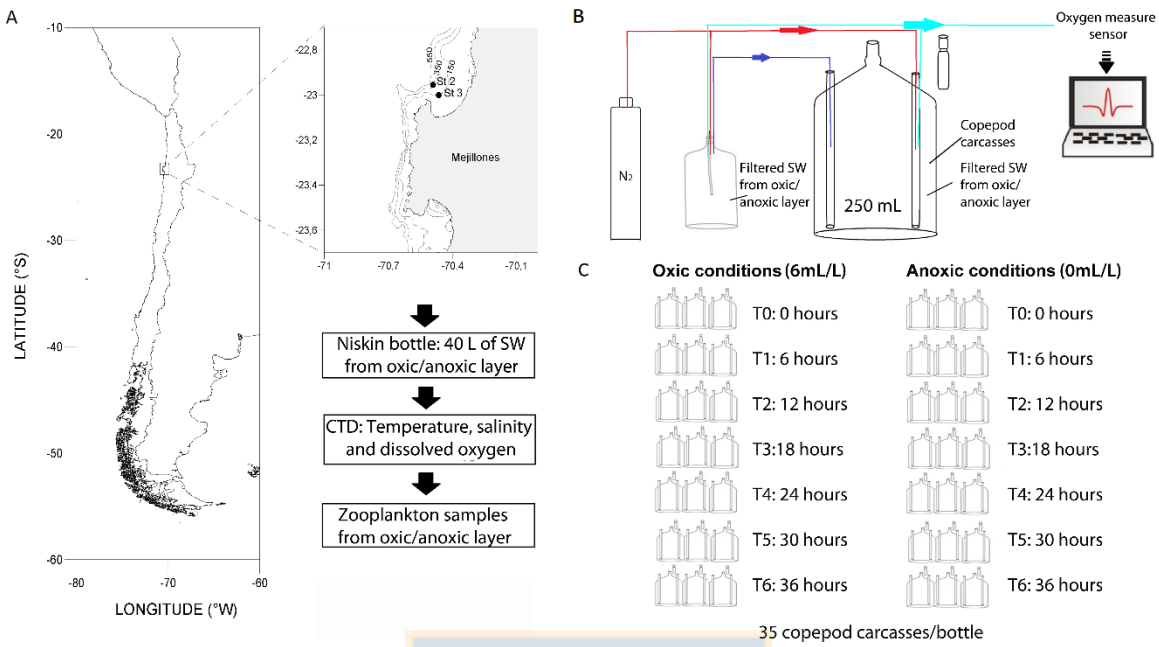
A
LATITUDE (°S)
LONGITUDE (°W)
Mejillones
St 2
St 3
Niskin bottle: 40 L of SW from oxic/anoxic layer
CTD: Temperature, salinity and dissolved oxygen
Zooplankton samples from oxic/anoxic layer
B
Oxygen measure sensor
N2
Filtered SW from oxic/ anoxic layer
250 mL
Copepod carcasses
Filtered SW from oxic/ anoxic layer
C
Oxic conditions (6mL/L)
Anoxic conditions (0mL/L)
T0: 0 hours
T1: 6 hours
T2: 12 hours
T3:18 hours
T4: 24 hours
T5: 30 hours
T6: 36 hours
35 copepod carcasses/bottle

Figure 1

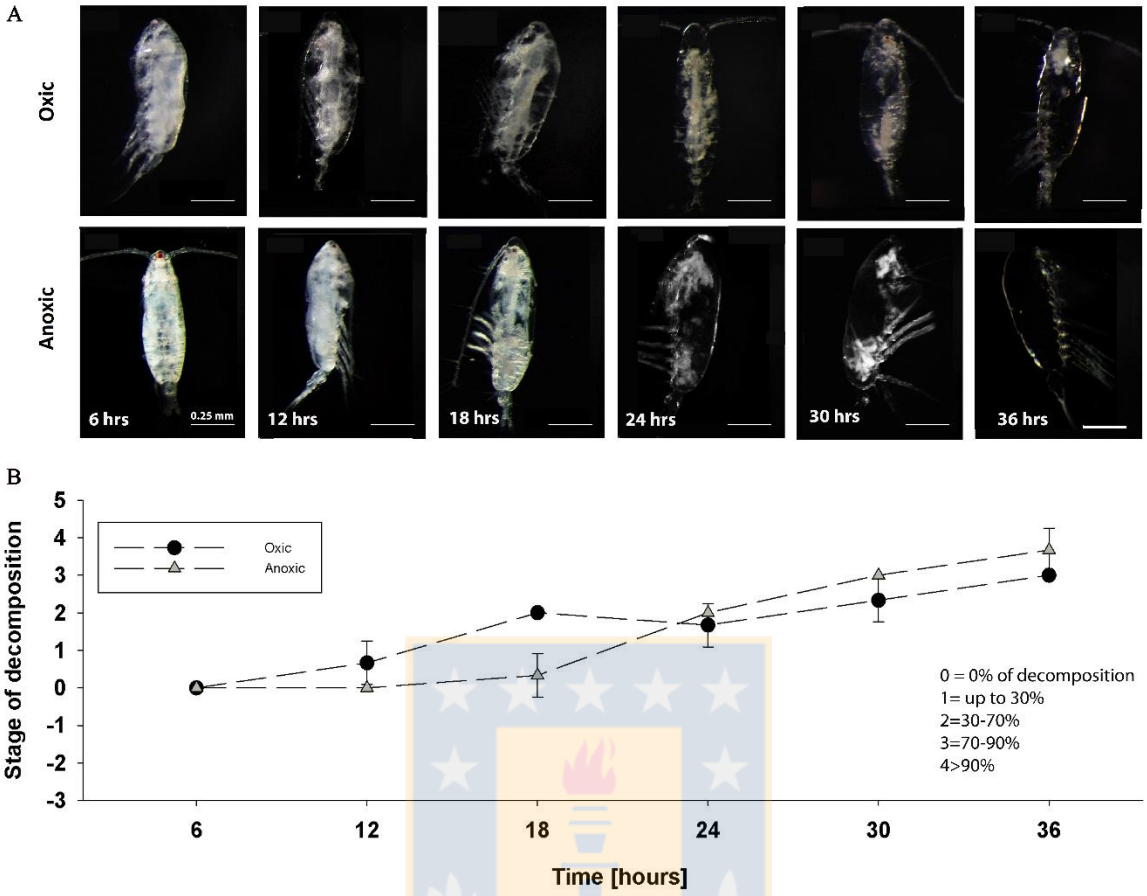
A
Oxic
Anoxic
6 hrs
0.25 mm
12 hrs
18 hrs
24 hrs
30 hrs
36 hrs
B
Stage of decomposition
Oxic
Anoxic
0 = 0% of decomposition
1= up to 30%
2=30-70%
3=70-90%
4>90%
Time [hours]

Figure 2

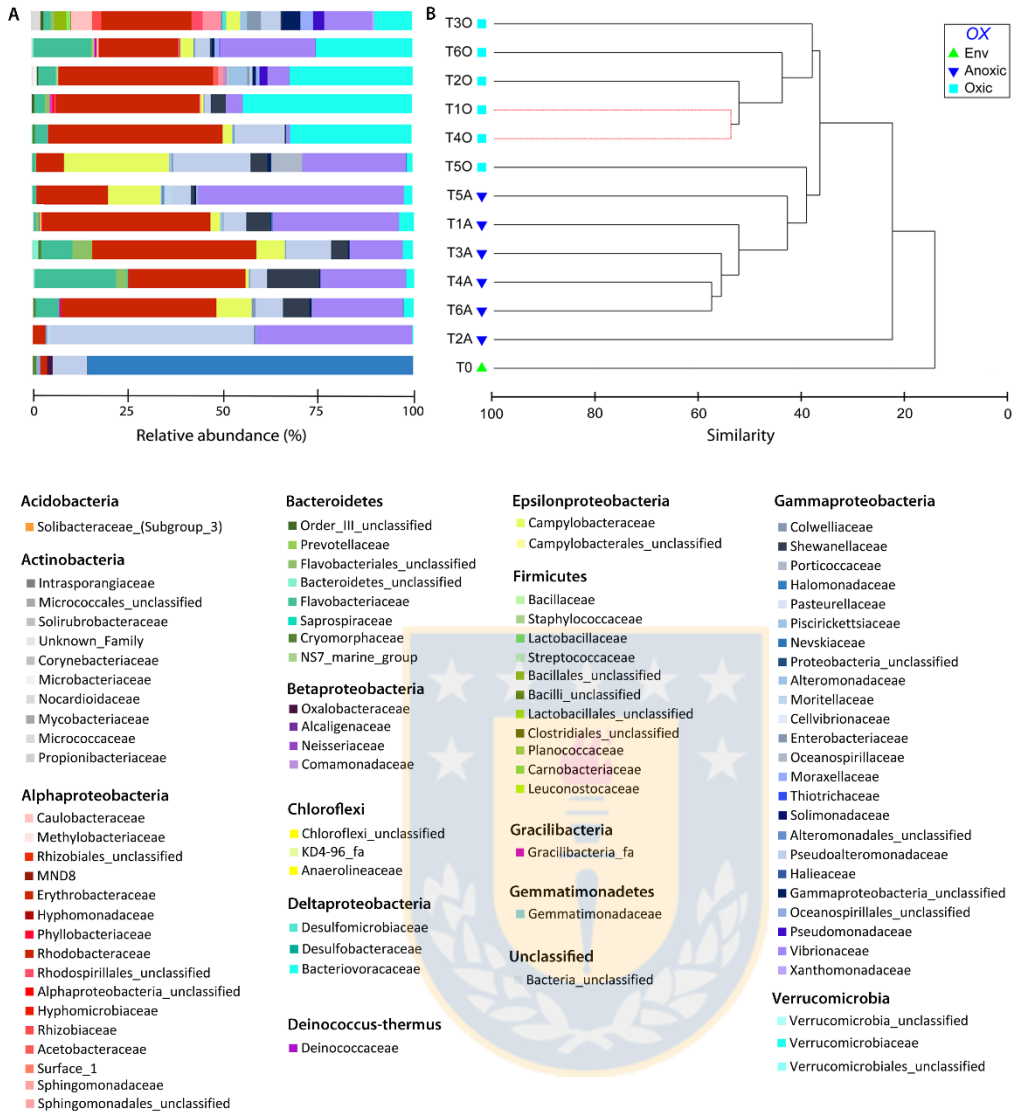
A
B
T3O
T6O
T2O
T1O
T4O
T5O
T5A
T1A
T3A
T4A
T6A
T2A
T0
OX
Env
Anoxic
Oxic
0
25
50
75
100
Relative abundance (%)
100
80
60
40
20
0
Similarity
Acidobacteria
Solibacteraceae_(Subgroup_3)
Actinobacteria
Intrasporangiaceae
Micrococcales_unclassified
Solirubrobacteraceae
Unknown_Family
Corynebacteriaceae
Microbacteriaceae
Nocardioidaceae
Mycobacteriaceae
Micrococcaceae
Propionibacteriaceae
Alphaproteobacteria
Caulobacteraceae
Methylobacteriaceae
Rhizobiales_unclassified
MND8
Erythrobacteraceae
Hyphomonadaceae
Phyllobacteriaceae
Rhodobacteraceae
Rhodospirillales_unclassified
Alphaproteobacteria_unclassified
Hyphomicrobiaceae
Rhizobiaceae
Acetobacteraceae
Surface_1
Sphingomonadaceae
Sphingomonadales_unclassified
Bacteroidetes
Order_III_unclassified
Prevotellaceae
Flavobacteriales_unclassified
Bacteroidetes_unclassified
Flavobacteriaceae
Saprospiraceae
Cryomorphaceae
NS7_marine_group
Betaproteobacteria
Oxalobacteraceae
Alcaligenaceae
Neisseriaceae
Comamonadaceae
Chloroflexi
Chloroflexi_unclassified
KD4-96_fa
Anaerolineaceae
Deltaproteobacteria
Desulfomicrobiaceae
Desulfobacteraceae
Bacteriovoracaceae
Deinococcus-thermus
Deinococcaceae
Epsilonproteobacteria
Campylobacteraceae
Campylobacterales_unclassified
Firmicutes
Bacillaceae
Staphylococcaceae
Lactobacillaceae
Streptococcaceae
Bacillales_unclassified
Bacilli_unclassified
Lactobacillales_unclassified
Clostridiales_unclassified
Planococcaceae
Carnobacteriaceae
Leuconostocaceae
Gracilibacteria
Gracilibacteria_fa
Gemmatimonadetes
Gemmatimonadaceae
Unclassified
Bacteria_unclassified
Gammaproteobacteria
Colwelliaceae
Shewanellaceae
Porticoccaceae
Halomonadaceae
Pasteurellaceae
Piscirickettsiaceae
Nevskiaceae
Proteobacteria_unclassified
Alteromonadaceae
Moritellaceae
Cellvibrionaceae
Enterobacteriaceae
Oceanospirillaceae
Moraxellaceae
Thiotrichaceae
Solimonadaceae
Alteromonadales_unclassified
Pseudoalteromonadaceae
Halieaceae
Gammaproteobacteria_unclassified
Oceanospirillales_unclassified
Pseudomonadaceae
Vibrionaceae
Xanthomonadaceae
Verrucomicrobia
Verrucomicrobia_unclassified
Verrucomicrobiaceae
Verrucomicrobiales_unclassified

Figure 3

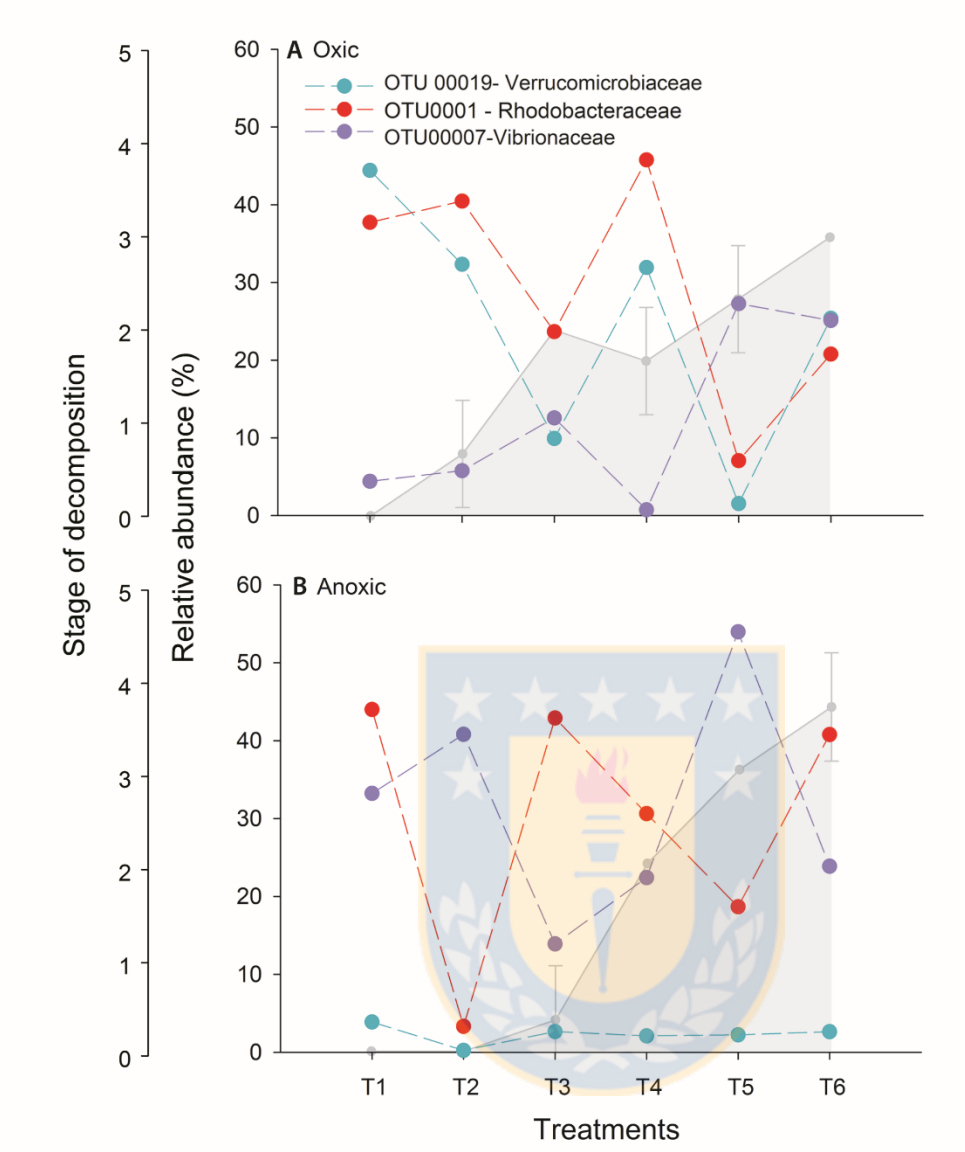
A Oxic
OTU 00019- Verrucomicrobiaceae
OTU0001 - Rhodobacteraceae
OTU00007-Vibrionaceae
B Anoxic
Stage of decomposition
Relative abundance (%)
Treatments
T1
T2
T3
T4
T5
T6

Figure 4

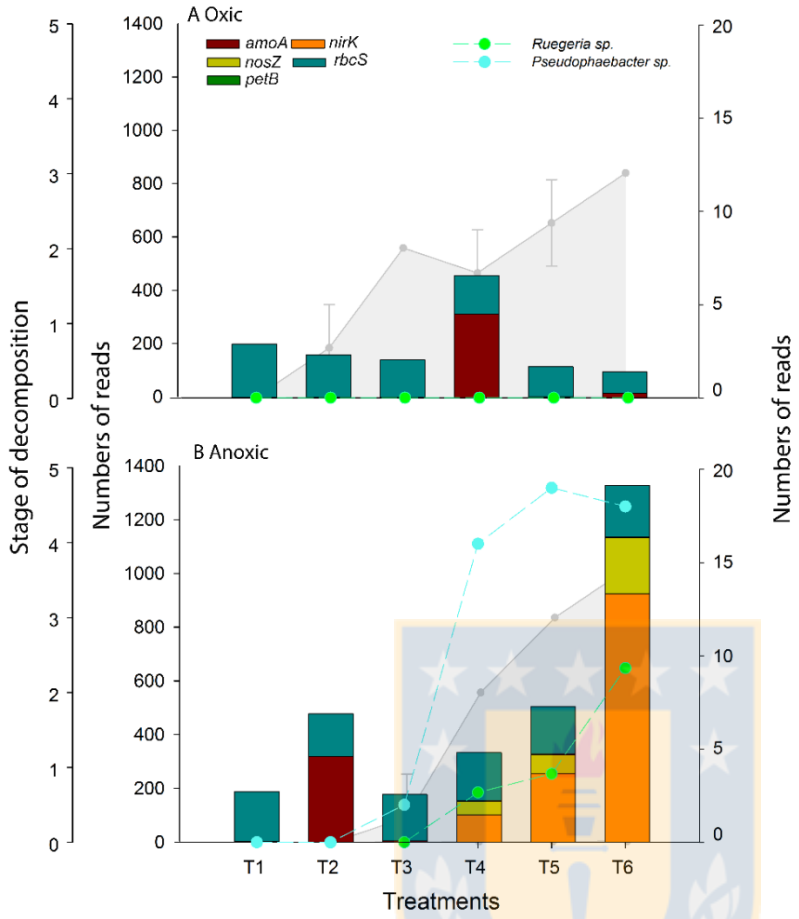
A Oxic
amoA
nirK
nosZ
rbcS
petB
Ruegeria sp.
Pseudophaebacter sp.
B Anoxic
Stage of decomposition
Numbers of reads
Numbers of reads
Treatments
T1
T2
T3
T4
T5
T6

Figure 5

4.2.2. Degradation of sinking copepods: exploring their importance for N and C cycling in oxygen depleted water

Artículo en preparación (resultados preliminares)

Sonia Yañez
Doctorado en Oceanografía
Universidad de Concepción

Resumen

Las carcasas de copépodos son densos paquetes de materia orgánica y su destino podría tener consecuencias importantes para el flujo de materia y energía. Aquí nos enfocaremos en su degradación y sedimentación. Estas carcasas son frecuentemente colonizadas por bacterias, manteniendo alta actividad y crecimiento bacteriano. La razón C:N de partículas de detrito es de un rango entre 5-20, y los aminoácidos representan entre un 8-51% de su contenido orgánico particulado, en comparación con un copépodo calanoideo, que posee un promedio de la razón C:N ~ 3, y entre un 30-70% de proteína de su peso seco. Por lo tanto, las carcasas de copépodos representan materia orgánica de mayor calidad para las bacterias que las partículas de detrito. Además, la rápida degradación y mineralización realizadas por estas bacterias canaliza la materia orgánica (MO) de estas carcasas dentro de la cadena trófica microbiana de la zona pelágica. De lo contrario, esta MO se deposita en el sedimento en la zona bentónica. En nuestros estudios de laboratorio se evidenció que, la producción de NH_4^+ a partir de la degradación bacteriana de carcasas de *Acartia tonsa* fue observada en todos los tratamientos en donde el oxígeno estaba muy bajo y estaría provocada por la mineralización del nitrógeno orgánico; y esta, podría potencialmente contribuir a la DNRA (del inglés Dissimilatory Nitrate reduction to ammonium). Además, la producción de NH_4^+ podría apuntar a que aquellas carcasas de copépodos que sedimentan y que podrían pasivamente transportar nitrógeno orgánico hacia aguas profundas, donde este se podría liberar parcialmente como NH_4^+ y allí las bacterias de vida libre podrían utilizar ese NH_4^+ y oxidarlo a N_2. Por lo tanto, estas carcasas estarían contribuyendo, indirectamente, a procesos de pérdida de N, a través de anammox.

Palabras claves: Carcasas de copépodos, degradación bacteriana, sedimentación, ciclos de C y N

Degradation of sinking carcasses of the marine copepod *Acartia tonsa* at different temperatures, and to explore their importance for C and N cycling in oxygen depleted waters

Sonia Yáñez[1,2], Rie Pors[3,], Pamela Hidalgo[2], Peter Stief [3], Ronnie N. Glud [3,4*]

[1]Doctoral Program in Oceanography, Department of Oceanography, Faculty of Natural Science and Oceanography, University of Concepcion, P.O. Box 160 C, Concepción, Chile
[2]Department of Oceanography and Millennium Institute of Oceanography, Faculty of Natural Science and Oceanography, University of Concepcion, P.O. Box 160 C, Concepción, Chile.
[3]Nordcee, Department of Biology, University of Southern Denmark, 5230 Odense M, Denmark
[4] Department of Ocean and Environmental Sciences, Tokyo University of Marine Science and Technology, Tokyo, Japan

***Corresponding author: rnglud@biology.sdu.dk**

Abstract

Copepod carcasses are dense packages of organic matter and their fate therefore has important implications for material and energy fluxes. Here we will focus on two possible fates: bacterial decomposition and sedimentation. These carcasses are often densely colonized by bacteria and support elevated bacterial activities and growth. The C:N ratio of the detrital particles ranges 5-20, with particulate combined amino acids accounting for 8-51% of their particulate organic content. By comparison, a calanoid copepod body has an average carbon-to-nitrogen ratio of ~3, and 30-70% of its dry weight are proteins. Copepod carcasses are therefore higher quality organic matter than detrital particles for bacteria. In addition, rapid decomposition and remineralization by bacteria will channel carcass materials to the microbial food web within the pelagic zone. The opposite side of the coin is deposition of carcass materials to the benthos. Because a copepod body is denser than the surrounding water, it tends to sink. Our laboratory studies showed that the production of NH_4^+ from decomposition of carcasses was observed in all treatments under low oxygen saturation levels and came from mineralization processes; thus, DNRA (Dissimilatory Nitrate reduction to ammonium) may contribute. Moreover, the production of NH_4^+ further suggests that sinking of copepods' carcasses passively transports bound nitrogen to depths where it could be partially released as ammonium and may fuel free-living anammox bacteria and thus contribute to pelagic N-loss by anammox.

Also, pelagic N-loss is potentially enhanced by carcasses of chitinous zooplankton indirectly through NH_4^+ production that may contribute to anammox. As copepods are some of the most abundant mesozooplankton in the oceans, anaerobic nitrogen cycling associated with these animals may have large implications for biogeochemical cycling in the oceans, and the fixed-nitrogen loss from marine pelagic environments.

Keywords: Sinking copepod carcasses, degradation, C and N cycles

Introduction

The pelagic food web plays a central role in regulating the exchange of CO_2 between the atmosphere and the surface ocean, as well as the transfer of organic carbon into the deep sea. Within this food web, zooplankton serve both as trophic links between primary producers and higher trophic levels (such as fish) and as recyclers that transform particulate carbon and nutrients into dissolved pools (Steinberg and Laundry, 2017). Copepods usually dominate the mesozooplankton in respect to numbers and biomass in all marine waters (Miller and Wheeler, 2012) and is increasingly recognized to host unique microenvironments in the pelagic macroenvironment (Tang et al., 2010).

Copepod carcasses i.e. the remains of dead copepods, which has been found to make up 12-60% of the total zooplankton population (Glud et al. 2015), and yet another, little studies. Studies have shown that the gut of copepods is potentially anoxic, and increasingly so with decreasing oxygen saturation in the surrounding water (Glud et al. 2015; Tang et al. 2011). Additionally, copepods and their carcasses constitute local sources of particulate and dissolved organic matter and nutrients, which attracts and feeds free-living and animal associated bacteria (Steinberg et al., 2000; Tang et al., 2006; Saba et al., 2011). Copepods are important components of the marine food web, and can be substantial contributors to biological pump export processes through production of sinking carcasses. Their significance as a link between primary producers and higher trophic levels has long been recognized (Cushing 1989; Møller and Nielsen 2001; Møller 2005; Olsen et al. 2005). Copepods also contribute to the microbial loop (Azam et al. 1983; Møller and Nielsen 2001) by releasing dissolved organic carbon (DOC) via the decomposition of copepod carcasses by bacteria (Tang et al. 2006a, b). Carcasses produced by copepods also can contribute of passively sinking copepod the particulate organic carbon (POC) export as well (Sampei et al., 2009). Carcasses are altered as they sink, and also their contribution to export changes with depth because of microbial degradation (Tang et al., 2009, Tang and Elliott, 2014). Indeed, most carcasses produced in the upper mixed layer are degraded by microbes such as bacteria and fungi (Tang et al., 2006) resulting in retention and recycling of particulate carbon in surface waters.

In addition, perhaps due to the fact that copepod carcass organic matter tends to be more labile and is turned over faster than the time needed to establish a microbial food chain

(Tang and Elliott, 2014). Then, rapid decomposition and remineralization by microbes will channel carcass materials to the microbial food web within the pelagic zone and oxygen depleted water. The opposite side of the coin is deposition of carcass materials to the benthos. Because a copepod body is denser than the surrounding water, it tends to sink.

The role of carcasses as hotspots of microbial activity might have an important indirect effect on the aquatic biogeochemical cycles as the conditions into those carcasses may host different levels of pH (Tang et al., 2011), oxygen (Stief et al., 2017, Glud et al 2015) and represent concentrated organic matter in relation to the surrounding water and therefore might be important in elemental cycling such as nitrogen cycling.

Here, we measured bacterial respiration as a proxy for carbon and nitrogen turnover/degradation directly associated with carcasses of the calanoid copepod *Acartia tonsa* in incubations at different temperatures.

Materials and methods

Copepod cultures

Adult A. tonsa were obtained from the Department of Science and Environment (Ph.D. Thomas Allan Rayner/Prof. Benni Winding Hansen, Roskilde University, RUC), and kept at 21-22 °C in filtered seawater (salinity 30) until incubations. A. tonsa were fed daily with *Rhodomonas sp.*, also obtained from RUC. Animal culture bottles were aerated with very light bubbling through glass tubes to resuspend algae, and algae bottles were shaken to resuspend the algae and given new media every 3-4 days. Animals and algae were exposed to the natural light:dark cycle in Denmark during February, 2017.

Microsensor Profiling

Prior to experiments, each optode was calibrated at 100% O_2 air saturation and at 0% O_2 air saturation (achieved by addition of sodium dithionite) in seawater (30‰) at 8, 17 and 23°C.

Microbial respiration experiments/Copepod degradation experiments

The oxygen air saturation was measured (converted to oxygen concentration) and then we have calculated the respiration rates follows equation (1), (2), (3) and (4) (see Table 1).

Experiments were carried out in order to observe degradation of copepod carcasses, using microbial respiration rates as proxy to degradation of *A. tonsa* carcasses. Carcasses were incubated at a density of 25 carcasses 25 mL^{-1} in 25-mL serum bottles sealed with butyl rubber stoppers. To make sure incubation vials were clean/had no bacteria on the bottles walls, they were rinsed with acid and MQ water prior to experiments (Kanda 2008), and placed in a plankton wheel for incubations.

The animals used in experiments were not fed on the day of counting and starved overnight. Copepod carcasses were produced by submerging live animals into 10% acetic acid for about 10 seconds, and after this into Petri dishes with MQ-water for rinsing before to start experiments. These intact carcasses were carefully transferred from Petri dishes to the serum bottles containing 0.2 µm- filtered seawater (Millipore, Isopore membrane filters, 0.2 µm GTTP). In total, 24 bottles were mounted on a plankton wheel rotating at 13 rpm in order to ensure proper mixing of the water, and keep particulates, including carcasses, suspended. Oxygen concentration was monitored over time with optode spots (SensorSpot, Pyroscience, Germany) fixed to the inside of the incubation bottles (Glud et al., 2015). Oxygen concentrations were measured with the optode spots from the outside by a FireSting optical O_2 meter (Pyro Science, Germany). Then, oxygen concentration data were used for choosing the moment when sacrifice bottles as well and to take samples for ammonium DIC analysis and microbial cell bacteria.

At each of 5 time points (put hours of experiments), 3 bottles containing carcasses and 3 bottles containing only 0.2 µm filtered seawater (controls) were sacrificed, and samples were taken for ammonium. At each sampling, 1 ml of water was sampled for ammonium analysis, and stored at -20°C until analysis.

Mineralization processes

The carcasses-associated O_2 consumption and NH_4^+ production can be used to asses the microbial mineralization of the carcasses. Oxygen concentration time series were re-constructed from the concentration decreases measured between consecutive sampling points, while NH_4^+ concentration time series were measured directly.

Bottle effects

The bottle effect may produce an evident deviation from linear rates at oxygen concentrations above the limiting oxygen range due to significant increases in bacterial abundance and/or activity on the bottle walls. Regarding this, after sacrificing those bottles incubated with carcasses and they were re- filled and sealed with butyl rubber stoppers. Then, the bottles were mounted again on plankton wheel and the oxygen concentration was measured as was described above.

Sample analyses

The NH_4^+ concentration of the samples was determined by the salicylate-hypochlorite method (Bower and Holm- Hansen 1980) using a spectrophotometer Genesys 10S UV-VIS (ThermoScientific).

Results

Oxygen dynamics

Oxygen consumption associated with degradation of *A.tonsa* carcasses are shown below for experiments at 8, 17 and 23°C (Figure 1).

At 8°C O_2 concentration decreased from 305 to near 200 µM in bottles with carcasses and from 305 to 272 µM was observed in the control bottles (Fig.1A). In a 17°C O_2 decreased throughout the incubation from 258 to 115 µM in bottles with carcasses. A small decrease O_2 was observed in the control bottles (Fig. 1B).

While in 23°C the O_2 concentration decreased near linearly during the first 12 hours, and the conditions only truly got anoxic. Comparably very small, if any, concentration changes were observed in the controls (Fig, 1C).

The effect of the bottle treatment was similar at all incubations, although some differences were noticed in 23°C (Fig.1 I,J,K)

Bacterial respiration experiment as proxy of degradation of *A.tonsa* carcasses

Bacterial respiration rates associated with *A.tonsa* carcasses were calculated from oxygen consumption data measured at different temperatures (8, 17 and 23°C) (see *Materials and Methods*).

In 8°C oxygen consumption by bacterial respiration rates varied on average about 41

nmol h^{-1} in bottles with carcasses and 35 nmol. h^{-1} was measured in control bottles over 3 first hours, about 41 nmol. h^{-1} in carcasses and 9 nmol. h^{-1} in control and over 31 hours, and about 13 nmol. h^{-1} in carcasses and small consumption of 5 nmol. h^{-1} in control over last 124 hours (Fig. 1E).

In the 17°C experiment oxygen consumption by bacterial respiration was more pronounced compared to 8 and 8°C, steadily high by about 184 nmol. h^{-1} on bottles with carcasses and 71 nmol. h^{-1} over 3 hours, and over 12 hours continued high at about 117 nmol. h^{-1} with carcasses and 34 nmol. h^{-1} in control, and decreased oxygen consumption during the last 45 hours to about 47 nmol. h^{-1} and small concentration changes were seen in the control bottles (Fig. 1F).

Finally, at 23°C similar results than at 17°C, a high oxygen consumption, about 183 nmol. h^{-1} was seen over 3 hours, and 75 nmol. h^{-1} over 45 h in bottles with carcasses. Comparably small concentrations changes were observed in the controls (Fig. 1G).

NH_4^+ dynamics

In the 8°C- treatment (Fig. 2A), a production of NH_4^+ on average in carcasses could be seen already during the first 24 hours of incubation, and this production continued, with a total average increase about 9 µM over the entire incubation.

In the 17°C-treatment (Fig. 2B), ammonium production was more pronounced compared to what was seen at 8°C, with increase of about 6 µM over the first 24 hours, and a total increase of 11 µM during the whole incubation.

Finally, in the 23°C- treatment, a similar increase (compared to that seen at 17°C) in NH_4^+ average in carcasses was observed over first 24 hours, and a total increase of 9 µM was observed throughout the whole incubation. At all temperatures, the concentration changes observed in the controls were very small (Fig. 2C).

Discussion (preliminary)

The presence of zooplankton carcasses in the water column results from non-predatory mortality, which allows extensive microbial degradation of carcasses during their descent to the seabed (Tang et al., 2011). Common causes of non-predatory mortality include senescence, temperature change, physical and chemical stresses (e. g turbulence, wind and

currents), parasitism and food-related factors. After death, these carcasses could remain in the water column until removed by sinking, necrophagy, or microbial decomposition. Thus, in pelagic ecosystems, copepods represent vastly abundant "microbial hotspots" with unique biogeochemical features (Tang, 2005; Tang et al., 2010; Nuester et al., 2014).

An important process in microbial food webs is nutrient regeneration, especially mineralization of organic nitrogen to ammonium (Harrison, 1992). These originally bound nutrients can be release directly by grazers during the feeding process (sloppy feeding) (Jumars et al. 1989**;** Møller and Nielsen 2001; Møller, 2005**)**, viral lysis of bacteria (Fuhrman, 2000) and protists (Miller and Wheeler, 2009) or during microbial decomposition of zooplankton carcasses (Tang et al., 2010).

In this investigation, we have measured bacterial respiration rate as a proxy for carbon turnover/degradation directly associated with carcasses of the calanoid *A. tonsa* , which seemed to be temperature dependent. Over time, bacteria initially associated with the animals may end up in the water during incubation and respire O_2 due to ammonium release by the decomposition of carcasses.

Bacteria release ammonium when C:N of the DOM utilized is <4.5, but take up ammonium when the C:N of the DOM utilized is >6.6 (Goldman et al., 1987;Kirchman 2000). By comparison, calanoid copepods, the most abundant marine mesozooplankton taxa, have an average C:N ratio close to 3, and proteins commonly account for 30–70% of their dry weight (Båmstedt 1986). This suggests that although, few in number, zooplankton carcasses provide higher quality POM than detrital aggregates. Also, unlike phytoaggregates, which rarely become anoxic (Ploug 2001), decomposing zooplankton carcasses can quickly become hypoxic or anoxic and support anaerobic microbial processes that otherwise could not occur in the water column (Glud et al. 2015).

There is some controversy over the relative roles of bacteria and protists for ammonium regenerations. Both can release ammonium, but bacteria collectively appear to take up as much ammonium as they release (Kirchman 2000). Therefore, the availability production of NH_4^+ from decomposition of carcasses observed in all treatments as oxygen was depleted, resulted from mineralization processes, and then DNRA may contribute (but this is a process that occurs in anoxic conditions, using nitrate instead of O_2 as an electron acceptor). Besides, the production of NH_4^+ further suggest that copepod carcasses sinking

passively transport bound nitrogen to depth where it is partially released as ammonium and may fuel free-living anammox bacteria and thus may contribute to pelagic N- loss by anammox.

Therefore, Pelagic N-loss is potentially enhanced by zooplankton carcasses indirectly through NH_4^+ production that may fuel free-living anammox bacteria. As copepods are some of the most abundant mesozooplankton in the oceans, anaerobic nitrogen cycling associated with these animals may have large implications for biogeochemical cycling in the oceans, and not least fixed-nitrogen loss from marine pelagic environments.

Contributions

SY, PS and RG led the design of the study, fieldwork and laboratory analyses. All authors interpreted results. SY and RP wrote the manuscript with contributions from all other authors.

Acknowledgements

This work was supported by Millennium Institute of Oceanography ICM 120019. Yañez was supported by the Scholarship of CONICYT-PCHA/Doctorado Nacional/2013-21130213. This work is a contribution by Millennium Institute of Oceanography ICM 120019.

References

Azam F, Fenchel T, Field JG, Gray JS, Meyer-Reil LA, Thingstad F. 1983. The ecological role of water-column microbes in the sea. Mar Ecol Prog Ser 10:257–263.

Båmstedt U. 1986. Chemical composition and energy content. In: Corner EDS, O'Hara SCM (Eds.), The Biological Chemistry of Marine Copepods, Clarendon Press, Oxford.

Cushing DH .1989. A difference in structure between ecosystems in strongly stratified waters and in those that are only weakly stratified. J Plankton Res 11: 1-13.

Fuhrman J. 2000. Impact of viruses on bacterial processes. In: Kirchman DL (ed) Microbial ecology of the oceans. Wiley, New York, p 327–350.

Glud, R. N., Grossart, H. P., Larsen, M., Tang, K. W., Arendt, K. E., Rysgaard, S., et al. 2015. Copepod carcasses as microbial hot spots for pelagic denitrification. Limnol.

Oceanogr. 60, 2026–2036. doi: 10.1002/lno.10149.

Goldman JC, Caron DA, Dennet MR.1987. Regulation of gross growth efficiency and ammonium regeneration in bacteria by substrate C:N ratio. Limnol Oceanogr 32:1239 − 1252.Harrison W.G. 1992. Regeneration of Nutrients. In: Falkowski P.G., Woodhead A.D., Vivirito K. (eds) Primary Productivity and Biogeochemical Cycles in the Sea. Environmental Science Research, vol 43. Springer, Boston, MA

Kanda, J. 2008. 'Vertical profiles of nitrate uptake obtained from in situ N-15 incubation experiments in the western North Pacific', Journal of Marine Systems, 71: 63-78.

Kirchman, D.L. 2000. Uptake and regeneration of inorganic nutrients by marine heterotrophic bacteria. In Kirchman, D.L. (ed), Microbial ecology of the oceans. John Wiley and Sons, New York, pp. 261-288.

Miller C.B., Wheeler P.A 2009. Biological Oceanography. John Wiley & Sons, 2009. 416 pp.

Møller EF, Nielsen TG. 2001. Production of bacterial substrate by marine copepods: Effect of phytoplankton biomass and cell size. J Plankton Res 23: 527-536.

Møller EF. 2005. Sloppy feeding in marine copepods: Prey-size-dependent production of dissolved organic carbon. J Plankton Res 27: 27-35.

Nuester, J., Shema, S., Vermont, A., Fields, D. M., and Twining, B. S. 2014. The regeneration of highly bioavailable iron by meso- and microzooplankton. Limnol. Oceanogr. 59, 1399–1409.

Olsen SN, Westh P, Hansen BW .2005. Real-time quantification of microbial degradation of copepod fecal pellets monitored by isothermal microcalorimetry. Aquat Microb Ecol 40:259–267.

Ploug H. 2001. Small-scale oxygen fluxes and remineralization in sinking aggregates. Limnol Oceanogr 46:1624–1631.

Saba, G. K., Steinberg, D. K., and Bronk, D. A. 2011. The relative importance of sloppy feeding, excretion, and fecal pellet leaching in the release of dissolved carbon and nitrogen by *Acartia tonsa* copepods. J. Exp. Mar. Biol. Ecol. 404, 47–56.

Sampei M., Sasaki H., Hattori H.,Forest A. and Fortier L. 2009. Significant contribution of passively sinking copepods to the downward export flux in Arctic waters. Limnol. Oceanogr 54(6) 1894–1900.

Steinberg, D. K., Goldthwait, S. A., and Hansell, D. A. 2000. Zooplankton vertical migration and the active transport of dissolved organic and inorganic nitrogen in the Sargasso S.

Steinberg D.K and Landry M.R. 2017. Zooplankton and the Ocean Carbon Cycle. Annu. Rev. Mar. Sci. 2017. 9:413–44.

Stief P, Lundgaard ASB, Morales-Ramírez Á, Thamdrup B and Glud RN. 2017. Fixed-Nitrogen Loss Associated with Sinking Zooplankton Carcasses in a Coastal Oxygen Minimum Zone (Golfo Dulce, Costa Rica). Front. Mar. Sci. 4:152.

Tang, K. W. 2005. Copepods as microbial hotspots in the ocean: effects of host feeding activities on attached bacteria. Aquat. Microb. Ecol. 38, 31–40.

Tang, K. W., Hutalle, K. M. L., and Grossart, H. P. 2006. Microbial abundance, composition and enzymatic activity during decomposition of copepod carcasses. Aquat. Microb. Ecol. 45, 219–227. doi: 10.3354/ame045219.

Tang, K. W., Bickel, S. L., Dziallas, C., and Grossart, H. P. 2009. Microbial activities accompanying decomposition of cladoceran and copepod carcasses under different environmental conditions. Aquat. Microb. Ecol. 57, 89–100.doi: 10.3354/ame01331.

Tang, K. W., Turk, V., and Grossart, H. P. 2010. Linkage between crustacean zooplankton and aquatic bacteria. Aquat. Microb. Ecol. 61, 261–277 doi: 10.3354/ame01424.

Tang, K.W., Glud, R.N., Glud, A., Rysgaard, S., and Nielsen, T.G. 2011 Copepod guts as biogeochemical hotspots in the sea: Evidence from microelectrode profiling of Calanus spp. Limnol Oceanogr 56: 666-672.

Tang, K. W., Gladyshev, M. I., Dubovskaya, O. P., Kirillin, G., and Grossart, H. P. 2014. Zooplankton carcasses and non-predatory mortality in freshwater and inland sea environments. J. Plankton Res. 36, 597–612.

Tang, K, W., Elliott D, T. 2014. Copepod carcasses: Occurrence, fate and ecological importance. Copepods: Diversity, Habitat and Behaviour, Pages: 255 – 278.

Table 1: Parameters and formulations for calculating bacterial respiration rates

Parameter	Symbol	Unit	Note
Oxygen concentration	O_2 conc.	µM	Where the solubility (µM) of O_2 change at 8, 12, 17 and 23 °C and 30‰, and slope (calibration) is the slope between nominal % air sat. values (e.g. 100% and 0%) and measured % air sat. values
Oxygen conversion rate	O_2 rate	nmol/h	O_2 conc.(µM) vs. time (hours)
Oxygen conversion rate by animals	O_2 rate by carcasses	nmol/h	
Individual-specific respiration rate	Ind-Rrate	nmol/ind./ h	Bacterial respiration rate from degradation of carcasses experiments
Calculations of factor:			
$O_2\ \text{conc.} = \frac{\text{Meas. } O_2\%\ \text{air. sat\% air sat. at 0\% cal.} \cdot \text{slope(cal.)}}{100\%} \cdot \text{solubility}$			(1)
$O_2\ \text{rate} = \text{slope}\ (O_2\ \text{conc. vs. time}) \cdot 25$			(2)
$O_2\ \text{rate by carcasses} = O_2\ \text{rate (bottle w. animals) [nmol/h]} - O_2\ \text{rate (bottles) [nmol/h]}$			(3)
$\text{Ind-R rate} = \frac{O_2 \text{conversion rate by animals [nmol/h]}}{\text{Abundance (no. ind.)}}$			(4)

Figure captions

Figure 1: Concentration time-series of oxygen. Oxygen consumption (µM) associated to *A. tonsa* incubated at temperatures of 8 (A), 12 (B), 17(C) y 23°C (D). Black diamonds symbols are carcasses and white diamonds are controls. Bacterial respiration experiment as proxy of degradation of *A.tonsa* incubated at temperatures of 8 (E), 12 (F), 17(G) y 23°C (H). Black barr are carcasses and white barr are controls. Oxygen consumption (µM) associated to bottle effects experiments associated to *A. tonsa* incubated at temperatures of 8 (I), 12 (J), 17(K) y 23°C (L). Black diamonds symbols are carcasses and white diamonds are controls.

Figure 2: NH_4^+ dynamics associated to *A. tonsa* incubated at temperatures of 8(A), 12(B), 17 (C) y 23°C (D). Red square are carcasses and white square are controls.

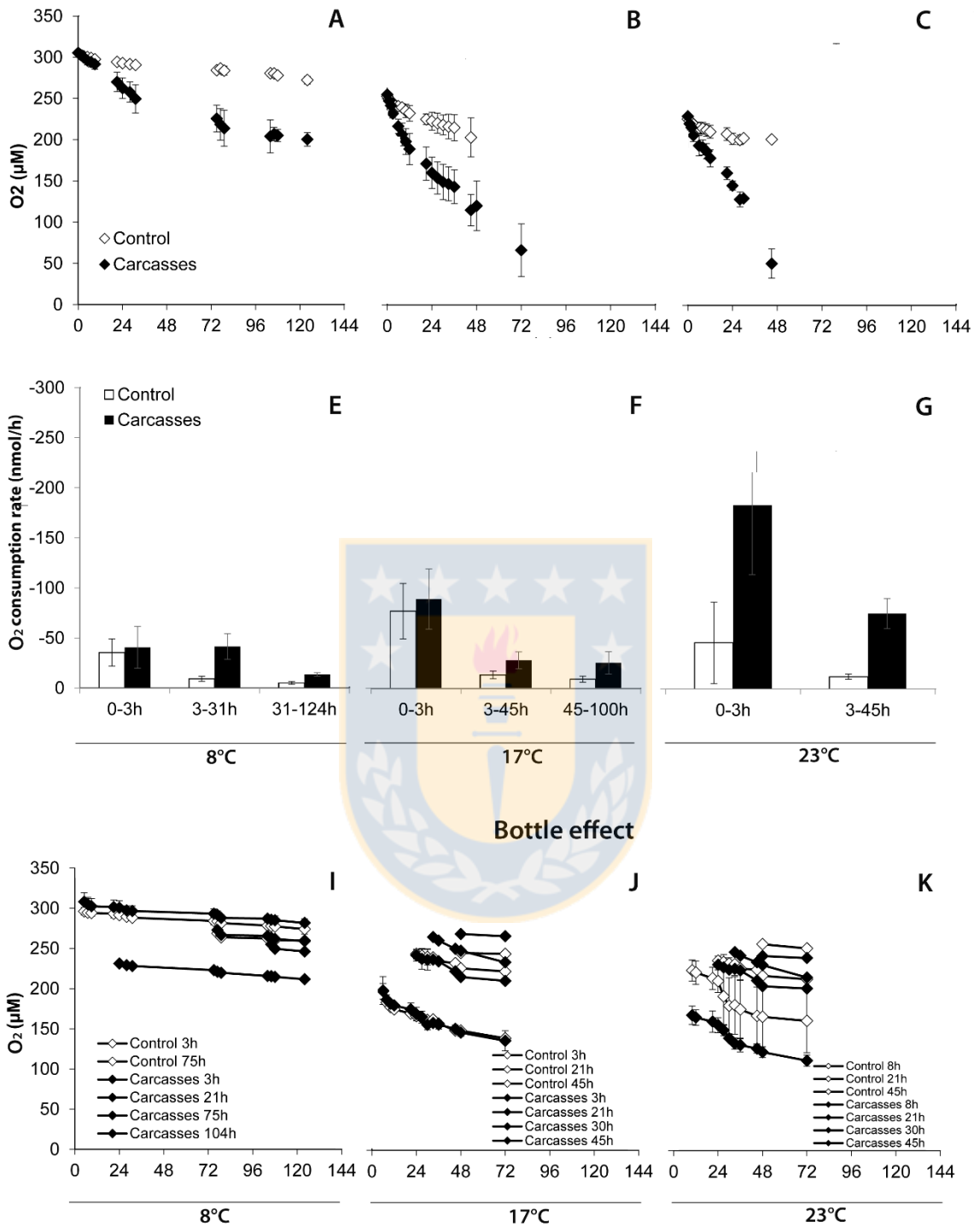
A
B
C
O2 (µM)
Control
Carcasses
E
F
G
O2 consumption rate (nmol/h)
0-3h
3-31h
31-124h
0-3h
3-45h
45-100h
0-3h
3-45h
8°C
17°C
23°C
Bottle effect
I
J
K
O2 (µM)
Control 3h
Control 75h
Carcasses 3h
Carcasses 21h
Carcasses 75h
Carcasses 104h
Control 3h
Control 21h
Control 45h
Carcasses 3h
Carcasses 21h
Carcasses 30h
Carcasses 45h
Control 8h
Control 21h
Control 45h
Carcasses 8h
Carcasses 21h
Carcasses 30h
Carcasses 45h
8°C
17°C
23°C

Figure 1

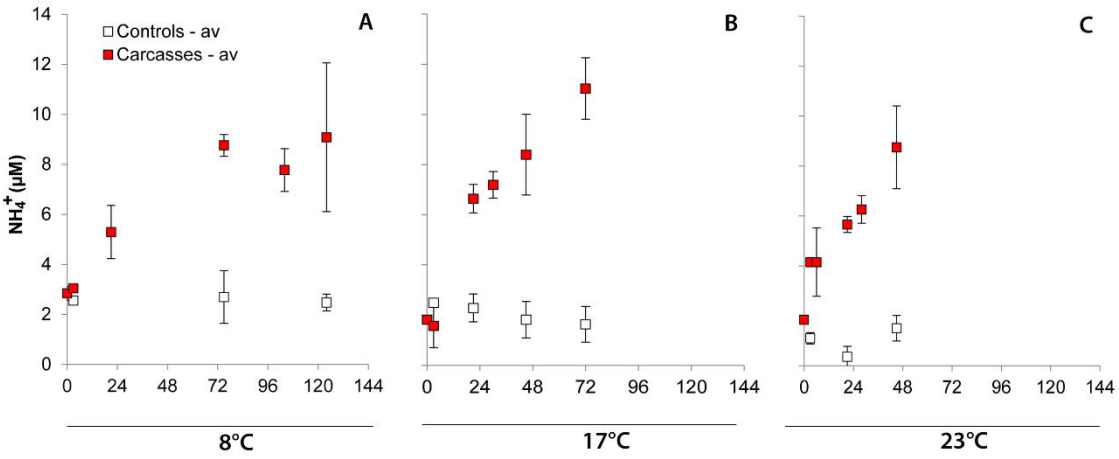
Controls - av
Carcasses - av
A
B
C
NH_4^+ (µM)
0
2
4
6
8
10
12
14
0
24
48
72
96
120
144
8°C
17°C
23°C

Figure 2

5. DISCUSIÓN

5.1. Copépodos pelágicos en el Sistema de Corrientes de Humboldt: aproximaciones de tasas de mortalidad no−depredatoria.

El Sistema de Corrientes de Humboldt (SCH), es uno de los sistemas más productivos del mundo, que incluye ecosistemas de surgencia costera frente a Chile (Morales & Lange, 2004). Esta producción es, en gran medida, transferida al pélagos a través de grandes pesquerías, sustentada principalmente por el zooplancton como parte de su alimento (Morales and Lange, 2004; Espinoza and Bertrand, 2008) y/o es exportado al sistema bentónico donde finalmente es acumulado y enterrado como sedimento rico en materia orgánica.

La mortalidad es uno de los parámetros más crítico y poco descrito en la dinámica poblacional de copépodos (Runge et al., 2004; Ohman & Wood 1995), siendo sus mecanismos de control espacial y temporal pobremente descritos hasta ahora. Las investigaciones tradicionales por mucho tiempo han asumido que la mortalidad siempre es causada por la depredación (Genin et al., 1995), y es esta quien regula los cambios en la abundancia de las poblaciones; no obstante, muchos otros factores no-depredarorios pueden ser también responsables de mortalidad, tales como enfermedades (Delgado & Alcaraz 1999), parásitos (Kimmerer & McKinnon 1990; Burns 1985; Dufy et al., 2005), estrés ambiental (Roman et al., 1993), inanición (Tsuda 1994), y senescencia (Ceballos & Kiørboe 2011; Saiz et al., 2015).

Hoy en día, sigue siendo una práctica común en muestreos zooplanctónicos de campo donde los científicos simplemente preservan y cuentan todos los organismos como "vivos" (Harris et al., 2000). Pero es simplemente ilógico creer que todos los copépodos *in situ* están vivos. Esto ha sido principalmente debido a la falta de métodos que permitan la identificación de individuos vivos y muertos en las muestras, y en parte debido a la percepción arraigada de que los copépodos solo mueren por depredación en el ambiente (Hirst & Kiørboe, 2002). Sin embargo, no existe una razón biológica (o lógica) válida para creer que los copépodos no mueran por mortalidad no-depredadora y que se observa como la presencia de cadáveres (carcasas) en el ambiente. Como lo señaló el ecologista R.G.

Wetzel, (1995):

"La idea común que existe sobre la producción neta en organismos, particularmente algas, microbios y también metazoos, deriva principalmente de la depredación, no sólo es poco comprobable sino también intuitivamente poco razonable. Muchos de los organismos, particularmente bacterias, hongos y también algas y muchos otros organismos simplemente maduran fisiológicamente, envejecen, y mueren, combinándose con el detrito particulado y disuelto disponible para la utilización heterotrófica microbiana. Solo porque no podamos medir bien la mortalidad no- depredadora no significa que no exista o incluso domine en la mayoría de las épocas del año"

Los resultados de esta investigación brindan un fuerte respaldo para estas audaces declaraciones.

Primero, desde recientes avances en el método de tinción de Rojo Neutro para distinguir entre los individuos vivos y muertos en muestreos de campo, se ha podido obtener una detallada cuantificación de la abundancia de carcasas de copépodos en el SCH (Yañez et al. 2012,2018; Elliott and Tang 2009). Este método había sido utilizado escasamente en el SCH, y en este estudio fue estandarizado para diferentes grupos de zooplancton, específicamente copépodos, sus huevos, nauplios y copepoditos. Además, fue testeado en dos diferentes zonas de surgencia costera y tres tipos de redes de muestreo, demostrándose su eficiencia en esas áreas luego de analizar más de 140 muestras de zooplancton.

Luego, estimamos por primera vez las tasas de mortalidad de tres copépodos dominantes en la bahía de Mejillones (23°S) dentro del SCH y examinamos su relación con las condiciones ambientales. Una interesante observación de este estudio es que las tasas de mortalidad aumentaron con los estadios de desarrollo en las tres especies. Las tasas de mortalidad se incrementa con la ontogenia, porque los estadíos tardíos poseen tiempos de desarrollo más largos (días a semanas) que los estadíos tempranos (horas a días), por lo tanto permanecen mucho más tiempo en el ambiente. Elliott and Tang (2011a) observaron que, en un ciclo anual en la bahía de Chesapeake, las tasas de mortalidad de copepoditos fueron más altas que las de los nauplios. En Lurejforden, Noruega, las tasas de mortalidad de *Calanus* spp. disminuyeron substancialmente a través de los estadios naupliares, pero incrementaron subtancialmente de los estadios C1 y C5 (Eiane et al., 2002). La mortalidad

depredatoria de las tres especies aumentaron con los estadios de desarrollo, por lo tanto, con el tamaño del cuerpo. Un mayor tamaño corporal puede lograr que los copépodos se vuelvan más evidentes para los depredadores, tales como los peces planctívoros, que a menudo prefieren una presa más grande (Brooks 1968, O'Brien et al. 1976). Dentro del HCS, los planctivoros principales incluyen sardinas y anchovetas dentro de la capa oxígenada (Espinoza y Bertrand 2008), que podrían explicar la relación la relación positiva de las tasas de mortalidad depredatoria con los estadios de copepoditos (e.g. tamaño del cuerpo), asi como tambien con el OD en dos de tres especies. La intrusión intermitente de aguas pobres en oxígeno asociadas a la surgencia costera es una característica común en esta región (Marín et al., 1993), que podría inducir episodios de hipoxia y mortalidad de copépodos como *Paracalanus* cf. *indicus*, *Acartia tonsa* y estadios tempranos de *Calanus chilensis* (Yañez et al., 2012; Elliott et al., 2010, 2013; Ruz et al., 2015; este estudio).

Así mismo, en este estudio las bajas concentraciones de DO fueron asociadas con altas tas de mortalidad no-depredatoria en *P.* cf. *indicus* y *A.tonsa*, coincidente con estudios previos (Yáñez et al., 2012; Ruz et al., 2015). Lo opuesto fue observado en *C. chilensis*, lo que refleja la mejor capacidad de esta especie para tolerar la hipoxia (Hirche et al., 2014, Ruz et al., 2018).

Este estudio sugiere, entonces, que el estrés ambiental generado por la hipoxia en aguas superficiales podría ser la causa principal de mortalidad no-depredatoria en copépodos, y por lo tanto refleja la importancia del estrés ambiental sobre el control de la dinámica poblacional de copépodos dentro del HCS. Futuros ajustes a esta aproximación son necesarios, particularmente para estimar el tiempo de residencia de las carcasas (τ) en nuestro ambiente. No obstante, esta aproximación podría permitir que los investigadores comiencen estudios de mortalidad no-depredatoria de copépodos, incitando la posibilidad de futuras discusiones e investigaciones sobre este tópico.

Entonces, las carcasas de copépodos no son necesariamente pérdidas desde la cadena trófica. Algunas de ellas pueden servir como alimento para planctívoros (Elliott et al., 2010), o ser incorporados en la cadena trófica microbiana (Tang et al., 2009; Bickel and Tang, 2010; este estudio, siguiente capítulo) y en los flujos de sedimentación de materia orgánica (Sampei et al., 2009, 2012; Ivory et al., 2014), debido al rápido hundimiento que éstas presentan (40-60 m por día, Yañez et al., 2012: Elliott et al., 2010). Sin embargo,

sabemos que los copépodos muertos obviamente muestran patrones de desplazamiento muy diferentes a los de copépodos vivos; por lo tanto, entender el destino de estas carcasas nos permitiría conocer como ellos influencian sobre el ecosistema. Mas significativo aun, hay que reconocer que estos individuos muertos no contribuyen al crecimiento poblacional, por lo que correcciones apropiadas son necesarias sobre las estimaciones de producción secundaria (PS).

Así, la estandarización del método de tinción rojo neutro junto a la aproximación de tasas de mortalidad no-depredatoria nos permitieron estimar los errores en estimaciones de PS asociados a la ocurrencia de carcasas en las muestras de campo y al uso del método de tasas de muda para estimar tasas de crecimiento. En este estudio, nosotros cuantificamos los errores en PS causados por la falta de consideración de los tiempos de duración de estadios y el crecimiento entre estadios, junto a la incapacidad de diferenciar copépodos vivos y muertos. En general, nuestro rango de datos calculados de error en la estimación de PS basados sobre muestras de campo fue comparable con los datos derivados de meta-análisis por Hirst et al., (2005, 2014). También, nuestros datos muestran que tanto el signo como la magnitud del error en las estimaciones de PS varían entre las especies de copépodos co-existentes, siendo en *P.* cf. *indicus* un orden de magnitud mayor que en *A.tonsa* y *C. chilensis*. *P.* cf. *indicus* es altamente abundante en el SCH y desempeña un rol importante en la ecología de este ecosistema (Escribano et al., 2012, 2016; Pino-Pinuer et al., 2014). Es más probable que esta especie contribuya con más carcasas que otras, proporcionando su mayor abundancia, una mortalidad potencialmente más alta. Esto, porque *P.* cf. *indicus* puede responder rápidamente a las variaciones ambientales (por ejemplo, aumentando sus tasas de desarrollo y crecimiento), y así incrementando sus tasas de mortalidad no-depredatoria como fue observado claramente en este estudio con la presencia de carcasas, así podemos afirmar que la estimación de producción secundaria de esta especie es particularmente propensa a errores, y que se requiere precaución adicional al considerar la dinámica de la red trófica regional y las pesquerías que involucran a esta especie. A pesar que los errores en PS promedio en *A. tonsa* y *C.chilensis* son más bajos que los observados en *P.* cf. *indicus*, es importante aún su consideración debido a que un error inicial pequeño que se propague a través de las generaciones, daría lugar a un error de gran magnitud a largo plazo (Elliott and Tang, 2011). Esto es particularmente relevante en

especies de tiempos generacionales cortos, tales como aquellas que habitan en el SCH (Hidalgo and Escribano, 2008; Escribano et al., 2014). Finalmente, es igualmente importante la observación que, entre especies, la distribución no fue uniforme a través de los meses y/o estadios. Esto es relevante ya que conocer cuándo y dónde ocurre la mayor parte del error podría ayudar a los científicos a diseñar métodos más adecuados de muestreo y modelar estrategias para minimizar el sesgo.

La región del Pacifico Suroriental, está fuertemente influenciada por El Niño Oscilación del Sur (ENSO). Se espera que el cambio climático intensifique la surgencia dentro del SCH (Echevin et al., 2012), con los correspondientes cambios en hidrografía, química del agua, diversidad de especies y fenología (Hays et al., 2005). Un aumento en los eventos de surgencia costera podría promover blooms de diatomeas que afectan negativamente el suministro de alimento para copépodos (Vargas et al., 2006; Poulet et al., 2007) y somerizar más aún la ZMO, intensificando el estrés relacionado con la hipoxia (Gilly et al., 2013). Estas predicciones podrían conducir a un aumento en los episodios de mortalidad no-depredatoria en copépodos. Basado en lo anterior, podemos afirmar que es relevante considerar la realización de esfuerzos parar diferenciar y cuantificar los copépodos vivos y muertos *in situ*, y por ende aplicar las correcciones apropiadas al estimar producción secundaria en estudios futuros.

5.2. Degradación y composición bacteriana de carcasas de copépodos en aguas con bajo contenido de oxígeno.

El curso de la degradación de las carcasas del copépodo marino *A. tonsa*. En condiciones óxicas, la descomposición comento rápidamente, en las siguientes horas esta fue relativamente estabe y lentamente se incremento en las ultimas horas de incubación. En contraste, el proceso de descomposición fue mucho mas bajo en condiciones anóxicas, incrementándose muy rapidamente en las últimas horas de la incubación. Las diferencias observadas en este estudio durante las primeras horas de incubación entre los tratamientos: alto porcentaje de perdida de tejidos internos en condiciones óxicas que anóxicas son comparables con observaciones realidadas por Tang et al., (2006). Nosotros tambien observamos que al final del experimento mucho del tejido interno tiende a desaparecer, quedando el exoesqueleto quitinoso intacto, coincidente con Tang et al., (2009). La

degradación de quitina en la naturaleza tiende a ser muy baja. Por ejemplo, incubaciones *in situ* de purificación de partículas muestran una "tasa de pérdida" < 1% por día (Kirchner, 1995; Kirchman &White, 1999; Tang & Elliott, 2014).

Entonces, las ZMOs en el SCH incrementan las tasas de sedimentación de las carcasas de copépodos, debido a que las tasas de degradación de estas son mas lentas las primeras horas, manteniendo una densidad mayor que la de agua de mar y como consecuencias estas carcasas se hunden hacia aguas más profundas.

Usando secuenciación masiva dirigida (Ilumina taq-sequencing) se identificaron las comunidades bacterianas asociadas a la degradación de carcasas del copépodo calanoideo *A.tonsa* bajo concentraciones de oxígeno controladas. Estas comunidades fueron significativamente diferentes entre los tratamientos.

Las Rhodobacteraceae, la familia más abundante en las comunidades bacterianas asociadas a carcasas de bacterias en nuestros experimentos de degradación, han sido reportadas en estudios previos asociadas a otros organismos marinos, tales como los corales, esponjas y microalgas (Ridley et al., 2005; Burke et al., 2011 y Roder et al., 2014; respectivamente) y también como responsables en la formación de biopelículas (Pujalte et al., 2014), sugiriendo entonces que este grupo desempeña un rol importante en la colonización del exoesqueleto de copépodos.

Otros grupos típicamente asociados con copépodos marinos son aquellos capaces de utilizar la quitina como fuente de carbono y nitrógeno, tales como *Vibrio* spp., *Sphingomonas sp*., y *Pseudoalteromonas spp*. (Svitil et al., 1997; Zhu et al., 2007; Tang et al., 2010; Gerdts et al., 2013), que son representantes de las familias Vibrionaceae, Sphingomonadaceae y Pseudoalteromonadaceae, respectivamente. En este estudio, Vibrionaceae fue una de las más dominantes en los experimentos de degradación, especialmente en los estadios iniciales y finales de degradación en condiciones anoxicas, en donde se observó que la quitina de las carcasas estaba rota y altamente degradada, respectivamente. Consecuentemente, se puede sugerir que Vibrionaceae es la principal responsable de la degradación de quitina en nuestros experimentos.

Inesperadamente, nosotros obtuvimos OTUs asociadas a la familia Verrucomicrobiaceae en las carcasas de copépodos. Representantes de esta familia habían sido reportados hasta ahora solamente como simbiontes de esponjas (Thiel et al., 2007) e

hidromedusas (Daley et al., 2016). En nuestro estudio, observamos que fueron consistentemente abundantes en carcasas de copépodos, especialmente en el tratamiento con condiciones oxigenadas; en contraste, obserbamos muy bajas abundancias en condiciones anóxicas. Lo que coincide con estudios previos realizados en donde se ha encontrado en muy bajas abundancias en el microbioma del intestino (anóxico) presente en copépodos marinos (Moinsander et al., 2015; Skovgaard, 2015). Por otro lado, los miembros del filo Firmicutes han sido encontrados en materia orgánica particulada marina (Vojvoda et al. 2014) y en el microbioma de mamíferos e invertebrados tanto terrestres como acuáticos (Ley et al. 2005; Wust et al. 2011). En el medio acuático, se ha documentado su rol específico en la digestión de copépodos de agua dulce, aunque están ausentes en aguas circundantes (Grossart et al. 2009; Homonnay et al. 2012). En este estudio, fueron identificados en muy baja abundancia, aunque distinguiendo más individuos en condiciones óxicas que anóxicas, representantes de los órdenes Clostridiales, Lactobacillales y Bacillales, pertenecientes también a este Phyllum.

Las comunidades bacterianas asociadas con carcasas de copépodos, incluyendo aquellas que colonizan el exoesqueleto, podrían cambiar y ser dominadas por organismos anaeróbicos o anaeróbicos facultativos, en comparación con las óxicas, al ser expuestas a ambientes con bajos niveles de oxígeno, reforzando la idea de la función de las carcasas de copépodos en un ambiente pelágico hipóxico como *hotspots* con potenciales implicancias a gran escala en los ciclos biogeoquímicos del ecosistema pelágico.

En esta investigación también se observó la presencia de dos genes marcadores de la presencia de desnitrificación, *nirK y nosZ* (producción N_2 y N_2O, respectivamente) los que fueron encontrados bajo condiciones anóxicas, principalmente asociados con el estadio final de degradación. Esto es concordante con estudios previos, en donde se ha reportado la presencia de los genes *nirS*, *nirK* y *nosZ* en el intestino de copépodos árticos (Glud et al. 2015), del Océano Atlántico norte (De Corte et al. 2018).

Por consiguiente, las carcasas de *Acartia tonsa* que permanecen en la columna de agua representan *hotspots* de desnitrificación en el ecosistema pelágico, aunque su importancia cuantitativa como sumidero de nitrógeno biodisponible es extremadamente dependiente de la concentración de OD del ambiente. Así, la importancia de las carcasas de copépodos asociadas a la desnitrificación podría ser altamente significativa en ambientes

pobres en oxígeno disuelto tales como la Zonas de Mínimo de Oxígeno (ZMO) presentes en el SCH.

5.3 Degradación de carcasas de copépodos: potenciales impactos en el ciclo de C y N.

La presencia de carcasas de zooplancton en la columna de agua es el resultado de la mortalidad no-depredatoria, cuyas causas están descritas arriba (ver sección 5.1). Una vez que los copépodos mueren, sus carcasas pueden permanecer en la columna de agua, sedimentar o ser removidas por necrofagia o degradación microbiana (Tang et al., 2011). Por lo tanto, las carcasas de zooplancton representan *"microbial hotspots"* enormemente abundantes en el ecosistema pelágico con características biogeoquímicas únicas (Tang, 2005; Tang et al., 2010; Nuester et al., 2014).

Un proceso importante en las redes tróficas microbianas es la regeneración de nutrientes, especialmente la mineralización de nitrógeno orgánico a amonio (Harrison, 1992). Estos nutrientes pueden ser liberados directamente por herbívoros durante el proceso de alimentación (*sloppy feeding*) (Jumars et al. 1989; Møller and Nielsen 2001; Møller, 2005), lisis viral de bacterias (Fuhrman, 2000), protistas (Miller and Wheeler, 2009), o durante la degradación microbiana de carcasas de zooplancton (Tang et al., 2010).

En esta investigación, hemos medido la tasa de respiración bacteriana como un proxy a la pérdida/degradación de nitrógeno asociado directamente con las carcasas del copépodo calanoideo *A. tonsa*, la que parece depender estrictamente de la temperatura. Se observó un incremento en las concentraciones de amonio hacia el final del experimento, cuando las concentraciones de oxígeno estaban muy bajas (hipoxia). Esto puede deberse a la liberación de bacterias inicialmente asociadas a las carcasas de copépodos a lo largo de la incubación, las cuales consumirían O_2 mientras se remineraliza el nitrógeno orgánico, liberado como amonio a través de la descomposición de las carcasas.

Las bacterias liberan amonio cuando la razón C:N de la DOM utilizada es < 4.5 y consumen amonio cuando ésta es > 6.6 (Goldman et al., 1987; Kirchman, 2000). Copépodos calanoideos, el taxa del mesozooplancton marino más abundante, presenta un radio de C:N promedio cercano a 3, con 30–70% de su peso seco correspondiente a proteínas (Båmstedt 1986). Basado en lo anterior, se puede sugerir que las carcasas de

copépodos proporcionan POM de mejor calidad para las bacterias que los agregados de detrito. Además, a diferencia de los fitoagregados, que rara vez se vuelven anóxicos (Ploug, 2001), estas carcasas en descomposición pueden convertirse rápidamente en hipóxicas o anóxicas y sostener procesos microbianos anaeróbicos que de otro modo no podrían ocurrir en la columna de agua (Glud et al., 2015).

Estos estudios siguen generando controversia, principalmente en relación a los roles relativos que bacterias y protistas tendrían como regeneradores de amonio. Ambos pueden liberar amonio, pero las bacterias parecen poder absorberlo, así como liberarlo (Kirchman 2000). Por lo tanto, la producción de NH_4^+ a partir de la degradación bacteriana de carcasas de *A.tonsa* observada en todos los tratamientos en donde el oxígeno estaba en muy bajas concentraciones, estaría provocada por la mineralización del nitrógeno orgánico; y ésta, a su vez, potencialmente podría contribuir a la DNRA (pero, este es un proceso que ocurre solo en condiciones anóxicas, utilizando nitrato en lugar de O_2 como aceptador de electrones). Por otra parte, el NH_4^+ producido en carcasas de copépodos que sedimentan arrastraría nitrógeno a través de transporte pasivo hacia aguas profundas donde podría liberarse parcialmente como amonio y ser oxidado a N_2 por bacterias de vida libre. Entonces, estas carcasas estarían contribuyendo, indirectamente, a procesos de pérdida de N a través de anammox.

Así, la pérdida de N en el piélago se ve potencialmente incrementada por las carcasas de copépodos directamente a través de la producción de N_2 y N_2O (ver sección 5.2), e indirectamente a través de la producción de NH_4^+ por anammox de bacterias de vida libre.

6. CONCLUSIONES

Considerando todos los resultados obtenidos en este estudio realizado para evaluar la mortalidad y degradación de copépodos pelágicos asociada a las Zonas de Mínimo de Oxígeno (ZMOs), podemos concluir lo siguiente:

- Los avances recientes en métodos de tinción para distinguir entre individuos vivos y muertos en muestras *in situ* junto a los ajustes a las condiciones locales realizados en este estudio han abierto la oportunidad de realizar una cuantificación detallada de la abundancia de carcasas de copépodos en Sistema de Corrientes de Humboldt (SCH).
- Las carcasas de tres copépodos marinos dominantes: *Paracalanus* cf. *indicus*, *Acartia tonsa*, y *Calanus chilensis*, fueron ubicuas en el SCH.
- Las tasas de mortalidad total aumentaron con los estadíos de desarrollo en las tres especies en la Bahía de Mejillones. Las tasas de mortalidad total de C5 fueron 3-4 veces más altas que las de C1. En promedio, la depredación representó 53,7 de la mortalidad total en *P.* cf. *indicus*, 56,4% en *A. tonsa* y hasta un 65,2% en *C. chilensis*. Mientras tanto, la mortalidad no depredadora representa entre 34.8 al 46.3% de la mortalidad total, y esto refleja la importancia del estrés ambientales sobre el control de la dinámica poblacional de copépodos en el HCS.
- Futuros ajustes a esta aproximación son necesarios, particularmente para estimar el tiempo de residencia de las carcasas (τ) en nuestro ambiente. No obstante, esta aproximación podría permitir que los investigadores comiencen estudios de mortalidad no-depredatoria de copépodos, estimulando la posibilidad de futuras discusiones e investigaciones sobre este tópico.
- No realizar correcciones apropiadas en las estimaciones de crecimiento e ignorar la presencia de carcasas, puede llevar a enormes errores en las estimaciones de producción secundaria (PS). El promedio anual de error en PS fue -39,2% en *P.* cf. *indicus*, 3,1% en *A.tonsa*, y 5,2% en *C.chilensis*.
- Este error puede variar en magnitud y signo a través de los meses, especies y estadios de desarrollo. Esto es relevante ya que conocer cuándo y dónde ocurre la mayor parte del error podría ayudar a los científicos a diseñar métodos más

adecuados de muestreo y modelar estrategias para minimizar el sesgo. Incluso en aquellos casos en que el porcentaje de error es pequeño, las proyecciones de producción pueden acumular errores significativos a largo plazo, principalmente especies con tiempos generacionales cortos.

- La degradación de carcasas del copépodo marino *A. tonsa* en condiciones óxicas, comenzó rápidamente, luego se observó relativamente estable, y se incrementó lentamente en las últimas horas de incubación. En contraste, el proceso de degradación fue mucho más lento en condiciones anóxicas, luego este incrementó enormemente, así continúo aumentando rápidamente hasta las últimas horas de incubación.
- Las ZMOs en el SCH incrementan las tasas de sedimentación de las carcasas, debido principalmente a dos procesos; 1) aumentan las tasas de mortalidad; 2) las tasas de degradación son mas lentas las primeras 18 h, por lo tanto se hunden.
- Distintas comunidades bacterianas fueron observadas entre los diferentes tratamientos desde los experimentos de degradación, además de cambios de estas comunidades a través de ambas incubaciones.
- Las carcasas de *A.tonsa* están asociados con tres phyla: Proteobacteria, Bacteroidetes y Verrucomicrobia. Vibrionaceae, Pseudoalteromonadaceae, Rhodobacteraceae, Flavobacteriaceae and Verrucomicrobiaceae fueron las familias de bacterias más abundantes.
- Presencia de genes marcadores de desnitrificación *nirK* y *nosZ*, (producción N_2 y N_2O, respectivamente) fueron encontrados bajo condiciones anóxicas, principalmente asociados con el estadio final de degradación. Entonces, la investigación de carcasas de copépodos asociados a bacterias es importante debido a la funcionalidad de estas carcasas y su degradación bacteriana como *hotspots* pelágicos que tienen implicancias biogeoquímicas en el ciclo del nitrógeno, a través de la desnitrificación.
- En otros estudios de laboratorio se evidenció que, la producción de NH_4^+ a partir de la degradación bacteriana de carcasas de *A. tonsa* fue observada en todos los tratamientos en donde el oxígeno estaba muy bajo y estaría siendo provocada por la

mineralización del nitrógeno orgánico; la cual, podría potencialmente contribuir a la DNRA.

- Además, la producción de NH_4^+ podría apuntar a aquellas carcasas de copépodos que sedimentan podrían pasivamente transportar nitrógeno orgánico hacia aguas profundas, donde este se podría liberar parcialmente como amonio y allí las bacterias de vida libre podrían utilizar ese NH_4^+ y oxidarlo a N_2. Por lo tanto, estas carcasas estarían contribuyendo, indirectamente, a procesos de pérdida de N, a través de anammox.
- Así, la pérdida de N en el pélagos se ve potencialmente incrementada por las carcasas de copépodos tanto directamente a través de la producción de N_2 y N_2O, como indirectamente a través de la producción de NH_4^+ que podría contribuir a anammox.
- Como los copépodos son algunos de los organismos del mesozooplancton más abundantes en el océano, por lo que el ciclo anaeróbico del nitrógeno asociado con estos individuos podría tener grandes implicancias sobre los ciclos biogeoquímicos del océano, y la pérdida de nitrógeno orgánico desde los ecosistemas pelágicos.

De acuerdo a los resultados obtenidos en la presente investigación se aceptan las hipótesis propuestas.

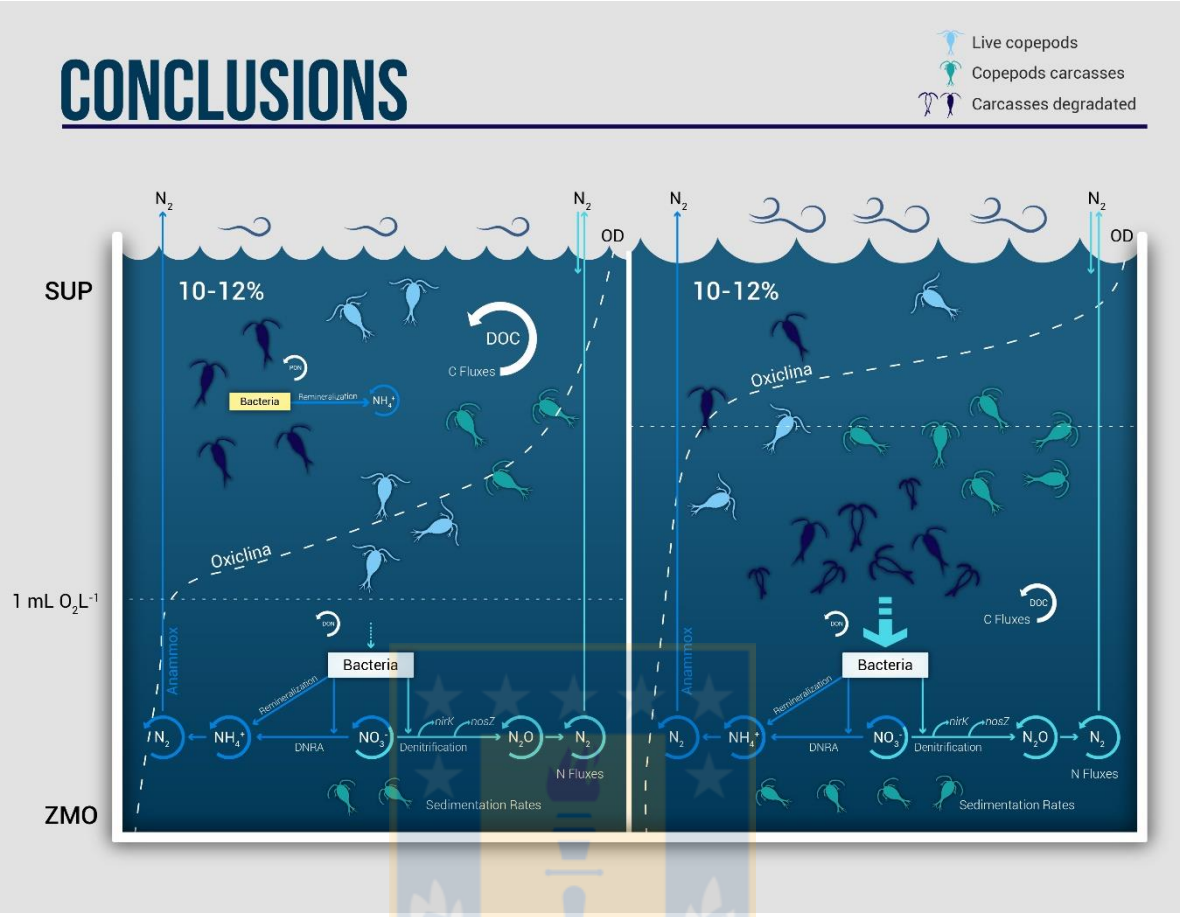

Figura 6.1.- Modelo conceptual de la dinámica poblacional de copépodos pelágicos, vivos (celestes), carcasas (verdes) y degradados por bacterias (azul oscuro y transparente) en un sistema de surgencia costera basado en la zona norte de Chile. La intensificación de vientos favorables aumenta la velocidad vertical de la surgencia (flechas azules sobre el agua), someriza la zona de mínimo oxígeno (ZMO) y la capa superficial oxigenada (SUP). La presencia de la ZMO incrementa las tasas de mortalidad- no depredatoria, aumentando la presencia de carcasas de copépodos en la capa de agua deficiente de oxígeno. Simultáneamente, las carcasas son resuspendidas por la surgencia, o tienden a hundirse hacia el bentos. La suma de estos eventos incrementa la disponibilidad de estas carcasas como materia orgánica lábil para degradación bacteriana, siendo estas carcasas degradadas en la capa superficial y en la ZMO de forma diferenciada. Se muestra el límite superior (1 mL O2 L-1) de la ZMO, perfiles típicos de oxígeno disuelto (OD), la oxiclina, y el potencial efecto de esta degradación sobre los flujos de C y N en el pélagos.

7. REFERENCIAS

Arcos, D.F., Cubillos, L.A., Nuñez, S.P., 2001. The jack mackerel fishery and El Niño 1997–98 effects of Chile. Progr. Oceanogr. 49, 597–617.

Auel H., and H.M. Verheye. 2007. Hypoxia tolerance in the copepod *Calanoides carinatus* and the effect of an intermediate oxygen minimum layer on copepod vertical distribution in the northern Benguela Current upwelling system and the Angola-Benguela Front. J. Exp. Mar. Biol. Ecol. 352: 234–243, doi: 10.1016/j.jembe.2007.07.020.

Azam F, Malfatti F. 2007. Microbial structuring of marine ecosystems. Nat. Rev. Micro. 5: 782-791.

Aksnes, D. L., and M. D. Ohman. 1996. A vertical life table approach to zooplankton mortality estimation. Limnology and Oceanography 41:1461-1469

Bèlehràdek, J. 1957. Physiological aspects of heat and cold. Annu. Rev. Physiol. 19: 59 - 82.

Bickel, S.L., Tang, K.W. 2010. Microbial decomposition of proteins and lipids in copepod versus rotifer carcasses. Mar. Biol. 157 (3), 1613–1624.

Bickel, S.L., Hammond, J.D.M., Tang, K.W. 2011. Boat-generated turbulence as a potential source of mortality among copepods. Journal of Experimental Marine Biology and Ecology 401:105-109.

Böttger-Schnack, R. 1995. Summer distribution of micro- and small mesozooplankton in the Red Sea and Gulf of Aden, with special reference to non-calanoid copepods. Mar. Ecol. Prog. Ser. 118: 81-102.

Båmstedt U (1986) Chemical composition and energy content. In: Corner EDS, O'Hara SCM (Eds.), The Biological Chemistry of Marine Copepods, Clarendon Press, Oxford.

Burns C.W., 1985. Fungal parasitism in a copepod population: the effects of Aphanomyces on the population dynamics of *Boeckella dilatata* Sars. J. Plankton Res. 7, 201–205.

Burke, C., Thomas, T., Lewis, M., Steinberg, P., and Kjelleberg, S. 2011. Composition, uniqueness and variability of the epiphytic bacterial community of the green alga *Ulva australis*.ISME J 5, 590–600.

Brooks L.J. 1968. The effects of prey size selection by lake planktivores. Systematic Biology, 17(3): 273–291.

Carman, K.R., Dobbs, F.C. 1997. Epibiotic microorganisms on copepods and other marine crustaceans. Microscopy Research and Techniques 37:116-135.

Ceballos S., Kiørboe T., 2011. Senescence and sexual selection in a pelagic copepod. PLoS One 6(4):18870. doi:10.1371/journal. pone.0018870.

Daley M.C., Urban-Rich J., and Moisander P. 2016. Bacterial associations with the hydromedusa *Nemopsis bachei* and scyphomedusa *Aurelia aurita* from the North Atlantic Ocean. Mar. Biol. Res. 12:10, 1088 –1100

Daneri, G., Dellarossa, V., Quiñonez, R., Jacob, B., Montero, P., Ulloa, O., 2000. Primary production and community respiration in the Humboldt Current System off Chile and associated oceanic areas. Mar. Ecol. Prog. Ser. 97, 41–49.

De Corte, D., Srivastava, A., Koski, M., Garcia, J. A. L., Takaki, Y., Yokokawa, T., Nunoura, T., Elisabeth, N. H., Sintes, E. and Herndl, G. J. 2018. Metagenomic insights into zooplanktonassociated bacterial communities. Environ Microbiol, 20: 492–505. doi:10.1111/1462-2920.13944.

Delgado M, Alcaraz M., 1999. Interactions between red tide microalgae and herbivorous zooplankton: the noxious effects of *Gyrodinium corsicum* (Dinophyceae) on *Acartia grani* (Copepoda: Calanoida). J. Plankton Res. 21, 2361–2371.

DeVries T, Deutsch C, Rafter PA, Primeau F. 2013. Marine denitrification rated determined from a global 3-D inverse model. Biogeosciences. 10, 2481−2496.

Dufy M.A., Hall S.R., Tessier A et al., 2005. Selective predators and their parasitized prey: are epidemics in zooplankton under top–down control? Limnol. Oceanogr. 50, 412–420.

Echevin, V., Goubanova, K., Belmadani, A., Dewitte, B., 2012. Sensitivity of the Humboldt Current system to global warming: a downscaling experiment of the IPSL-CM4 model. Climate Dynam. 38, 761–774.

Eiane K., Aksnes D.L., Ohman M.D., Wood S., Martinussen M.B .2002. Stage-specific mortality of *Calanus* spp. under different predation regimes. Limnol. Oceanogr 47:636-645.

Elliott, D.T., Tang, K.W., 2009. Simple staining method for differentiating live and dead marine zooplankton in field samples. Limnol. Oceanogr. Methods 7, 585–594.

Elliott D.T., Harris C.K., Tang K.W., 2010. Dead in the water: The fate of copepod carcasses in the York River estuary, Virginia. Limnol. Oceanogr. 55,1821–1834.

Elliott, D. T. and Tang, K.W. 2011. Spatial and temporal distributions of live and dead copepods in the lower Chesapeake Bay (Virginia, USA). Estuar. Coasts. 34, 1039–1048.

Escribano, R. 1998. Population dynamics of *Calanus chilensis* in the Chilean Eastern Boundary Humboldt Current. Fish. Oceanogr., 7(3/4): 245-251.

Escribano, R., Hidalgo, P. 2000. Spatial distribution of copepods in the north of the Humboldt Current region off Chile during coastal upwelling. Journal Marine. Biol. Ass. U. K., 80, 283–290.

Escribano R, Schneider W. 2007. The structure and functioning of the coastal upwelling system off central/southern Chile. Progress in Oceanography, 75: 343 – 347.

Escribano, R., Hidalgo, P., González, H.E., Giesecke, R., Riquelme-Bugueño, R., Manríquez, K. 2007. Interannual and seasonal variability of metazooplancton in the Central/South upwelling region off Chile. Prog. Oceanogr. 75: 470-485

Escribano, R., Hidalgo, P., Fuentes, M., Donoso, K. 2012. Zooplankton time series in the coastal zone off Chile: Variation in upwelling and responses of the copepod community. Prog. Oceanogr., doi: 10.1016/j.pocean.2011.11.006.

Escribano R., P. Hidalgo, V. Valdés, and L. Frederick. 2014. Temperature effects on development and reproduction of copepods in the Humboldt Current: the advantage of rapid growth. J. Plankton Res. 36: 104–116.

Escribano, R., Bustos-Ríos, E., Hidalgo, P., Morales C.E., 2016. Non-limiting food conditions for growth and production of the copepod community in a highly productive upwelling zone. Cont. Shelf Res. 126, 17–14.

Espinoza, P., Bertrand, A., 2008. Revisiting Peruvian anchovy (*Engraulis ringens*) trophodynamics provides a new vision of the Humboldt Current system. Progr. Oceanogr. 79,215–227.

Fernández-Álamo, M., and J. Färber-Lorda. 2006. Zooplankton and the oceanography of the eastern tropical Pacific: A review. Prog. Oceanogr. 69: 318–359.

Fuhrman J. 2000. Impact of viruses on bacterial processes. In: Kirchman DL (ed) Microbial ecology of the oceans. Wiley, New York, p 327–350.

Genin A, Gal G, Haury L.1995. Copepod carcasses in the ocean. II. Near coral reefs. Mar. Ecol. Prog. Ser. 123, 65–71.

Gerdts, G., Brandt, P., Kreisel, K., Boersma, M., Schoo, K. L., and Wichels, A. 2013. The microbiome of North Sea copepods. Helgoland Mar. Res. 67, 757–773. doi: 10.1007/s10152-013-0361-4. 3

Gilly, W. F., Beman, J., Litvin, S.Y. and Robison, B. H. (2013) Oceanographic and biological effects of shoaling of the oxygen minimum zone. *Ann. Rev. Mar. Sci.*,**5**, 393–420.

Giraldo, A., Escribano, R., Marin, V.H., 2002. Spatial distribution of Calanus chilensis off Mejillones Peninsula (northern Chile): ecological consequences upon coastal upwelling. Mar. Ecol. Progr. Ser. 230, 225–234.

Grossart, H.P., Dziallas, C., and Tang, K.W. 2009. Bacterial diversity associated with freshwater zooplankton. Env Microbiol Rep 1: 50-55.

Goldman JC, Caron DA, Dennet MR.1987. Regulation of gross growth efficiency and ammonium regeneration in bacteria by substrate C:N ratio. Limnol Oceanogr 32:1239 − 1252.

Glud, R. N., Grossart, H. P., Larsen, M., Tang, K. W., Arendt, K. E., Rysgaard, S., et al. 2015.Copepod carcasses as microbial hot spots for pelagic denitrification. Limnol. Oceanogr. 60, 2026–2036.

Harding, G.C.H .1973. Decomposition of marine copepods. Limnology & Oceanography 18: 670-673.

Harris, R., Wiebe, P., Lenz, J., Skjoldal, H.R., Huntley, M., 2000. ICES Zooplankton Methology Manual. Academic Press. San Diego, USA.

Hays, G., A. Richardson, and C. Robinson. 2005. Climate change and marine plankton. Trends Ecol. Evol. 20 (6): 337- 344

Hidalgo, P. & R. Escribano .2001. Succession of pelagic-copepod species during the period 1996/1998 in northern Chile: the influence of the 1997–98 El Niño. Hydrobiology. 453, 153–160.

Hidalgo P, R Escribano & C Morales. 2005a. Annual life cycle of the copepod *Eucalanus inermis* at a coastal upwelling site off Mejillones (23º S), northern Chile. Marine Biology 146: 995–1003.

Hidalgo P, R Escribano & C Morales. 2005b. Ontogenetic vertical distribution and diel migration of the copepod *Eucalanus inermis* in the oxygen minimum zone off northern Chile. Journal of Plankton Research 27: 519-529.

Hidalgo, P., Escribano, R., 2008. The life cycles of two coexisting copepods, *Calanus chilensis* and *Centropages brachiatus*, in the upwelling zone off northern Chile (23ºS). Mar. Biol. 155, 429–442.

Hidalgo, P., Escribano, R., Vergara, O., Jorquera, E, Donoso, K. & Mendoza, P. 2010. Patterns of copepod diversity in the Chilean coastal upwelling system. Deep-Sea Res., Part II 57: 2089-2097.

Hidalgo P, R Escribano, M Fuentes, E Jorquera & O Vergara. 2012. How coastal upwelling influences spatial patterns of size-structured diversity of copepods off central-southern Chile (summer 2009). Progress in Oceanography 92-95: 134-145.

Hirst, A.G., and R.S. Lampitt. 1998. Towards a global model of in situ weight-specific growth in marine planktonic copepods. Mar. Biol. 132: 247-257.

Hirst AG, Kiørboe T. 2002. Mortality of marine planktonic copepods: global rates and patterns. Mar. Ecol. Prog. Ser. 230, 195–209.

Hirst, A.G., Peterson, W.T., Rothery, P., 2005. Errors in juvenile copepod growth rate estimates are widespread: problems with the Moult Rate method. Mar. Ecol. Progr. Ser. 296, 263–279.

Hirst, A.G., Keister, J.E., Richardson, A.J., Ward, P., Shreeve, R.S., Escribano, R., 2014. Reassessing copepod growth using the Moult Rate Method. J. Plankton Res. 36, 1224–1232.

Hirche H.J., K. Barz, P. Ayon, and J. Schulz .2014. High resolution vertical distribution of the copepod *Calanus chilensis* in relation to the shallow oxygen minimum zone off northern Peru using LOKI, a new plankton image system. Deep-Sea Res. I. 188: 63–7.

Homonnay ZG, Keki Z, Marialigeti K et al. 2012.Bacterial communities in the gut of the freshwater copepod *Eudiaptomus gracilis*. J Basic Microbiol. 52, 86–90.

Huntley, M.E., and M.D.G. López. 1992. Temperature-dependent production of marine copepods: a global synthesis. Amer. Nat. 140: 201-242.

Ivory, J.A., Tang, K.W., Takahashi, K., 2014. Use of Neutral Red in short-term sediment traps to distinguish between zooplankton swimmers and carcasses. Mar. Ecol. Progr. Ser. 505, 107–117.

Jumars PA, Penry DL, Baross JA, Perry MJ, Frost BW. 1989. Closing the microbial loop: dissolved carbon pathway to heterotrophic bacteria from incomplete ingestion, digestion and absorption in animals. Deep Sea Res Part A 36: 483–495.

Kimmerer, W. J., McKinnon, D., 1987. Growth, mortality, and secondary production of the copepod *Acartia tranteri* in Westernport Bay, Australia. Limnol. Oceanogr. 32, 14–28.

Kimmerer, W. J., McKinnon, D., 1990. High mortality in a copepod population caused by a parasitic dinoflagellate. Marine Biology 107(3):449-452. DOI: 10.1007/BF01313428.

Kirchner, M .1995. Microbial colonization of copepod body surfaces and chitin degradation in the sea. Helgoland Marine Research. 49:201-212.

Kirchman, D.L., White, J. 1999. Hydrolysis and mineralization of chitin in the Delaware Estuary. Aqua. Microb. Ecol. 18: 187-196.

Kirchman, D.L. 2000. Uptake and regeneration of inorganic nutrients by marine heterotrophic bacteria. In Kirchman, D.L. (ed), Microbial ecology of the oceans. John Wiley and Sons, New York, pp. 261-288.

Mann K.H., Lazier J.N.R.,1991. Dynamics of marine ecosystems: biological-physical interactions in the oceans. Blackwell Scientific Publications, Oxford, United Kingdom. 394 pp.

EscribanoMarín, V., Rodríguez, L., Vallejo, L., Fuenteseca, J., Oyarce, E., 1993. Efectos de la surgencia costera sobre la productividad primaria primavera de la Bahía Mejillones de Sur (Antofagasta, Chile). Rev. Chil. Hist. Nat. 66, 479–491.

Marín, V., Olivares, G., 1999. Estacionalidad de la productividad primaria en Bahía Mejillones del Sur (Chile): una aproximación proceso-funcional. Rev. Chil. Hist. Nat. 72, 629–641.

Marín V, L Delgado & R. Escribano. 2003. Upwelling shadows at Mejillones bay (northern Chilean coast): a remote sensing in situ analysis. Investigaciones Marinas 31(2): 47-55.

Manríquez, K., R. Escribano, and P. Hidalgo. 2009. The influence of coastal upwelling on the mesozooplankton community structure in the coastal zone off Central/Southern Chile as assessed by automated image analysis. J. Plankton Res. 31(9): 1075 – 1088

Martínez, M., Espinosa, N. & Calliari, D. 2014. Incidence of dead copepods and factors associated with non-predatory mortality in the Río de la Plata estuary. J. Plankton Res., 36, 265–270.

Miller C.B., Wheeler P.A 2009. Biological Oceanography. John Wiley & Sons, 2009. 416 pp.

Møller EF, Nielsen TG. 2001. Production of bacterial substrate by marine copepods: Effect of phytoplankton biomass and cell size. J Plankton Res 23: 527-536.

Møller EF. 2005. Sloppy feeding in marine copepods: Prey-size-dependent production of dissolved organic carbon. J Plankton Res 27: 27-35.

Møller EF, Riemann L, Søndergaard M. 2007. Bacteria associated with copepods: Abundance, activity and community composition. Aquat. Microb. Ecol. 47: 99–106.

Moisander, P. H., Sexton, A. D., and Daley, M. C. 2015. Stable associations masked by temporal variability in the marine copepod microbiome. PLoS ONE 10:e0138967. doi: 10.1371/journal.pone.0138967.

Nagasawa, S., Nemoto, T. 1988. Presence of bacteria in guts of marine crustaceans and on their fecal pellets. Journal of Plankton Research 10: 559-564.

Nuester, J., Shema, S., Vermont, A., Fields, D. M., and Twining, B. S. 2014. The regeneration of highly bioavailable iron by meso- and microzooplankton. Limnol. Oceanogr.59, 1399–1409.

Ley R.E., Backhed F., Turnbaugh P. et al. 2005. Obesity alters gut microbial ecology. P Natl Acad Sci USA.102,11070–5.

O'Brien W.J., Slade, N.A., Vinyard G. L.1976. Apparent size as the determinant of prey selection by bluegill sunfish (*Lepomis macrochirus*). Ecology 57(6): 1304–1310.

Omori, M., and T. Ikeda. 1984. Methods in zooplankton ecology. J. Wiley & Son

Ohman, M. D., & S. N. Wood. 1995. The inevitability of mortality. ICES Journal of Marine Science 52: 517-522.

Ohman M. 2012. Estimation of mortality for stage-structured zooplankton populations: What is to be done? Journal of Marine Systems 93: 4-10.

Paulmier, A. & D. Ruiz-Pino. 2009. Oxygen minimum zones (OMZs) in the modern ocean. Progress in Oceanography 80 (3-4), 113-128.

Paulmier, A., P. Ruz-Pino, and V. Garçon. 2011. CO_2 maximum in the oxygen minimum zone (OMZ). Biogeosciences 8: 239 – 252.

Peterson, W. 1998. Life cycle strategies of copepods in coastal upwelling zones. J. Mar. Syst. 15: 313-326

Peterson W.T., 2001. Patterns in stage duration and development among marine and freshwater calanoid and cyclopoid copepods: a review of rules, physiological constraints, and evolutionary significance. Hydrobiologia. 453/454, 91–105.

Pino-Pino, P, Escribano R., Hidalgo P., Riquelme-Bugueño R. & Schneider W. 2014. Copepod community response to variable upwelling conditions off central-southern Chile during 2002−2004 and 2010−2012. Mar. Ecol. Prog. Ser. 515: 83–95.

Poulet, S. A., R. Escribano, P. Hidalgo, A. Cueff, T. Wichardc, V. Aguilera, C.A. Vargas, and G. Pohnert. 2007. Collapse of *Calanus chilensis* reproduction in a marine environment with high diatom concentration. J. Exp. Mar. Biol. Ecol. 352: 187 - 199

Ploug H. 2001. Small-scale oxygen fluxes and remineralization in sinking aggregates. Limnol Oceanogr 46:1624–1631.

Plourde S, Maps F, Joly P. 2009a. Mortality and survival in early stages control recruitment in *Calanus finmarchicus*. J Plankton Res 31:371–388.

Plourde, S., P. Pepin, and E. J. H. Head. 2009b. Long-term seasonal and spatial patterns in mortality and survival of *Calanus finmarchicus* across the Atlantic Zone Monitoring Programme region, Northwest Atlantic. ICES Journal of Marine Science 66:1942-1958.

Pujalte, M.J., Lucena, T., Ruvira, M.A., Arahal, D.R., and Macian, M.C. 2014. The family Rhodobacteraceae. In The Prokaryotes: Alphaproteobacteria and Betaproteobacteria. Rosenberg, E., DeLong, E.F., Lory, S., Stackebrandt, E., and Thompson, F. (eds). Berlin, Heidelberg: Springer Berlin Heidelberg, pp. 439–512.

Ridley, C.P., Faulkner, D.J., and Haygood, M.G. 2005. Investigation of Oscillatoria spongeliaedominated bacterial communities in four dictyoceratid sponges. Appl Environ Microb 71, 7366–7375.

Roder, C., Arif, C., Bayer, T., Aranda, M., Daniels, C., Shibl, A., et al. 2014. Bacterial profiling of White Plague Disease in a comparative coral species framework. ISME J 8, 31–39.

Roman M.R., Gauzens A.L., Rhinehart W.K., White J.R., 1993. Effects of low oxygen waters on Chesapeake Bay zooplankton. Limnol Oceanogr 38, 1603–1614.

Runge JA, Franks PJS, Gentleman WC, Megrey BA, Rose KA, Werner FE, & Zakardjian B. 2004. Diagnosis and prediction of variability in secondary production and fish recruitment processes: developments in physical-biological modeling. In: Robinson AR, Brink KH (eds) The sea, Vol 13. Harvard University Press, Cambridge, MA, p 413–473.

Runge, J. A., and Roff, J. C. 2000. The measurement of growth and reproductive rates, p. 401–454. In Harris, R. P., P. Wiebe, J. Lenz, H. R. Skjoldal, and M. Huntley [eds.], ICES Zooplankton Methodology Manual. Academic Press.

Runge, J.A., Franks, P.J., Gentleman, W.C., Megrey, B.A., Rose, K.A., Werner, F.E., and Zakardjian, B., 2004. Diagnosis and prediction of variability in secondary production and fish recruitment processes: developments in physical-biological modelling. In: Robinson AR, Brink KH (eds) The sea, vol. 13. Harvard University Press, pp. 413–473.

Ruz, P. M., P. Hidalgo, S. Yáñez, R. Escribano, and J. E. Keister. 2015. Egg production and hatching success of Calanus chilensis and Acartia tonsa in the northern Chile upwelling zone (23° S), Humboldt Current System. J. Marine. Syst. 148: 200–212.

Ruz, P. M., Hidalgo P., Escribano R., Keister J. E., Yebra L., Franco-Cisterna B. 2018. Hypoxia effects on females and early stages of *Calanus chilensis* in the Humboldt Current ecosystem (23°S). J. Exp. Mar. Biol. Ecol. 498, 61–71.

Roman, M. R., W. K. Rhinehart and J. R. White. 1993. Effects of low oxygen waters on Chesapeake Bay zooplankton. Limnol. Oceanogr. 38(8): 1603 – 1614. doi: 10.4319/lo.1993.38.8.1603.

Sampei M, H Sasaki, H Hattori, A Forest & L Fortier. 2009. Significant contribution of passively sinking copepods to the downward export flux in Arctic waters. Limnology and Oceanography 54: 1894-1900.

Sampei, M., Sasaki, H., Forest, A., Fortier, L., 2012. A substantial export flux of particulate organic carbon linked to sinking dead copepods during winter 2007-2008 in the Amundsen Gulf (southeastern Beaufort Sea, Arctic Ocean). Limnol. Oceanogr. 57, 90–96.

Schneider W, R. Fuenzalida, J. Garcés-Vargas, L. Bravo & C. Lange, Carina. 2006. Vertical and horizontal extension of the oxygen minimum zone in the easterns south Pactific Ocean. Gayana (Concepción), 70(Supl. 1), 79-82.

Saiz E., Calbet A., Grifell K., Guilherme J., Bersano F., Isari S., Solé M., Peters J., Alcaraz M., 2015. Ageing and caloric restriction in a marine planktonic copepod. Sci Rep 5:14962.

Stalder, L.C. and N.H. Marcus. 1997. Zooplankton responses to hypoxia: behavioral patterns and survival of three species of calanoid copepods. Mar. Biol. 127: 599–608

Steele JH, Henderson EW .1992. The role of predation in plankton models. J Plankton Res 14:157– 172.

Stevens H, Ulloa O. 2008. Bacterial diversity in the oxygen minimum zone of the eastern tropical South Pacific. Environmental Microbiology, 10 (5): 1244-1259.

Stewart FJ, Ulloa O, DeLong EF. 2012. Microbial Metatranscriptomics in a Permanent Marine Oxygen Minimum Zone. Environmental Microbiology, 14.1: 23–40.

Sobarzo M & D Figueroa. 2001. The physical structure of a cold filament in a Chilean upwelling zone (Peninsula de Mejillones, Chile, 23°S). Deep Sea Research Part I: Oceanographic Research Papers 48: 2699-2726.

Svitil AL, Chadhain SMN, Moore JA, Kirchman DL.1997. Chitin degradation proteins produced by the marine bacterium Vibrio harveyi growing on different forms of chitin. Appl Environ Microbiol. 63, 408–13.

Tang, K.W., 2005. Copepods as microbial hotspots in the ocean: effects of host feeding activities on attached bacteria. Aquatic Microbial Ecology 38: 31-40

Tang, K.W., Freund, C. S. and Schweitzer, C. L. 2006 a. Occurrence of copepod carcasses in the lower Chesapeake Bay and their decomposition by ambient microbes. Estuar. Coastal Shelf Sci., 68, 499–508.

Tang, K. W., K. M. Hutalle & Grossart, H. P. 2006 b. Microbial abundance, composition and enzymatic activity during decomposition of copepod carcasses. Aquat. Microb. Ecol. 45: 219–227, 2006

Tang, K. W., S. L. Bickel, C. Dziallas, & Grossart, H. P. 2009. Microbial activities accompanying decomposition of cladoceran and copepod carcasses under different environmental conditions. Aquat. Microb. Ecol. 57: 89-100.

Tang, K. W., V. Turk, & Grossart, H. P. 2010. Linkage between crustacean zooplankton and aquatic bacteria. Aquat. Microb. Ecol. 61: 261–277.

Tang K. W., M. I. Gladyshev, O. Dubovskaya, G. Kirillin & Grossart H. P.2014. Zooplankton carcasses and non-predatory mortality in freshwater and inland sea environments. Journal of Plankton Research 36: 597–612

Tang K.W. & D.T. Elliott. 2014. Chapter: Copepod carcasses: occurrence, fate and ecological importance. In: Copepods: Diversity, Habitat and Behavior. 28 pp.

Thiel V., Neulinger S C., Staufenberger T., Schmaljohann R., and Imhoff J. F. 2007. Spatial distribution of sponge-associated bacteria in the Mediterranean sponge *Tethya aurantium*.FEMS Microbiol Ecol. 59, 47–63.

Turner, J.T. and P.A. Tester. 1997. Toxic marine phytoplankton, zooplankton grazers, and pelagic food webs. Limnol. Oceanog. 42(5, part. 2): 1203 - 1214

Tsuda A., 1994. Starvation tolerance of a planktonic marine copepod *Pseudocalanus newmani* frost. J Exp Mar Biol Ecol 181, 81–89.

Trujillo-Ortiz, A. 1986. Life cycle of the marine calanoid copepod *Acartia californiensis* Trinast reared under laboratory conditions. CalCOFI Rep. XXVII: 188 – 204

Ulloa O, Pantoja S. 2009. The oxygen minimum zone of the eastern South Pacific. Deep Sea Research II, 56: 987 – 991.

Ulloa O, Canfield DE, DeLong EF, Letelier RM, Stewart FJ. 2012. Microbial oceanography of anoxic oxygen minimum zones. Proc. Nat. Acad. Sci., 109 (40):15996-16003.

Ulloa O, Wright JJ, Belmar L, Hallam SJ. 2013. Pelagic Oxygen Minimum Zone Microbial Communities. In: Rosenberg E. Delong EF. Lory S. Stackebrandt E. Thompson F. (Eds.). The Prokaryotes. Springer-Verlag. Berlin Heidelberg, pp. 528.

Vargas, C.A., Escribano, R., Poulet, S., 2006. Phytoplankton diversity determines time windows for successful zooplankton reproductive pulses. Ecol. 87, 2992–2999

Vargas C.A., Martínez R.A., Escribano R.E., Lagos N.A., 2010. Seasonal relative influence of food quantity, quality, and feeding behaviour on zooplankton growth regulation in coastal food webs. J. Mar. Biol. Assoc. U.K. 90,1189–1201.

Vojvoda J, Lamy D, Sintes E et al. 2014.Seasonal variation in marine snow-associated and ambient-water prokaryotic communities in the northern Adriatic Sea. Aquat Microb Ecol. 73, 211–24.

Wetzel RG. 1995. Death, detritus, and energy flow in aquatic ecosystems. Fresh. Biol. 33, 83 – 89.

Wust P.K., Horn M.A., Drake H.L. 2011. Clostridiaceae and Enterobacteriaceae as active fermenters in earthworm gut content. ISME J. 5, 92–106.

Yáñez, S., 2009. Tasa de mortalidad y desarrollo de *Paracalanus cf. indicus* (Copepoda: Calanoida) (Wolfender, 1905) en la zona Centro-Sur de Chile (36°S) asociada con la zona de mínimo de oxígeno. Seminario de título, Facultad de Ciencias Naturales y Oceanográficas, Universidad de Concepción, Concepción, 65 pp.

Yañez, S., Hidalgo P., Escribano, R., 2012. Mortalidad natural de *Paracalanus indicus* (Copepoda, Calanoida) en áreas de surgencia asociada a la zona de mínimo oxígeno en el Sistema de Corrientes de Humboldt: implicancias en el transporte pasivo del flujo de carbono. Rev. de Biol. Mar. Oceanogr. 47,Nº2: 295-310.

Yañez S., Hidalgo P., Ruz P. & Tang K. 2018. Copepod secondary production in the sea: errors due to uneven molting and growth patterns and incidence of carcasses. Progress in Oceanography. 165, 257-267. https://doi.org/10.1016/j.pocean.2018.06.008.

Zhu X-f, Zhou Y, Feng J-l .2007. Analysis of both chitinase and chitosanase produced by *Sphingomonas sp*. Cj-5. J Zhejiang Univ 8: 831-8.